# THE ROLE OF DBF4-DEPENDENT KINASE IN MAINTAINING GENOME STABILITY

By

Nanda Kumar Sasi

## A DISSERTATION

Submitted to
Michigan State University
in partial fulfilment of the requirements
for the degree of

Genetics-Doctor of Philosophy

2017

#### **ABSTRACT**

## THE ROLE OF DBF4-DEPENDENT KINASE IN MAINTAINING GENOME STABILITY

By

#### Nanda Kumar Sasi

DBF4-dependent kinase (DDK) is a two subunit kinase composed of the CDC7 kinase and its regulatory subunit, DBF4. It is essential for initiating DNA replication at individual origins and also has less understood roles in DNA repair, mitosis, and meiosis. Both DDK subunits are highly expressed in many diverse tumor cell lines and primary tumors, which is correlated with poor prognosis. Inhibiting DDK causes apoptosis of tumor cells, but not normal cells, through a largely unknown mechanism. The aim of this dissertation is to improve our understanding of the role of DDK in maintaining genome stability, in tumorigenesis, and to identify ways to better utilize DDK as a target for tumor therapy.

First, we studied the role of DDK in initiating and maintaining the replication checkpoint pathway. This pathway ensures complete and accurate replication of DNA before chromosomes segregate during mitosis. We found a novel role for DDK in the nucleolytic processing of stalled replication forks, structures generated upon inhibition of DNA replication. DDK-mediated fork processing is essential for generating single stranded DNA at stalled forks, which in turn is required for activating a replication-checkpoint pathway. Our results suggest that high levels of DDK expression might enable tumor cells to tolerate replication stress, a by-product of increased rate of proliferation. Indeed, gene expression signature of tumors with high levels of DDK correlated with increased resistance to genotoxic chemotherapies. Surprisingly, the level of DDK expression is also strongly correlated with genome-wide gene mutation frequencies suggesting that increased DDK levels promote elevated mutation frequency. This is consistent with the role of DDK in

promoting an error-prone trans-lesion DNA repair pathway, a possible mechanism for the increased rate of mutagenesis. Finally, using an RNA interference screen we identified 23 kinases and phosphatases that promote apoptosis of both breast and cervical carcinoma cell lines when DDK is inhibited. These hits include checkpoint genes, G2/M cell cycle regulators and known tumor suppressors. Initial characterization of the LATS2 tumor suppressor suggests that it promotes apoptosis independently of the upstream MST1/2 kinases in the Hippo signaling pathway. A clear understanding of this pathway would enable better use of DDK inhibitors for tumor therapy and also suggest possible mechanisms by which tumors might become resistant to DDK-targeting drugs.

These results have increased our understanding of DDK's role in cellular response to replication perturbation, an important function beyond its essential role in DNA replication. Our studies highlight the importance of DDK in tumor cells and explain the survival advantage gained by its increased expression. Finally, this work lays out strategies for targeting DDK to limit tumor growth and overcome resistance to existing genotoxic chemotherapies.

#### **ACKNOWLEDGEMENTS**

First and foremost, I would like to thank Dr. Michael Weinreich for being a kind and patient mentor to me. His steadfast support and encouragement made this journey intellectually stimulating. He gave me the freedom to explore questions that fascinated me and acknowledged my successes. Over the years I have not only benefitted from his scientific expertise but also learnt a great deal regarding all aspects of a career in scientific research. I also thank my co-advisor Dr. Jeff MacKeigan for providing a laboratory environment conducive to free thinking and encouraging me through the last and challenging phases of my dissertation. I spent several productive months working in Dr. Katheryn Meek's lab and her enthusiasm for science has been a source of inspiration to me. I thank her for her unwavering support through the years as a member of my thesis advisory committee. I also thank Dr. David Arnosti and Dr. Michele Fluck for their role as members of my thesis advisory committee. They always had my best interests in mind and guided me through my Ph.D. with care and affection.

Over the years many individuals have invested their time into my scientific training and I am greatly indebted to them. I thank FuJung Chang for being an amazing teacher to me and for expertly troubleshooting experiments. She is also a dear friend who ensured that I had an endless supply of banana bread and chocolate chip cookies. I thank my fellow lab-mates for creating a positive work environment in the lab. I especially thank Dr. Sunetra Roy, Smitha Yerrum, Dr. Kristin Dittenhafer-Reed, Dr. Lucas Chan, Dr. Aditi Bagchi, and Kellie Sisson for putting up with my frequent forays into random trivia. They encouraged and engaged me in intelligent discussions, helped me with new assays and experimental techniques, and were always a great source of support.

I am also thankful for the fantastic institutional support that has ensured stability while I split my time studying at Michigan State University (MSU) and working at Van Andel Institute (VAI). I thank Dr. Barbara Sears, Dr. Cathy Ernst, Jeannine Lee, and Cindy Robinson of the MSU Genetics program for recruiting me and supporting me through several semesters. I thank Dr. Peter Jones, Dr. Steve Triezenberg, and Dr. Julie Turner of VAI for supporting my research and for including me in all graduate school activities. I thank the core facilities at VAI for maintaining state of the art instruments, without which it would have been impossible to do good science. I will especially remember all the help I received from my fellow graduate students both at MSU and VAI. Special thanks to Dr. Sander Frank, Dr. Megan Goodall, and Dr. Arkadeep Sinha for making the long and frequent trips to MSU enjoyable.

I would like to thank my newfound family members Tony, Jincy, Aleena, and Joel Varghese. They took me in as a member of their family, which somewhat made up for the fact that all my family was thousands of miles away. I made many new friends in the last five years. As a student from a foreign country my first few months would have been extremely challenging if not for the camaraderie that surrounded me. I will forever cherish memories of our collective excitement upon seeing the skyscrapers in New York and Chicago, our trips to Cedar Point, and the numerous birthdays, weddings, and other special occasions we celebrated together.

Finally, and most importantly, I would like to express my heartfelt gratitude to my family. My parents Ambika and Sasi Kumar and my sister Saumya Pillai have been a source of great joy for me. They lifted me up when I fell and celebrated when I succeeded. Without their unconditional love, I would not have finished graduate school successfully. I owe them all my achievements and I am ever so grateful to them.

## TABLE OF CONTENTS

LIST OF TABLES	ix
LIST OF FIGURES	X
KEY TO ABBREVIATIONS	xii
CHAPTER 1. INTRODUCTION	1
Initiation of Eukaryotic DNA replication	2
Origin Licensing	2 2 3 9
Origin Firing	3
DNA Replication Checkpoint	9
Mechanism of Checkpoint Activation	9
Inhibition of Late Origin Firing	11
Cell Cycle Arrest	12
Dormant Origin Firing	13
Stabilization of Stalled Forks	13
Role of DDK in Replication Checkpoint	19
Rationale for this study	24
CHAPTER 2. DDK HAS A PRIMARY ROLE IN PROCESSING STALLED REPLICATION FORKS TO INITIATE DOWNSTREAM CHECKPOINT SIGNALING	26
ABSTRACT	27
INTRODUCTION	28
RESULTS	31
ATR kinase mediates cell death upon inhibition of DDK	31
Canonical replication-checkpoint pathway is not activated	51
upon DDK inhibition	37
An established replication-checkpoint response prevents cell death	51
induced by DDK inhibition	41
DDK has a primary role in initiating replication checkpoint signaling	46
DDK is required for the processing of stalled replication forks	52
DDK is required for restart of stalled replication forks	57
DDK might promote fork processing by regulating the activity	
of nucleases at stalled forks	60
Low dose DDKi causes aberrant mitotic structures	65
DISCUSSION	68
MATERIALS AND METHODS	76
Cell Lines and Reagents	76
RNAi Interference	77
Immunoblotting	77
Analysis of Caspase 3/7 activity	78

Cell Cycle Analysis	79
DNA Fiber Spreading	79
ACKNOWLEDGEMENTS	81
CHAPTER 3. DDK PROMOTES TUMOR CHEMORESISTANCE AND	
SURVIVAL VIA MULTIPLE PATHWAYS	82
ABSTRACT	83
INTRODUCTION	84
RESULTS AND DISCUSSION	87
Gene expression signature of tumors differentially expressing CDC7 kinase	87
DDK likely drives increased tumor mutagenesis	94
RB1 mutation is strongly correlated with high DDK expression in tumors	100
Functional RNAi screen to identify mediators of apoptosis induced	
following DDK inhibition	105
Proteins involved in mitotic progression are enriched among hits	
obtained from primary screen	107
LATS2 kinase mediates cell death upon DDK inhibition	112
MATERIALS AND METHODS	117
Computational data analysis	117
ChIP-seq data analysis	119
Cell lines and reagents	119
Primary RNAi screen	119
Secondary RNAi screen	121
RNAi interference	121
Immunoblotting	122
Analysis of Caspase 3/7 activity	122
ACKNOWLEDGEMENTS	124
CHAPTER 4. THE POTENT CDC7-DBF4 (DDK) KINASE INHIBITOR XL413	
HAS LIMITED ACTIVITY IN MANY CANCER CELL LINES AND	
DISCOVERY OF POTENTIAL NEW DDK INHIBITOR SCAFFOLDS	125
ABSTRACT	126
INTRODUCTION	127
RESULTS	132
DDK inhibitors exhibit very different cellular potencies	132
PHA-767491 and XI413 are potent DDK inhibitors in vitro	138
XL413 is defective in inhibiting DDK-dependent MCM2	1.41
phosphorylation in HCC1954 cells	141
Screen to determine cross reactivity of known kinase inhibitors with DDK	145
DISCUSSION	155
MATERIALS AND METHODS	159
Synthesis of PHA-767491 and XL413	159
Cell lines	159 160
DDK protein induction DDK purification	160
In vitro kinase activation assays	160
HI VIII O NIHANO ACHIVAHUH ANNAYN	1 ( ) 1

Analysis of cell viability	161
Analysis of Caspase 3/7 activity	162
Immunoblot Analysis	162
Thermal Stability Shift Assay (TSA)	163
ACKNOWLEDGEMENTS	164
CHAPTER 5. SUMMARY AND FUTURE DIRECTIONS	165
Nucleolytic processing of stalled replication forks	166
DDK has a primary role in processing stalled replication forks	167
High levels of DDK expression confers a survival advantage to tumor cells	168
DDK likely drives increased tumor mutagenesis	168
DDK as a chemotherapeutic target	169
REFERENCES	171

## LIST OF TABLES

Table 1.1.	Conserved replication initiation and checkpoint proteins in		
	yeast and metazoans	8	
Table 4.1.	DDK inhibitors synthesized by various pharmaceutical companies	131	
Table 4.2.	Structures of potential DDK inhibitors	154	

## LIST OF FIGURES

Figure 1.1.	Initiation of eukaryotic DNA replication.	6
Figure 1.2.	Activation and transduction of the replication checkpoint.	15
Figure 1.3.	Replication checkpoint-mediated activation of dormant origins.	17
Figure 1.4.	Replication checkpoint-mediated inhibition of late origins.	22
Figure 2.1.	Non-canonical role of ATR kinase in mediating apoptosis upon DDK inhibition.	33
Figure 2.2.	Canonical replication-checkpoint pathway is not activated upon DDK inhibition.	39
Figure 2.3.	An established checkpoint response prevents cell death induced by DDK inhibition.	43
Figure 2.4.	DDK is essential for initiating the replication checkpoint pathway.	47
Figure 2.5.	DDK is essential for initiating the replication checkpoint pathway in response to multiple replication inhibitors.	50
Figure 2.6.	DDK has a primary role in processing stalled replication forks.	54
Figure 2.7.	DDK plays an important role in the restart of stalled replication forks.	58
Figure 2.8.	DDK might promote fork resection by directly regulating the activity of nucleases.	63
Figure 2.9.	DDK inhibition induces mitotic abnormalities.	66
Figure 2.10.	Model for DDK's role at stalled replication fork and events downstream of DDK inhibition.	73
Figure 3.1.	DDK is overexpressed in tumors and is a predictor of poor survival.	89
Figure 3.2.	Characterization of tumors that differentially express DDK.	92
Figure 3.3.	DDK likely drives increased tumor mutagenesis.	96
Figure 3.4.	E2F family of transcription factors strongly bind DDK promoters.	102

Figure 3.5.	RNAi screen to identify mediators of cell death induced upon DDK inhibition.	
Figure 3.6.	LATS2 mediates cell death upon DDK inhibition.	115
Figure 4.1.	Two DDK inhibitors, PHA-767491 and XL413, exhibit differential activity against cultured tumor cells.	134
Figure 4.2.	PHA-767491 and XL413 are similarly effective DDK inhibitors in vitro.	139
Figure 4.3.	XL413 is defective in inhibiting DDK-dependent MCM2 phosphorylation in HCC1954 cells but is effective in Colo-205 cells.	143
Figure 4.4.	Discovery of potential new DDK inhibitor scaffolds.	148
Figure 4.5.	A PKR inhibitor and a CHK1 inhibitor also inhibits DDK activity and induces apoptosis in breast cancer cells.	151

#### **KEY TO ABBREVIATIONS**

APH Aphidicolin

ATM Ataxia telangiectasia mutated

ATMi ATM kinase inhibitor

ATR Ataxia telangiectasia and Rad3-related protein

ATRi ATR kinase inhibitor

BLM Bloom syndrome protein

CDC7 Cell division cycle 7-related protein kinase

CHK1 Cell cycle checkpoint kinase 1

CHK1i CHK1 kinase inhibitor

CHK2 Cell cycle checkpoint kinase 2

CldU 5-Chloro-2'-deoxyuridine thymidine analog

CPT Camptothecin

CtIP CtBP-interacting protein

DBF4 Dumbbell forming protein 4 – homolog A

DBF4B Dumbbell forming protein 4 – homolog B

DDK DBF4-dependent CDC7 kinase

DDKi DDK kinase inhibitor

DMSO Dimethyl sulfoxide

DNA-PKcs DNA-dependent protein kinase catalytic subunit

DNA-PKcsi DNA-PKcs kinase inhibitor

E2F Transcription factor E2F

Eto Etoposide

EXO1 Exonuclease 1

HU Hydroxyurea

IdU 5-Iodo-2'-deoxyuridine thymidine analog

LATS Large tumor suppressor homolog

MCM Minichromosome maintenance proteins

MST Mammalian STE20-like protein kinase

ORC Origin recognition complex

PARP Poly [ADP-ribose] polymerase 1

RB1 Retinoblastoma-associated protein

RPA Replication protein A

SAV1 Protein salvador homolog 1

Thy Thymidine

YAP1 Yes-associated protein 1

zVAD Pan caspase inhibitor Z-VAD-FMK (carbobenzoxy-valyl-alanyl-aspartyl-[O-

methyl]-fluoromethylketone)

## CHAPTER 1.

## INTRODUCTION

## Modified from

Sasi, N.K., and Weinreich, M. (2016). DNA Replication Checkpoint Signaling. In The Initiation of DNA Replication in Eukaryotes, L.D. Kaplan, ed. (Cham: Springer International Publishing), pp. 479-502.

## **Initiation of Eukaryotic DNA Replication**

Eukaryotes have large genomes that are tightly packed into chromatin and dispersed among multiple chromosomes and therefore utilize multiple origins of replication to replicate their genomes. Tight regulation of the initiation of DNA replication is required since re-initiation from any single origin during S-phase would result in over-replicated regions that could cause chromosome breakage during chromosome segregation. When DNA replication is perturbed or DNA is damaged during S-phase, checkpoint mechanisms inhibit initiation events at late origins, which conserves limiting initiation proteins, and stabilize replication forks. Checkpoints also inhibit mitotic entry to allow time for the repair of DNA damage and replisome reactivation.

The initiation of eukaryotic DNA replication is separated into two mutually exclusive steps during the cell cycle. Origins are "licensed" in late M to early G1 phase by the loading of an inactive form of the replicative MCM (mini-chromosome maintenance) helicase. The MCM helicase is subsequently remodeled by the recruitment of CDC45 and the four-subunit GINS (Go-Ichi-Ni-San) complex to form the active CMG (CDC45-MCM-GINS) helicase, which is required to unwind origin DNA and moves with each replication fork. Helicase activation signals the beginning of S-phase but occurs continuously at each individual origin that is utilized (or fires) during S-phase. In this section, the general concepts of DNA replication initiation are discussed with special emphasis on the role of DDK in these processes.

## Origin Licensing

Origin licensing requires binding of the hetero-hexameric origin recognition complex (ORC) to DNA (Figure 1.1). Budding yeast origins are comprised of specific DNA sequences that bind ORC, but fission yeast and more complex eukaryotes specify ORC binding sites with

little or no DNA sequence specificity. Instead secondary DNA structures and chromatin features have been proposed to be important in origin determination in mammalian cells (Leonard and Méchali, 2013). ORC is an ATP binding protein comprised of ORC1 through ORC6 subunits, five of which (ORC1 to ORC5) have AAA<sup>+</sup> (or AAA<sup>+</sup>-like) ATPase domains (Yan and Hiroyuki, 2013; Yardimci and Walter, 2013). To initiate DNA replication ORC first recruits CDC6, another AAA+ ATPase protein. CDC6 is homologous to the ORC1 subunit and its ATPase activity is also important for replication initiation (Yan and Hiroyuki, 2013; Yardimci and Walter, 2013). The next step in origin licensing is recruitment of the eukaryotic replicative MCM helicase, which is a hetero-hexamer of MCM2-7 subunits (Remus et al., 2009; Yardimci and Walter, 2013). Each of the six subunits of the MCM complex also contains AAA+ ATPase domains. The MCM2-7 complex interacts with a mediator protein CDT1. In budding yeast CDT1 aids in the nuclear import of MCM complex, which allows docking of CDT1-MCM2-7 complex onto the DNA-ORC-CDC6 complex (Yardimci and Walter, 2013). Subsequent recruitment of another CDT1-MCM2-7 complex forms a stable head-to-head double hexamer (dhMCM) followed by the dissociation of CDT1 and CDC6 (Silvia et al., 2014). The dhMCM bound to origin DNA forms what is known as the "pre-replicative complex" (pre-RC) and these origins are considered licensed for initiation. Although the precise biochemical roles of ATP hydrolysis by CDC6, ORC, and the MCM subunits in pre-RC formation are not fully understood, several models have been proposed (Yardimci and Walter, 2013).

#### Origin Firing

The dhMCM complex can slide freely on dsDNA but it has no helicase activity (Remus et al., 2009; Silvia et al., 2014). As mentioned above, the CDC45 and GINS proteins form a complex

with MCM to generate the active CDC45-MCM-GINS (CMG) helicase (Silvia et al., 2014; Yan and Hiroyuki, 2013). The transition of dhMCM to two CMG complexes involves multiple loading factors and another intermediate known as the pre-initiation complex (pre-IC, see **Figure 1**). MCM helicase loading and activation is thus highly regulated and later sections will justify the need for these regulatory networks.

Two Ser/Thr protein kinases, DDK (DBF4-dependent kinase) and CDK (cyclin-dependent kinase), are critical regulators of MCM loading and activation. CDK activity is lowest in G1 phase but increases at the G1- to S-phase transition (Figure 1). G1-CDK inhibits the ubiquitin ligase APC/C, thereby stabilizing targets of this degradation pathway (e.g. DBF4) to promote S phase entry (Khalid et al., 2013). Hence G1-CDK indirectly promotes DDK activity. At the G1-S phase transition, distinct S-CDKs are activated and cooperate with DDK to initiate DNA replication at individual origins. S-CDK and additional kinases like ATR phosphorylate the MCM complex in the pre-RC. This priming phosphorylation can facilitate DDK phosphorylation, which targets multiple MCM subunits (Randell et al., 2010; Sheu and Stillman, 2006). DDK phosphorylates S/T residues and prefers acidic or phospho-S/T in the +1 position. Purified DDK phosphorylates individual MCM 2,3,4,6,7 subunits in vitro (Karim, 2010) and the dhMCM complex (Sun et al., 2014), but DDK phosphorylation does not cause dissociation of hexamers (On et al., 2014). Instead one essential function of DDK in budding yeast is to phosphorylate the N-termini of MCM4 and MCM6 to relieve an inhibitory effect on DNA replication (Randell et al., 2010; Sheu and Stillman, 2010) and promote recruitment of the SLD3-SLD7-CDC45 complex to dhMCM (Yan and Hiroyuki, 2013) (Figure 1.1). S-CDK is also required for CMG formation by phosphorylating SLD3 and SLD2 (Tanaka et al., 2007; Zegerman and Diffley, 2007) to prime interaction with the scaffolding protein DPB11. DPB11 loads GINS to form the CMG helicase and

also recruits DNA polymerase  $\varepsilon$  to the origin (Silvia et al., 2014; Yan and Hiroyuki, 2013). Each active CMG helicase complex, in association with the DNA polymerase  $\varepsilon$ , encircles ssDNA and moves along the leading strand in the 3' – 5' direction (Fu et al., 2011; Kang et al., 2012a) (**Figure 1.1**).

CMG formation in fission yeast and higher eukaryotes is similar but with some notable differences (Silvia et al., 2014; Yan and Hiroyuki, 2013) since phosphorylation of DRC1<sup>SLD2</sup> and SLD3 by S-CDK is less important in fission yeast than in budding yeast. In metazoans S-CDK mediated phosphorylation of RECQ4<sup>SLD2</sup> is dispensable but that of Treslin<sup>SLD3</sup> is essential for recruitment of TopBP1<sup>DPB11</sup>, CDC45, and GINS (Itou et al., 2014; Kumagai et al., 2010; Sangrithi et al., 2005). See **Table 1.1** for comparison of protein names.

The precise role(s) of CDC45 and GINS in promoting the helicase activity of the MCM2-7 complex is under active investigation. In recent years, a number of additional proteins, e.g. MCM10 (Watase et al., 2012), CTF4 (Simon et al., 2014), DUE-B (Chowdhury et al., 2010), and GEMC1 (Balestrini et al., 2010) have also been shown to be important for origin unwinding (MCM10), CDC45 recruitment (GEMC1), and coupling of polymerases and CMG helicase at the replication fork (CTF4). Finally, the CMG complex recruits DNA polymerase α-primase, which is the only polymerase capable of initiating DNA synthesis *de novo* (Silvia et al., 2014; Simon et al., 2014).

Figure 1.1. Initiation of eukaryotic DNA replication.

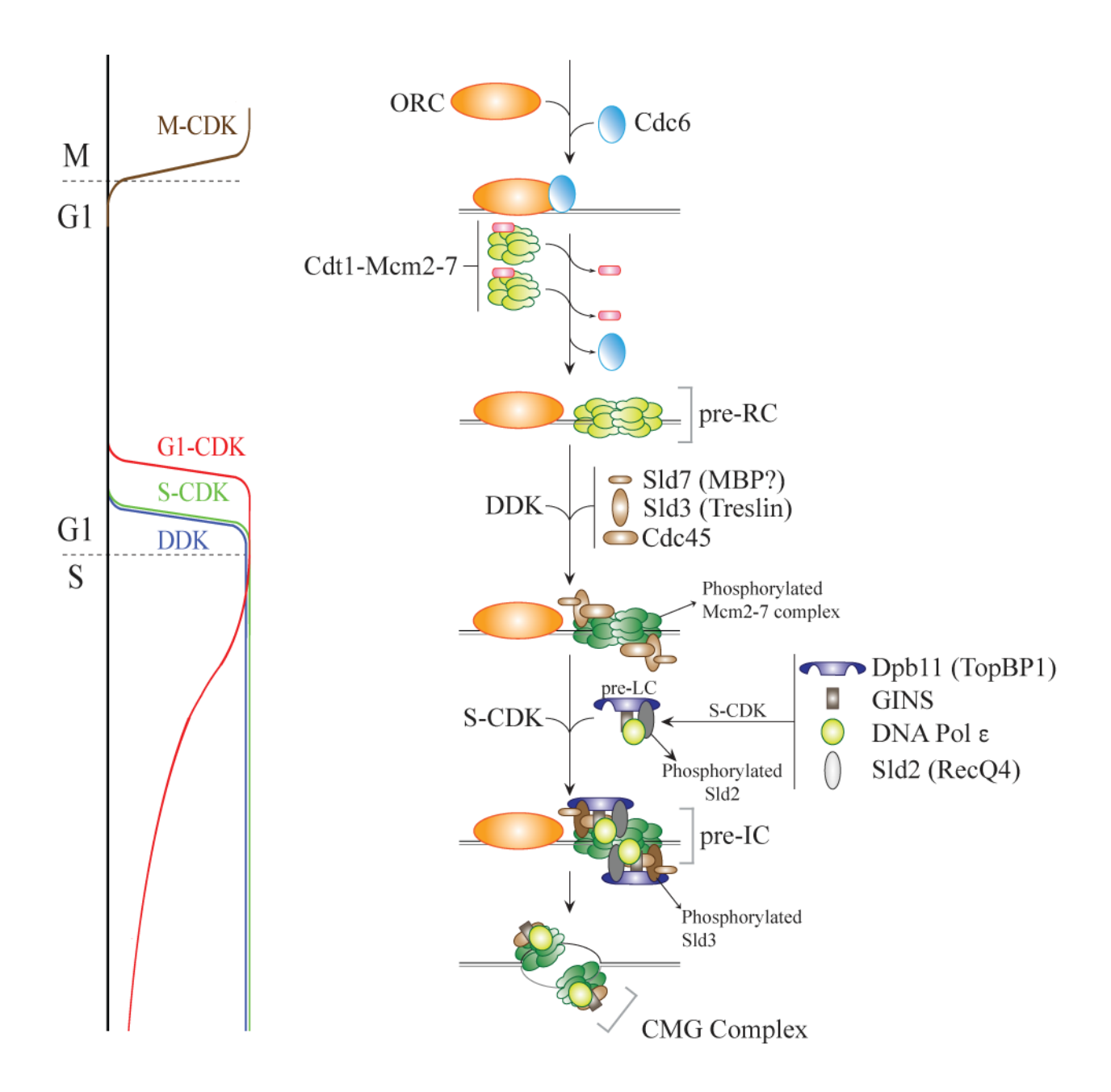


**Figure 1.1 (cont'd).** In G1-phase ORC-Cdc6, recruit Cdt1-Mcm2-7 to form a double hexameric form of the MCM helicase (dhMCM) encircling dsDNA. This is also called the pre-replicative complex (pre-RC). Upon entering S-phase the dhMCM helicase is activated by two protein kinases, DDK and CDK, which facilitate formation of a pre-initiation complex (pre-IC) that ultimately forms the active Cdc45-Mcm2-7-GINS (CMG) helicase. The *S. cerevisiae* pathway shown here is broadly conserved in higher eukaryotes with some notable differences in pre-IC formation. See text for details. Also shown are the cell cycle regulated levels of M-, G1-, S-CDK, and DDK.

Table 1.1. Conserved replication initiation and checkpoint proteins in yeast and metazoans

S. cerevisiae	S. pombe	Metazoans
Replication initiation	proteins	
ORC 1-6	ORC 1-6	ORC 1-6
Cdc6	Cdc6	Cdc6
Cdt1	Cdt1	Cdt1
Mcm 2-7	Mcm 2-7	Mcm 2-7
DDK	DDK	DDK
Cdc7	Hsk1	Cdc7
Dbf4	Dfp1/Him1	Dbf4
-	_ ^	Drf1
S-CDK	S-CDK	S-CDK
Cdc28	Cdc2	Cdk2
Clb5/Clb6	Cig1/Cig2	CyclinA/CyclinE
Sld7	-	MBP (?)
Sld3	Sld3	Treslin/ticrr
Cdc45	Cdc45/Sna41	Cdc45
Dpb11	Cut5/Rad4	TopBP1/Cut5/Rad4
GINS	GINS	GINS
Pol ε	Pol ε	Pol ε
Sld2	Drc1	RecQ4/RecQL4
Mcm10	Mcm10	Mcm10
Replication checkpoi	nt proteins	
RPA	RPA	RPA
Ddc2	Rad26	ATRIP
Mec1	Rad3	ATR
Rad24	Rad17	Rad17
RFC2-5	RFC2-5	RFC2-5
Ddc1	Rad9	Rad9
Mec3	Hus1	Hus1
Rad17	Rad1	Rad1
Chk1	Chk1/Rad27	Chk1
Rad53	Cds1	Chk2
Mrc1	Mrc1	Claspin
Csm3	Swi3	Tipin
Tof1	Swi1	Timeless (Tim1)
Ctf4	Mc11	And1
Swe1	Mik1	Wee1, Myt1
Mih1	Cdc25	Cdc25 A-C
Bmh1, Bmh2	Rad24, Rad25	14-3-3
M-CDK	M-CDK	M-CDK
Cdc28	Cdc2	Cdk1
Clb1/Clb2/	Cig2/Cdc13	CyclinA/CyclinB
Clb3/Clb4		

## **DNA Replication Checkpoint**

Eukaryotic DNA replication occurs efficiently and accurately due to the high number of replication origins and the fidelity of replicative polymerases. Coupling DNA repair with replication also increases overall accuracy. Nevertheless, DNA replication faces many hurdles even in an unperturbed cell cycle. Tight coordination of replication with other DNA specific processes like transcription and chromatin remodeling pose major challenges since conflict between these processes can result in genomic instability. Oncogene driven tumor cells are more susceptible to such conflicts since they have increased replication initiation events (Jones et al., 2013). Other challenges arise due to the complex nature of eukaryotic genomes, which contain repetitive elements and heterochromatin. For example, chromosomal fragile sites often occur in late replicating or heterochromatic regions where replication is more prone to stall (Debatisse et al., 2011). Genotoxic agents including reactive oxygen species, heavy metals, byproducts of metabolic processes, and exposure to harmful radiation from sunlight are all sources of replication stress. The DNA replication checkpoint is activated in response to stalled or damaged forks to help ensure genome integrity. The following section introduces the basic concepts of replication checkpoint signaling with an emphasis on the less understood role of DDK in this process.

## Mechanism of Checkpoint Activation

The general mechanism of replication checkpoint activation is shown in **Figure 1.2**. Long stretches of ssDNA formed at stalled replication forks are stabilized and protected from nucleolytic degradation by association with the single-stranded binding protein, replication protein A (RPA). RPA bound ssDNA is at least partially responsible for initiating the replication checkpoint response (Alexandre and Lee, 2015). Reduced levels of RPA result in attenuated checkpoint

activation in response to replication stress (Zou et al., 2003). RPA bound ssDNA recruits ATR through interactions with an essential ATR cofactor, ATRIP (Costanzo et al., 2002; Hustedt et al., 2012; Zou and Elledge, 2003). ATR in turn phosphorylates the 32kD subunit of the RPA complex and also mediates the recruitment of an ubiquitin ligase PRP19 that preferentially ubiquitylates hyper-phosphorylated RPA (Alexandre et al., 2014). Polyubiquitylated RPA induces the recruitment of additional ATR-ATRIP complexes onto RPA coated ssDNA, forming a feedforward loop that is important for amplification of the replication checkpoint response (Alexandre et al., 2014). Some forms of replication stress, however, do not result in large stretches of RPA bound ssDNA. In such cases, DNA resection by repair mechanisms or collapse of stalled forks result in replication-associated double strand breaks (DSBs). DSB-binding proteins amplify ATR checkpoint response at such DNA structures (Vidal-Eychenie et al., 2013). The DSBs are bound by the KU70/KU80 heterodimer, which then recruits the DNA repair protein DNA-dependent protein kinase catalytic subunit (DNA-PKcs). ATR kinase, initially activated by the small stretch of RPA-ssDNA, phosphorylates DNA-PKcs, which in turn phosphorylates RPA and other proteins downstream of ATR thereby amplifying the ATR signal (Vidal-Eychenie et al., 2013).

In the ATR checkpoint pathway a donut-shaped clamp composed of RAD9, RAD1, and HUS1 (the 9-1-1-complex) is loaded onto dsDNA adjacent to RPA-coated ssDNA by the RAD17-RFC2-5 clamp loader complex (Cimprich and Cortez, 2008; Edward and David, 2011) (Figure 1.2). Independent recruitment of 9-1-1 and ATR-ATRIP complexes to stalled replication forks promotes autophosphorylation of ATR and kinase activation (Liu et al., 2011). ATR phosphorylates RAD9 protein in the 9-1-1-complex (Cimprich and Cortez, 2008), which then recruits TopBP1, another mediator of the checkpoint response. The 9-1-1 interacting nuclear orphan protein (RHINO) promotes the stable association of TopBP1 with 9-1-1-complex (Cecilia

et al., 2011). TopBP1, the homologue of budding yeast DPB11, further stimulates ATR kinase activity and also acts as a platform to bring several other targets of ATR to the vicinity of stalled replication forks (Cimprich and Cortez, 2008; Edward and David, 2011).

Major downstream ATR targets are the checkpoint kinase CHK1, and replisome components like RPA and Claspin (Cimprich and Cortez, 2008) (Figure 1.2). ATR directly phosphorylates CHK1, which then transduces the replication checkpoint signals to downstream effector proteins (Cimprich and Cortez, 2008). Activated CHK1 kinase is subsequently released from the chromatin to target various downstream effector proteins. The human homolog of *C. elegans* sex determination fem1 protein (FEM1B) is thought to be important for the release of active CHK1 from chromatin (Sun and Shieh, 2009). FEM1B directly interacts with CHK1 kinase and with RAD9, a component of the 9-1-1 complex, which could facilitate the recruitment of CHK1 kinase to stalled forks. Upon phosphorylation of CHK1 by upstream proteins like ATR, FEM1B-CHK1 interaction is disrupted suggesting a mechanism by which active CHK1 could be released from chromatin (Sun and Shieh, 2009). The multiple effects of activated DNA replication checkpoint signaling influence both local (replication fork stabilization, DNA repair, dormant origin firing, fork restart) and global processes (cell cycle arrest, inhibition of origin firing, transcriptional regulation) that preserve genome integrity (Figure 2).

## Inhibition of Late Origin Firing

In normal cells, X-ray and UV-induced DNA damage results in inhibition of DNA synthesis mainly by preventing further initiation events and, to a lesser extent, by slowing replication fork elongation (Kaufmann and Cleaver, 1981; Walters and Hildebrand, 1975). This suggested that inhibition of origin firing is an important mechanism for increasing the length of S-

phase upon DNA damage. The mechanism for inhibiting origin firing is well studied in budding yeast. Mutants in *MEC1*, the budding yeast ATR ortholog, and *RAD53* (the CHK2 ortholog) inappropriately activate late replicating origins in response to the alkylating agent MMS or to nucleotide depletion by HU (José Antonio and John, 2001; Santocanale and Diffley, 1998; Shirahige et al., 1998). *mec1* and *rad53* mutants exhibited no effect on early origin firing and also did not disrupt the temporal nature of origin initiation (Wenyi et al., 2006). Replication fork progression in HU treated cells was greatly reduced (caused by decreased dNTP pools) but fork rates were similar in MMS-treated *mec1* and *MEC1* cells (Paulovich and Hartwell, 1995). Late origin firing was inhibited by blocking an early step in initiation, presumably MCM helicase activation (Jaime et al., 2010; Santocanale and Diffley, 1998; Zegerman and Diffley, 2010). As described above, CDK and DDK are the main kinases involved in helicase activation, and in budding yeast the replication checkpoint blocks origin firing by modulating the functional activity of these kinases.

## Cell Cycle Arrest

Another global effect of the replication checkpoint is to arrest the cell cycle. Cell cycle progression requires the ordered activation of multiple CDKs at each stage of cell cycle. Inhibitory kinases WEE1 and MYT1 prevent cell cycle progression by inactivating mitotic CDKs. They phosphorylate two key residues in the ATP binding domain: T14 and Y15. These phosphates are removed by the dual specificity phosphatase CDC25. While yeasts have a single CDC25 phosphatase, mammalian cells have three isoforms: CDC25A, B, and C. All three isoforms have been shown to promote G1-S and G2-M cell cycle progression with CDC25A being more important for G1-S while CDC25B and CDC25C being primarily responsible for G2-M transition

(Christina and Jonathan, 2006). The inactivating kinases and activating phosphatases described above are important downstream targets of the ATR-CHK1 signaling induced by replication stress (Christina and Jonathan, 2006). CHK1 directly phosphorylates CDC25A resulting in its ubiquitin-mediated degradation (Mailand, 2000). CHK1 mediated phosphorylation of CDC25B and CDC25C causes increased binding with 14-3-3 proteins and subsequent sequestration in the cytoplasm (Lindqvist et al., 2004; Peng et al., 1997). In the absence of CDC25 phosphatase activity CDK complexes remain inactive and the cell cycle is arrested. CHK1 can also phosphorylate and activate WEE1 to enhance cell cycle arrest (Raleigh and O'Connell, 2000).

## **Dormant Origin Firing**

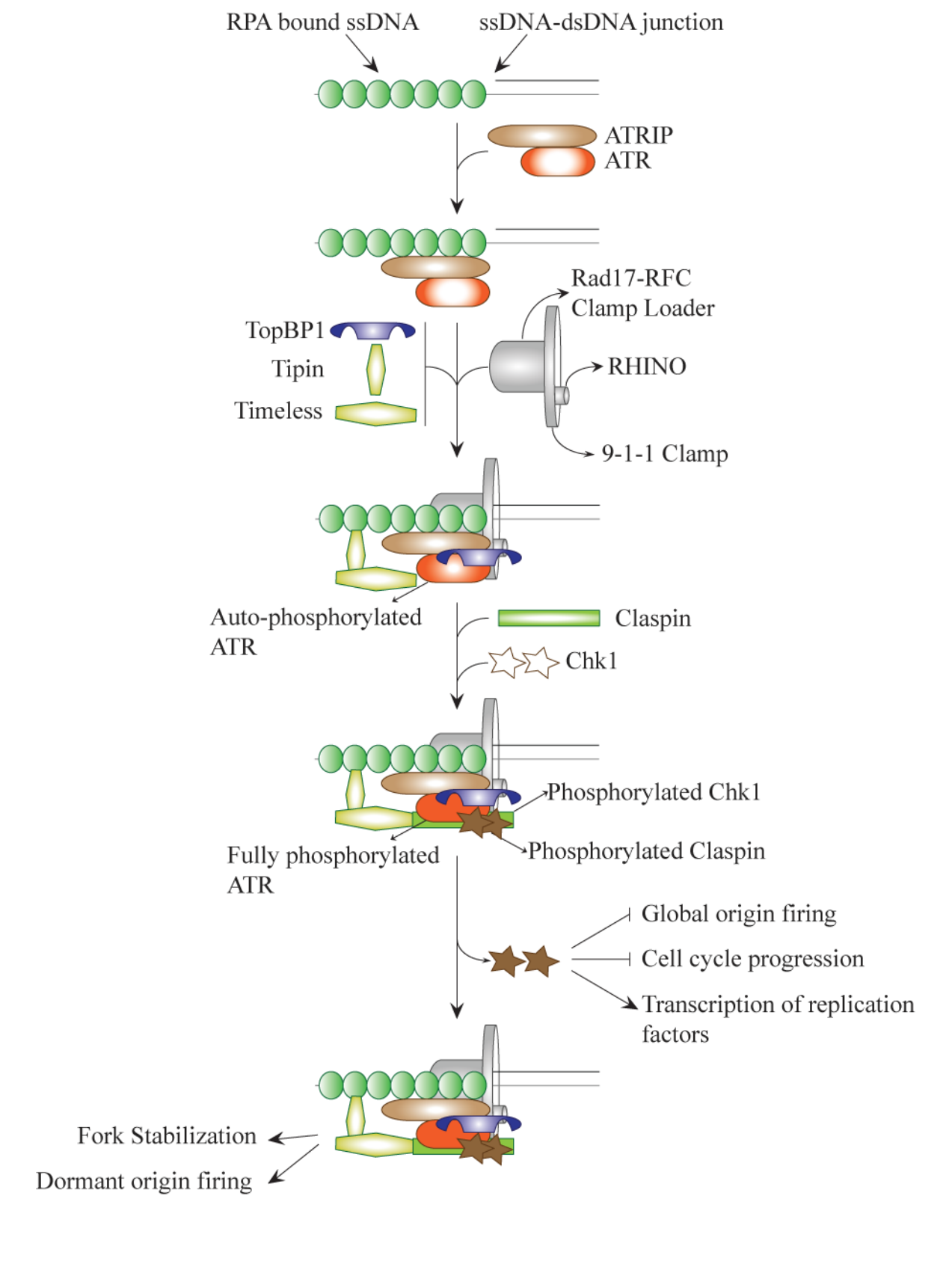
Although checkpoint activation inhibits global initiation events, one way to replicate DNA in the vicinity of a stalled replication fork is through activation of nearby dormant origins. Eukaryotic cells initiate DNA replication from origins spaced from 40 to ~200 kb apart depending on the organism, however more origins are licensed than are actually used (Blow et al., 2011). Current estimates suggest that only ~10% of licensed origins are used in each S phase of metazoan cells (Blow et al., 2011). When replication forks stall these dormant origins are activated to complete replication in the stressed regions of the genome, although the mechanism for this unclear. Several models have been proposed for dormant origin activation following replication stress (Blow et al., 2011; Yekezare et al., 2013) (Figure 1.3).

## Stabilization of Stalled Forks

Stalled forks are prone to aberrant recombination events and collision with active transcriptional and co-transcriptional machineries (Branzei and Foiani, 2010). The tethering of

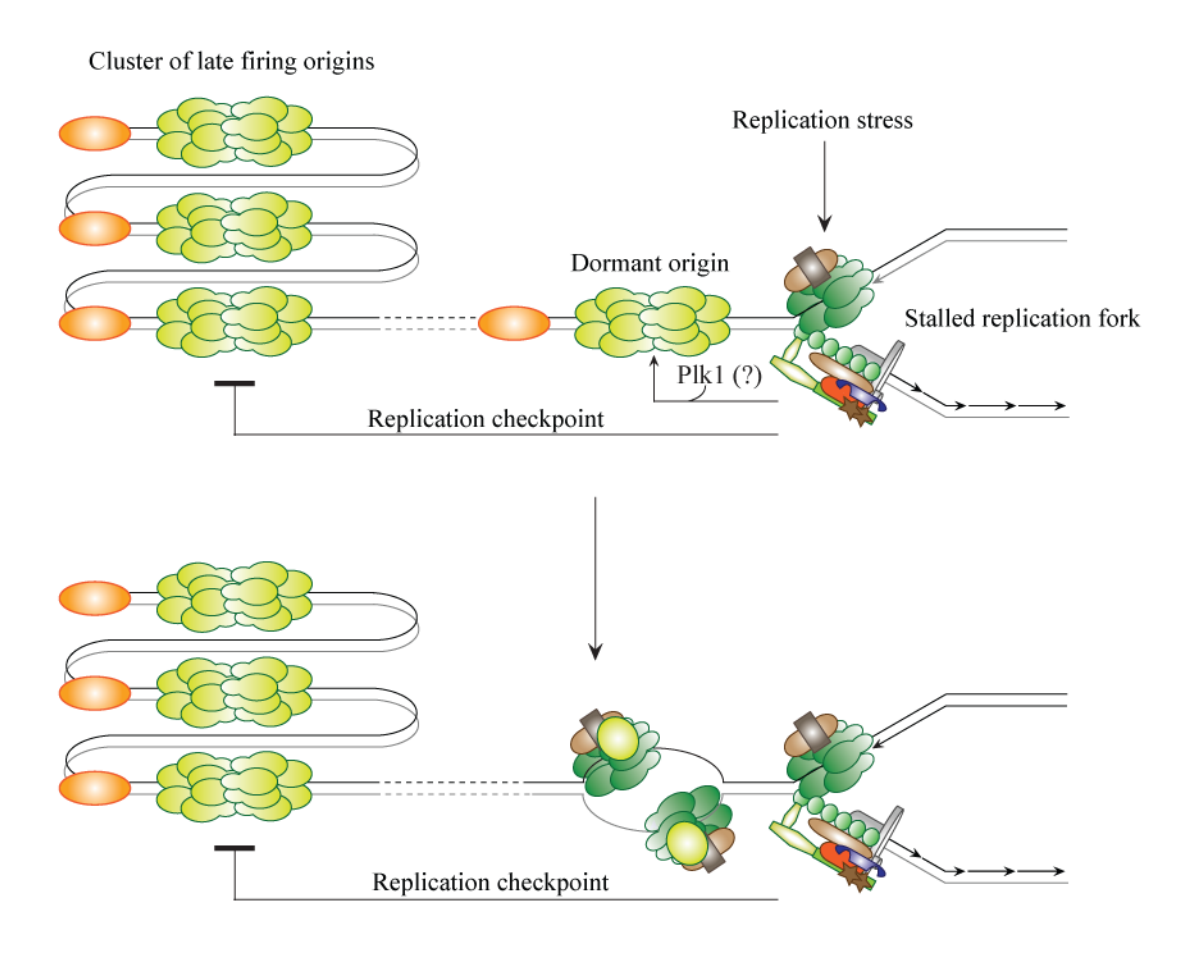
transcriptionally active genes to the nuclear pore complex (NPC) also increases torsional stress in the DNA increasing the chance of nearby fork reversal and collapse (Bermejo et al., 2011). Collapsed forks pose a challenge to DNA replication restart and promote genomic instability. Stabilization of forks and the resumption of DNA replication is especially important when a particular genomic region is devoid of extra origins, such as fragile site loci and telomeres. Hence one of the key roles played by the DNA replication checkpoint is to maintain the integrity of stalled replication forks (Branzei and Foiani, 2010). While homologous recombination is a DNA repair pathway that can be used by cells to repair collapsed or reversed forks (Branzei and Foiani, 2010), aberrant recombination at stalled forks would be deleterious to cells. Some nucleases like EXO1 and MUS81-EME1 initiate deleterious fork cleavage and DNA resection at stalled forks. Their activities, therefore, are inhibited upon phosphorylation by replication checkpoint proteins (Branzei and Foiani, 2010; Hustedt et al., 2012). Helicases like DNA2, which also possess nuclease activity, and SGS1/WRN/BLM, however, are required to maintain fork stability and are recruited to stalled forks upon phosphorylation (Branzei and Foiani, 2010; Hustedt et al., 2012). Other targets of the replication checkpoint include replisome components like DNA polymerases and helicases (Cimprich and Cortez, 2008).

Figure 1.2. Activation and transduction of the replication checkpoint.



**Figure 1.2 (cont'd).** Replication stress generates long stretches of RPA bound ssDNA, which recruits ATR-ATRIP. ATR phosphorylates RPA and also mediates the recruitment of PRP19 ubiquitin ligase. Hyper-phosphorylation and polyubiquitylation of RPA forms a feed-forward loop that recruits multiple ATR-ATRIP complexes. Subsequent interaction with 9-1-1-RHINO complex and TopBP1 promotes auto phosphorylation of ATR kinase. Recruitment of Claspin, aided by Tipin and Timeless proteins, is essential for full activation of ATR kinase. Claspin also stabilizes and activates the downstream effector kinase CHK1, which is released from the chromatin to execute global checkpoint responses while ATR executes the local response. The core pathway is well conserved from yeast to humans with several additional proteins being involved in higher eukaryotes.

Figure 1.3. Replication checkpoint-mediated activation of dormant origins.



**Figure 1.3 (cont'd).** Stalled forks can be rescued by initiating replication from an adjacent dormant origin. The mechanism by which such dormant origins escape global inhibition of origin firing is not known. One possibility is the ATR mediated recruitment of proteins like Plk1 could phosphorylate and activate a nearby inactive replicative helicase and promote dormant origin firing.

## Role of DDK in Replication Checkpoint

DDK, or DBF4-dependent CDC7 kinase, is an essential S-phase kinase that regulates replication initiation. While CDC7 kinase levels remain constant, the levels of its regulatory subunit DBF4 (and/or DRF1 in metazoans) are cell cycle regulated. DRF1 is a DBF4 homologue expressed during embryonic cell cycles in *Xenopus* and perhaps other organisms. DBF4 expression peaks in S phase and remains high through early M phase followed by APC/C mediated degradation (Khalid et al., 2013). Among the many target proteins of DDK are the MCM2-7 helicase subunits. Phosphorylation of the helicase is required for its activation and thereby for initiation of replication. Moreover, DBF4 is among the limiting factors that determine replication timing in budding yeast (Mantiero et al., 2011). Therefore, upon exposure to replication stress DDK activity at origins is blocked to inhibit global origin firing. Studies from multiple organisms support this idea.

In budding yeast, DBF4 is a direct target of RAD53 phosphorylation in response to HU (Duncker et al., 2002; Weinreich and Stillman, 1999b) and the hyper-phosphorylated version of DDK has modestly reduced kinase activity (Weinreich and Stillman, 1999b). RAD53-phosphorylated DBF4 inhibits late origin firing by an unknown mechanism (Zegerman and Diffley, 2010) (Figure 1.4 A). In fission yeast, HU treatment leads to CDS1(RAD53)-dependent hyper-phosphorylation of DFP1(DBF4) (Brown and Kelly, 1999). An early study using *Xenopus* egg extracts also showed that CDC7-DBF4 complex dissociates upon treatment with etoposide, a topoisomerase inhibitor (Costanzo et al., 2002). Studies using human cell lines also supported that DDK is a target of replication checkpoint. In a BCR-ABL tumor cell line, etoposide treatment resulted in dissociation of CDC7-DBF4 complex (Dierov et al., 2004). Multiple cancer cell lines exposed to sub-lethal doses of UV light showed similar phenotypes (Heffernan et al., 2007). CHK1

was shown to interact with DBF4 *in vivo* and phosphorylate it *in vitro*. Increased expression of DBF4 also abrogated the ATR-CHK1 mediated intra-S phase checkpoint induced by UV.

Although these studies indicate that the replication checkpoint targets DDK to inhibit origin firing, several studies point towards a more complex regulation. A non-essential N-terminal region of DBF4 that interacts with CDC5 and RAD53 has been found to be critical for survival in rad53 but not mec1 mutants; MEC1 is upstream of RAD53 (Gabrielse et al., 2006). In Xenopus egg extracts, CDC7-DRF1 complex, the dominant form of DDK, was unaffected by aphidicolin treatment and the overall kinase activity of DDK was also unperturbed (Yanow et al., 2003). Finally, MCM2 was hyper-phosphorylated at CDC7-dependent sites in human cells arrested in S phase with HU (Montagnoli et al., 2006a), and CDC7-DBF4/CDC7-DRF1 complexes were stable upon etoposide and HU treatment (Tenca et al., 2007; Yamada et al., 2013b). The more recent study has shown that chromatin bound CDC7-DBF4 complex is stabilized upon replication stress in an ATR-CHK1 dependent pathway. CHK1 phosphorylates and inhibits CDH1, a component of the APC/C ubiquitin ligase. CHK1 also phosphorylates other components of the APC/C complex. Upon inhibition by CHK1, APC/C is unable to degrade DBF4 thereby resulting in DDK stabilization on chromatin. The stable form of DDK at stalled replication forks recruits trans-lesion synthesis polymerase to replicate through the DNA lesion (Figure 1.4 B). Stabilization of DDK could therefore act as a switch in determining the type of DNA repair pathway that is recruited to the stalled fork. Only in the absence of DDK does cisplatin treatment lead to recruitment of RAD51 (mediates homologous recombination) and mono-ubiquitylated forms of FANCD2 (mediates Fanconi anemia DNA repair pathway) at stalled forks. Therefore, DDK might stabilize stalled forks by preventing aberrant recombination mediated repair and thereby avoid genomic instability (Figure 1.4 B).

DDK's role in checkpoint signaling is complex. Perhaps a soluble fraction of DDK is phosphorylated to block firing of late origins upon replication stress but a chromatin-bound fraction is altered to enable lesion bypass through TLS. Replication checkpoint signaling could also regulate the role of DDK through phosphatases that are specific to DDK targets. Protein phosphatase 1 (PP1) is recruited to chromatin in a checkpoint dependent manner and dephosphorylates sites that are targeted by DDK, which could inhibit origin firing (Poh et al., 2013). PP1 interacts with RIF1, an important determinant of origin firing timing (Satoshi et al., 2013), and RIF1 targets PP1 to DDK-phosphorylated proteins (Hiraga et al., 2014). Through this mechanism DDK function could be regulated by the replication checkpoint without the direct inhibition of DDK kinase activity (Figure 1.4 B).

Figure 1.4. Replication checkpoint-mediated inhibition of late origins.

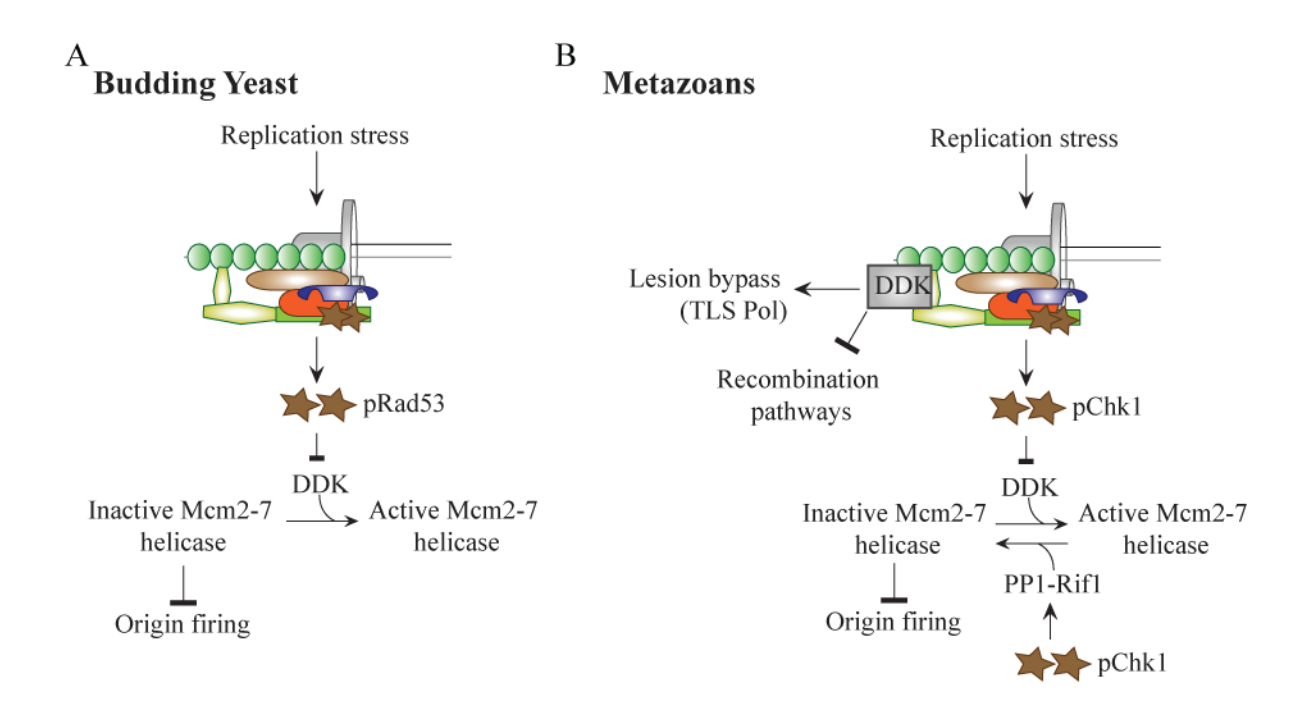


**Figure 1.4 (cont'd).** The replication checkpoint inhibits late origin firing primarily by targeting two key kinases CDK and DDK. Shown here are details of DDK inhibition by the checkpoint proteins. The differences in the mechanism of action between budding yeast and metazoans have been highlighted.

# Rationale for this study

DDK is over expressed in a number of primary tumors and tumor cell lines (Bonte et al., 2008; Chen et al., 2013a; Cheng et al., 2013; Hou et al., 2012a, b; Malumbres, 2011; Menichincheri et al., 2010). DDK over expression is prognostic of poor survival in lung adenocarcinoma (Chapter 3), breast cancers (Choschzick et al., 2010), advanced clinical stage in ovarian carcinoma (Kulkarni et al., 2009), and with aggressive phenotype in papillary thyroid carcinomas (Fluge et al., 2006). Within the last decade, DDK has emerged as a possible chemotherapeutic target. Depleting CDC7 kinase or inhibiting DDK activity induces apoptosis in tumor cells, while normal cells undergo a reversible cell cycle arrest (Montagnoli et al., 2004; Montagnoli et al., 2008; Tudzarova et al., 2010).

The mode of cell death induced in tumor cells upon DDK inhibition is independent of the canonical S-phase checkpoint kinases like CHK1 and CHK2 (Montagnoli et al., 2004; Montagnoli et al., 2008; Sasi et al., 2016). Despite the finding that DDK is required to activate CHK1 kinase, which is downstream of ATR (Figure 1.4 B), CDC7 depletion in HeLa cells was reported to activate a p38-MAPK-dependent apoptotic pathway, which is also downstream of ATR (Im and Lee, 2008). While tumor cells underwent apoptosis irrespective of their p53 status and p53 was not induced upon CDC7 knockdown in p53-positive tumor cells (Montagnoli et al., 2004), it has been suggested that p53 status could determine the timing and mode of cell death induced upon DDK inhibition (Ito et al., 2012). Moreover, DDK inhibition does not cause replication fork stalling but rather a slight increase in speed was observed at established forks (Montagnoli et al., 2008). Hence a detailed cellular response to DDK inhibition in tumor cells is still unclear.

In **Chapter 2** I provide direct evidence that ATR kinase is activated upon DDK inhibition and that ATR is required for apoptosis. I also show that DDK has a novel role to promote resection

of stalled replication forks, which helps explain the lack of full checkpoint activation when cells are depleted of DDK. Lastly, cells that are depleted of DDK progress through mitosis with anaphase bridges and other aberrant structures similar to low-dose aphidicolin-treated cells, indicative of problems in completing DNA replication. Based on these findings I propose a model for DNA damage and cell death induced upon DDK inhibition in tumor cells.

In **Chapter 3** I investigate how tumors induce and benefit from high levels of DDK. I show a strong correlation between DDK expression and tumor mutation load suggesting a role for DDK in driving tumor mutagenesis. I also show that chemoresistance genes are positively correlated with DDK expression, which could partly explain the poor clinical survival of patients with DDK-high expressing tumors. Furthermore, using a functional RNAi screen I investigate how DDK inhibition induces cell death and report a number of kinases and phosphatases that mediate tumor cell death in diverse tumor cell lines when DDK is inhibited.

Finally, in **Chapter 4** I describe extensive biochemical and cellular characterization of two DDK inhibitors. Although both compounds are comparable biochemical inhibitors, PHA-767491 exhibited superior activity to XL413 in multiple cell lines. To aid in the development of additional DDK inhibitors, we tested whether known protein kinase inhibitors (i.e., those not designed to inhibit DDK) exhibited cross-reaction with DDK. Using a thermal stability shift assay (TSA) we identified 12 molecules that shifted the thermal stability of DDK, several with nearly equivalent potency as PHA-767491. These 12 small molecule inhibitors are therefore unlikely to be highly specific for a single target. Our results highlight the opportunity to design additional specific, biologically active DDK inhibitors for use as chemotherapeutic agents.

## **CHAPTER 2.**

# DDK HAS A PRIMARY ROLE IN PROCESSING STALLED REPLICATION FORKS TO INITIATE DOWNSTREAM CHECKPOINT SIGNALING

## Modified from

Sasi, N., Coquel, F., Lin, Y., MacKeigan, J., Pasero, P., and Weinreich, M. (2016). DDK has a primary role in processing stalled replication forks to initiate downstream checkpoint signaling. *Under Review*.

#### **ABSTRACT**

CDC7-DBF4 kinase (DDK) is required to initiate DNA replication. When DDK is inhibited, tumor cells often progress through an abortive S-phase and induce apoptosis through an unknown mechanism. We report that DDK promotes limited resection and processing of newly synthesized strands behind stalled forks, which is essential to initiate replication-checkpoint signaling and for efficient fork restart. Following DDK inhibition, ATR is partially activated and is required for apoptosis. Low level DDK inhibition causes tumor cells to enter mitosis with a high level of aberrant mitotic structures. However, preventing S-phase progression protects cells from apoptosis. Based on these findings we propose that in the absence of DDK, defective processing of stalled or damaged replication forks results in incomplete DNA replication. This, coupled with the absence of normal checkpoint signaling and a robust G2/M arrest, causes a mitotic catastrophe and cell death.

#### INTRODUCTION

DBF4-dependent kinase (DDK) is essential to initiate DNA replication at individual replication origins by phosphorylating and activating the MCM2-7 replicative helicase, which is loaded in an inactive form at all origins in G1 (Sasi and Weinreich, 2016). DBF4 binds to CDC7 and is required for its kinase activity. DBF4 abundance, and therefore DDK activity, is cell cycle regulated, peaking in S phase but absent during late mitosis and early G1 (Sasi and Weinreich, 2016). DDK is overexpressed in a number of primary tumors and in the majority of cancer cell lines tested (Bonte et al., 2008; Chen et al., 2013a; Cheng et al., 2013; Hou et al., 2012b), although it is not understood how tumor cells benefit from high levels of DDK activity. Consistent with an important role for DDK in tumor phenotype, depletion of DDK subunits or inhibition of DDK activity leads to apoptosis in multiple cancer cell lines whereas normal fibroblast cells undergo a reversible p53-dependent cell cycle arrest (Montagnoli et al., 2004; Montagnoli et al., 2008; Tudzarova et al., 2010). In normal fibroblasts depleted of CDC7, the FOXO3a transcription factor upregulates the CDK inhibitor p15<sup>INK4B</sup> and also activates a p14<sup>ARF</sup>-p53-p21signaling axis. p21 directly inhibits CDK activity while p53 also activates DKK3, an inhibitor of MYC and Cyclin D1 expression, further halting cell cycle progression (Tudzarova et al., 2010). Since these pathways are non-redundant, inactivating any one axis, as occurs commonly in tumor cells, is sufficient to abrogate the cell cycle arrest induced upon DDK inhibition (Tudzarova et al., 2010). Inhibiting DDK activity could therefore be an excellent strategy to specifically kill tumor cells while reducing the lethal side effects on normal cells (Montagnoli et al., 2010).

The essential role of DDK is to activate the replicative MCM helicase. Budding yeast with *CDC7* or *DBF4* deletions are not viable, but this lethality (although not the normal growth rate or

response to fork stalling) can be rescued by a mutation in one of the helicase subunits (Hardy et al., 1997; Weinreich and Stillman, 1999a). Since DDK is required to initiate DNA replication at each origin, DDK inhibition would likely cause replication stress since far fewer origins would be activated during S-phase. However, the exact nature of this replication stress is unknown. One intriguing feature of the cellular response to DDK inhibition is the absence of canonical markers of checkpoint activation like phosphorylated CHK1, CHK2, or stabilized p53 (Montagnoli et al., 2004; Montagnoli et al., 2008). In budding yeast, DDK is a target of the Rad53 kinase (human CHK2) that is activated following replication stress (Duncker et al., 2002; Weinreich and Stillman, 1999a). Rad53-mediated phosphorylation of DBF4 modestly reduces DDK activity (Weinreich and Stillman, 1999a) and also inhibits late origin firing (Zegerman and Diffley, 2010). In addition, specific mutations in DBF4 are lethal in combination with RAD53 mutations, suggesting some overlap of checkpoint function between DDK and Rad53 (Chen et al., 2013b). While similar checkpoint inhibition of DDK activity in human cells has been reported (Dierov et al., 2004; Heffernan et al., 2007), recent studies have shown that human DDK is active during replication stress and has an upstream role to fully activate the checkpoint kinase CHK1. In response to exogenous replication inhibitors, there is increased recruitment of DDK to chromatin (Tenca et al., 2007; Yamada et al., 2013b), more stable complex formation between CDC7-DBF4 (Tenca et al., 2007), and increased phosphorylation of MCM helicase at DDK-specific phosphorylation sites (Montagnoli et al., 2006b; Tenca et al., 2007). DDK is also required for full activation of CHK1 kinase downstream of ATR (Kim et al., 2008; Rainey et al., 2013). This role of DDK is at least in part mediated through a DDK interaction with and phosphorylation of Claspin, which stabilizes Claspin-CHK1 interaction and thereby contributes to full CHK1 activation (Kim et al., 2008; Rainey et al., 2013). DDK has also been shown to have a role in promoting trans-lesion synthesis

across bulky DNA damage induced by UV and cisplatin (Brandao et al., 2014; Yamada et al., 2013b). DDK phosphorylates RAD18 ubiquitin ligase; this modification is essential for RAD18-POLη interaction (trans-lesion polymerase) and for efficient recruitment and distribution of POLη at stalled replication forks (Day et al., 2010).

Despite the finding that DDK is required to activate CHK1 downstream of ATR, CDC7 depletion in HeLa cells was reported to activate a p38-MAPK-dependent apoptotic pathway. which is also downstream of ATR (Im and Lee, 2008). While tumor cells underwent apoptosis irrespective of their p53 status and p53 was not induced upon CDC7 knockdown in p53-positive tumor cells (Montagnoli et al., 2004), it has been suggested that p53 status could determine the timing and mode of cell death induced upon DDK inhibition (Ito et al., 2012). Moreover, DDK inhibition does not cause replication fork stalling but rather a slight increase in speed was observed at established forks (Montagnoli et al., 2008). Hence a detailed cellular response to DDK inhibition in tumor cells is still unclear. In this study we provide direct evidence that ATR kinase is activated upon DDK inhibition and that ATR is required for apoptosis. We also show that DDK has a novel role to promote resection of stalled replication forks, which helps explain the lack of full checkpoint activation when cells are depleted of DDK. Lastly, cells that are depleted of DDK progress through mitosis with anaphase bridges and other aberrant structures similar to low-dose aphidicolin-treated cells, indicative of problems in completing DNA replication. Based on these findings we propose a model for DNA damage and cell death induced upon DDK inhibition in tumor cells.

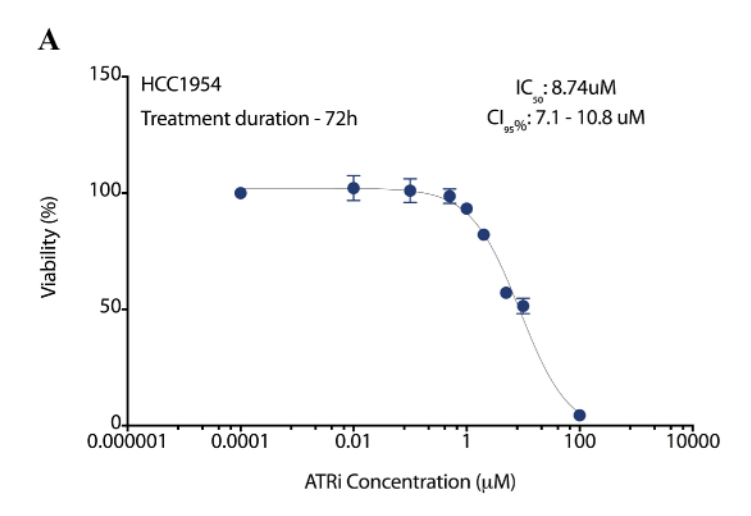
#### **RESULTS**

#### ATR kinase mediates cell death upon inhibition of DDK

We first tested if apoptosis induced upon inhibition of DDK activity in HCC1954 breast cancer cells is dependent on ATR kinase. A potent and selective inhibitor of ATR kinase, VE-821 (ATRi) (Reaper et al., 2011), does not induce significant cell death in HCC1954 cells and has an IC<sub>50</sub> of 8.7μM 72 hours after treatment (**Figure 2.1 A**). DDK was inhibited using the prototype inhibitor PHA-767491 (DDKi) (Montagnoli et al., 2008). 2μM of DDKi induces very robust apoptosis in HCC1954 cells within 8 to 12 hours (Figure 2.1 B). When the cells were co-treated with DDKi and increasing doses of ATRi we saw a reduction in cell death, most significantly 8 and 12 hours after treatment (Figure 2.1 B). Since PHA-767491 also inhibits CDK9 to some extent (Hughes et al., 2012), we confirmed this result using a structurally distinct and more specific inhibitor of DDK, XL413 (Koltun et al., 2012). Although XL413 has poor bioavailability in most cell lines tested, it inhibited DDK and cell proliferation, and induced apoptosis in the colorectal cell line Colo-205 (Sasi et al., 2014). XL413 induces significant Caspase 3/7 activity in Colo-205 cells 24 hours after treatment (Figure 2.1 F). Induction of caspase activity by XL413 or PHA-767491 in Colo-205 cells was inhibited upon co-treatment with increasing doses of ATRi (Figure 2.1 E, F). A reduction in PARP cleavage 12 hours after ATRi+DDKi treatment when compared to DDKi alone confirmed the rescue of apoptotic cell death in HCC1954 cells (Figure 2.2 B). The involvement of ATR kinase was also confirmed using an siRNA against ATR kinase. ATR knockdown partially rescues cell death induced by DDKi, as seen by reduction in PARP cleavage and Caspase 3/7 activity (Figure 2.1 C, D). Similar to ATR, ATM and DNA-PKcs are PI-3-like kinases that play an important role in initiating a DNA-damage response under certain conditions

(Sirbu and Cortez, 2013). However, inhibiting ATM or DNA-PKcs had no effect on cell death induced by DDKi (Figure 2.1 G, H). It has been shown that inhibition of ATR kinase induces aberrant origin firing leading to increased accumulation of chromatin-bound RPA1 and RPA2 (Buisson et al., 2015) (Figure 2.1 I, lane 3 vs 15). Co-treatment with ATRi and DDKi prevented accumulation of RPA1 and RPA2 indicating that increased origin firing seen upon ATR inhibition also requires DDK activity (Figure 2.1 I, lane 15 vs 18) (Buisson et al., 2015). Therefore, ATRimediated rescue of origin firing cannot explain the rescue of cell death induced by DDK inhibition. These results confirm that ATR kinase is activated and mediates apoptosis induced upon DDK inhibition.

Figure 2.1. Non-canonical role of ATR kinase in mediating apoptosis upon DDK inhibition.



В Caspase 3/7 activity per cell 15<sub>1</sub> HCC1954 Vehicle Control DDKi - PHA767491 ATRi 10μM ■ DDKi 2µM 10 DDKi  $2\mu M + ATRi \ 1\mu M$ DDKi  $2\mu M + ATRi 5\mu M$ DDKi 2μM + ATRi 10μM 5 24hrs 4hrs 8hrs 12hrs Time after drug addition

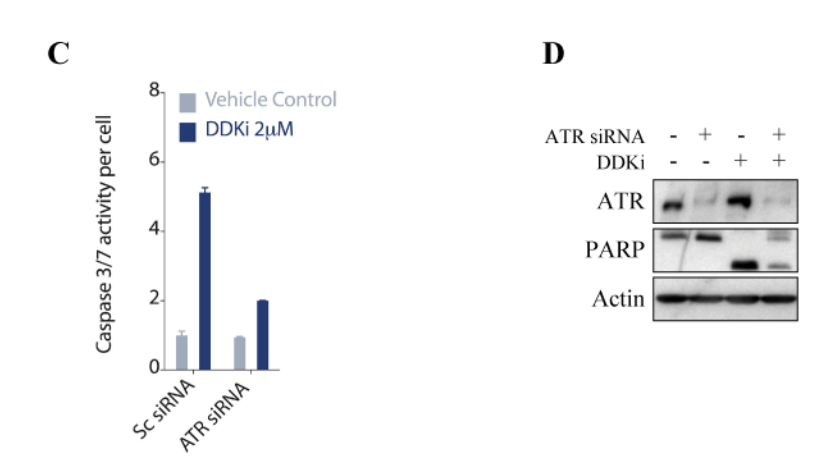
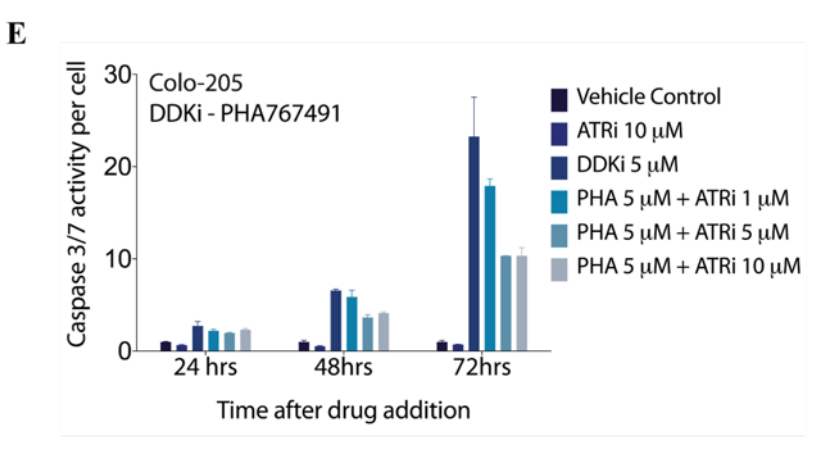
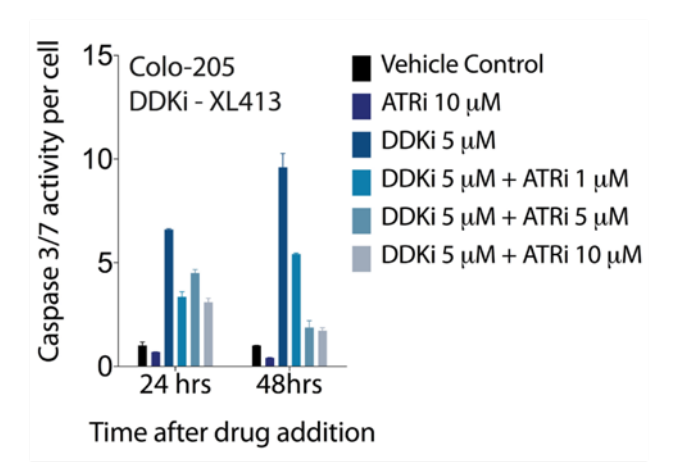


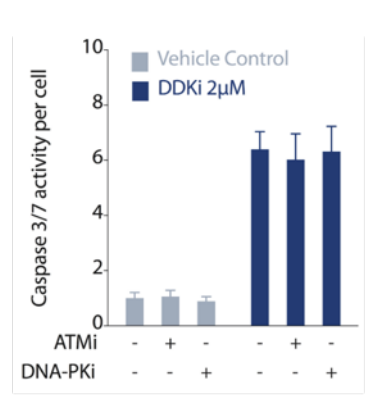
Figure 2.1 (cont'd)

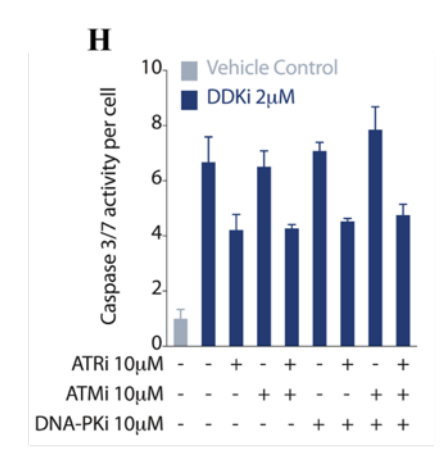


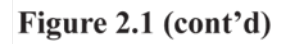
F



G







I

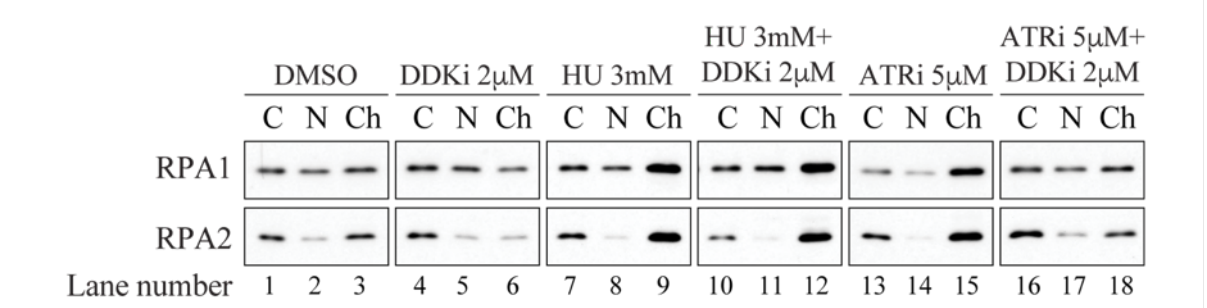


Figure 2.1 (cont'd). (A) HCC1954 cells were treated with DMSO or increasing doses of ATRi [VE-821] and cell viability was measured using CellTiter-Glo assay 72h after treatment. IC<sub>50</sub> value was calculated using Graph Pad. Viability was calculated as a percentage of DMSO-treated cells. (B) HCC1954 cells were treated with DMSO or DDKi with or without increasing doses of ATRi and apoptosis measured using Caspase-Glo assay at indicated time points. (C, D). HCC1954 cells were transfected with scrambled siRNA or ATR siRNA and 48 hours later treated with DDKi for 8 h. Apoptosis was measured using Caspase-Glo assay (C) and the remaining cells harvested for western blot (D). (E, F) Colo-205 cells were treated with DMSO or DDKi (PHA-767491, E; XL413, F) with or without increasing doses of ATRi and apoptosis measured using Caspase-Glo assay at indicated time points. (G, H) HCC1954 cells were treated with indicated drugs and apoptosis was measured 8h later using Caspase-Glo assay. (I) HCC1954 cells were treated with indicated drugs for 2h and were subsequently harvested and subjected to cell fractionation and western blot. C - Cytoplasmic fraction, N - Nuclear soluble fraction, Ch - Chromatin fraction.

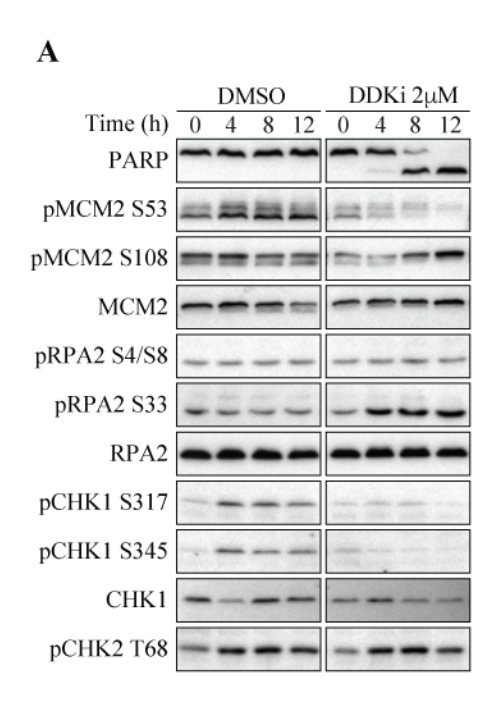
#### Canonical replication-checkpoint pathway is not activated upon DDK inhibition

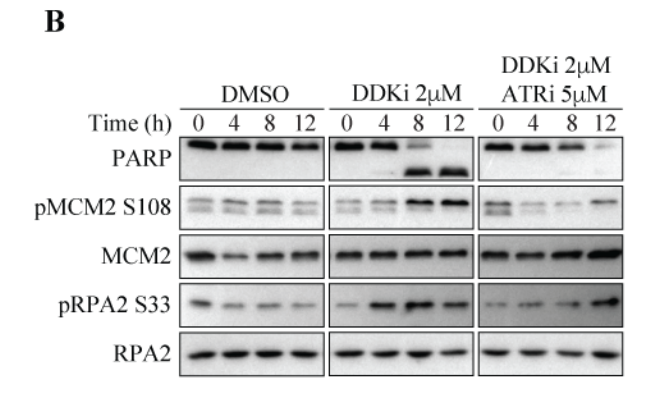
We next examined canonical markers of ATR activation in DDKi-treated cells, ATR kinase is activated during S-phase in response to a variety of DNA damaging agents and in response to stalled replication forks (Sasi and Weinreich, 2016). RPA-bound ssDNA at stalled replication forks serves as a scaffold for the recruitment and activation of ATR. Active ATR subsequently phosphorylates many downstream proteins such as RPA2 and CHK1. Phosphorylated CHK1-S317, -S345 and RPA2-S33 (and to a lesser degree RPA2-S4/S8) are markers of ATR activation (Sasi and Weinreich, 2016). CHK1 was not phosphorylated at S317 and S345 upon DDK inhibition alone (Figure 2.2 A). Lack of CHK1 activation could be due to a direct loss of DDK, since DDK is important for proper activation of CHK1 under conditions of replication stress (Kim et al., 2008; Rainey et al., 2013), or due to some upstream defect in checkpoint activation. We therefore looked at changes in chromatin accumulation of RPA and RPA2 phosphorylation following DDK inhibition as two early events in replication checkpoint signaling, i.e., events that occur before CHK1 activation. Chromatin accumulation of both RPA1 and RPA2 were unaffected by DDK inhibition (Figure 2.2 C). RPA2 was phosphorylated at S33 but not S4/S8 upon treatment with DDKi (Figure 2.2 A). Phosphorylated RPA2-S33 bands correspond to mild phosphorylation and not hyper-phosphorylation patterns observed upon treatment with replication inhibitors (Vassin et al., 2009). We also looked at another upstream marker of ATR activation, MCM2 phosphorylation. MCM2-S108 is a known target site for ATR kinase (Cortez et al., 2004). Interestingly, MCM2-S108 is also a predicted phosphorylation site for DDK (Montagnoli et al., 2006b). Treatment with DDKi decreased phosphorylation at MCM2-S53, a DDK-specific site. However, phosphorylation at MCM2 S108 was *increased* by 8 and 12 hours after treatment with DDKi (Figure 2.2 A, B). To confirm that phosphorylation at RPA2-S33 and MCM2-S108 was

specific to ATR kinase, we treated cells with both DDKi and ATRi. ATR inhibition eliminated phosphorylation at these sites indicating an ATR-specific effect (Figure 2.2 B). Phosphorylation at these sites increased somewhat by 12 hours of ATRi treatment, possibly due to activation of other kinases like ATM and DNA-PKcs or inhibitor turnover. We also looked at CHK2 phosphorylation, a marker for ATM activation in response to double stranded breaks. CHK2-T68 phosphorylation remained at low background levels upon DDKi treatment, further arguing against a role for ATM downstream of DDK inhibition (Figure 2.2 A).

Cells from conditional CDC7-knockout mice showed an increase in RAD51 accumulation on chromatin (Kim et al., 2002). A slight increase in RAD51 accumulation was also seen upon DBF4 knockdown in mammalian cells (Yamada et al., 2013a). We therefore examined RAD51 accumulation at early time points after acute DDK inhibition. We saw no accumulation of RAD51 up to 6 hours after DDK inhibition (Figure 2.2 C), and if anything, we find a slight reduction in chromatin-bound RAD51. RAD51 accumulation at stalled replication forks is not observed by immunofluorescence in the first 2 hours after fork stalling (Petermann et al., 2010). We cannot rule out the possibility that RAD51 accumulates on chromatin at much later time points when DDK is inhibited, however it is not an early event. Together, our data suggests that DDK inhibition does not result in widespread ssDNA formation nor the activation of normal replication-checkpoint signaling.

Figure 2.2. Canonical replication-checkpoint pathway is not activated upon DDK inhibition.





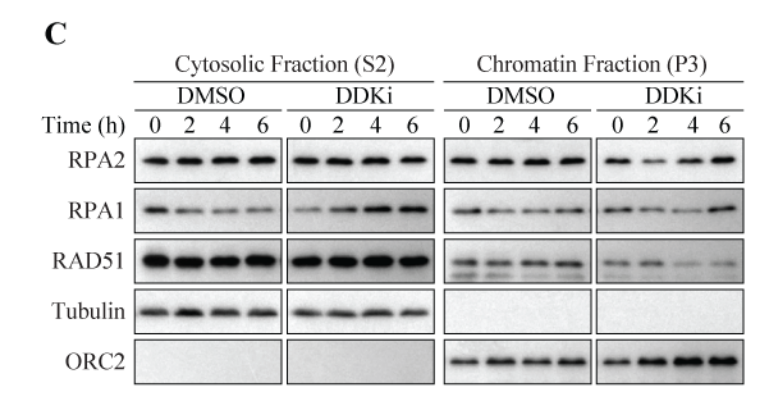


**Figure 2.2 (cont'd).** (**A, B, C**) HCC1954 cells were treated with DMSO/DDKi (**A, C**) or DMSO/DDKi/DDKi+ATRi (**B**) and harvested for western blot at indicated time points. Samples for (**C**) were subjected to cell fractionation.

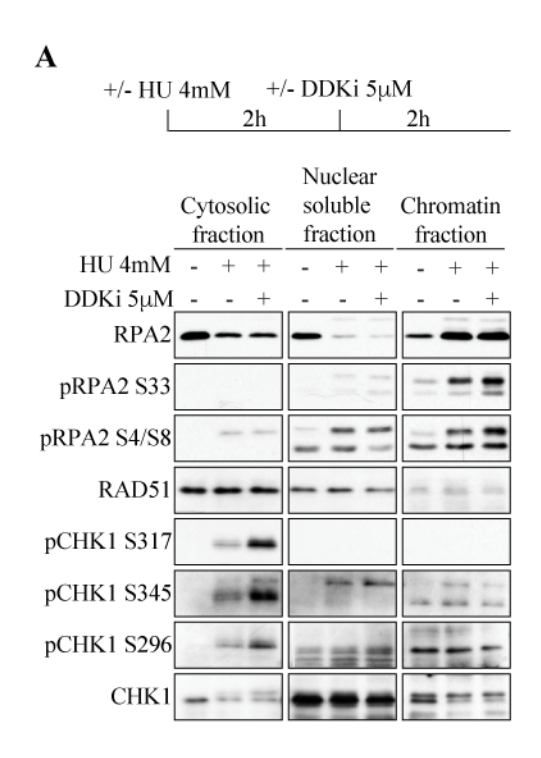
# An established replication-checkpoint response prevents cell death induced by DDK inhibition

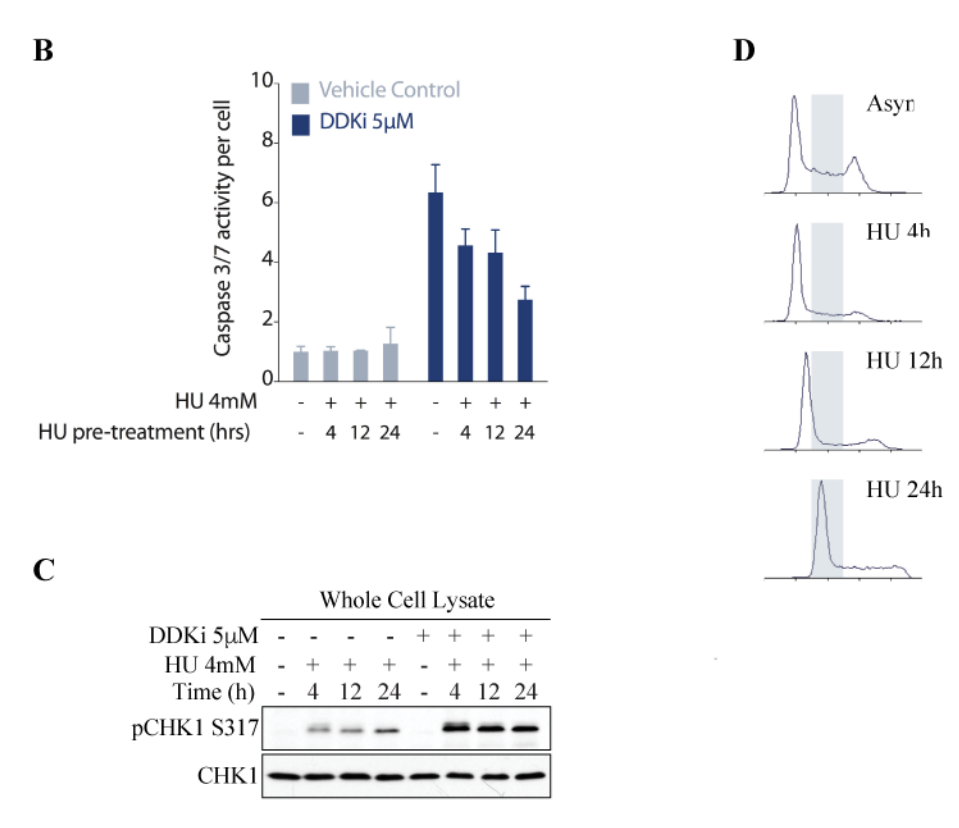
Our results suggest that DDK inhibition does not enhance ssDNA formation. Our interpretation of these results, however, is complicated by two factors: (1) DDK inhibition does not stall replication forks (Montagnoli et al., 2008) and, (2) in the absence of DDK fewer replication forks would exist as DDK is essential for initiation of DNA replication. Both RPA and RAD51 are required for unperturbed DNA replication fork progression. So, in the absence of fork stalling and new origin firing following DDKi, the dynamics of ongoing replication forks might mask the accumulation of these proteins on chromatin. If DDK inhibition alters ssDNA formation, using exogenous replication inhibitors to stall replication forks prior to DDKi treatment should allow us to detect ssDNA binding proteins on chromatin. We therefore pretreated cells with HU for 2 hours to stall replication forks and then added DDKi or vehicle control for another 2 hours. We saw no increase in RPA2 accumulation on chromatin following DDKi indicating that ssDNA generation was not increased (Figure 2.3 A). While ATRi-mediated increase in RPA accumulation was prevented upon co-treatment with DDKi (Figure 2.1 I, lane 15 vs 18), HU-mediated RPA1 and RPA2 accumulation on chromatin was unaffected by co-treatment with DDKi (Figure 2.1 I, lane 9 vs 12). These results also suggest that DDKi-mediated reduction in origin firing, and therefore reduced number of replication forks, does not significantly affect the extent of checkpoint activation and ssDNA at stalled forks.

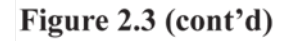
Since an increase in checkpoint activation (i.e. phosphorylated RPA2, CHK1) was seen upon DDK inhibition *after* HU exposure (**Figure 2.3 A**), we wondered if HU would protect cells against cell death induced by DDKi. To test this, we pretreated HCC1954 cells for increasing periods of time with 4mM HU and then treated them with 5μM DDKi for 12 hours followed by measurement of apoptosis. HU pretreatment rescued cell death and was positively correlated with

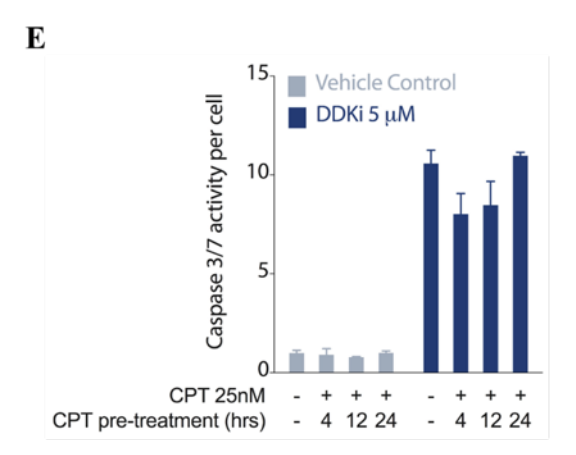
2.3 B). Phospho-CHK1 levels were induced by HU regardless of DDK inhibition (Figure 2.3 C). Cell cycle analysis showed a very robust arrest of cells in G1/S and within S upon exposure to HU (Figure 2.3 D). To test if active CHK1 is sufficient to rescue cell death that follows DDK inhibition, we pretreated cells with a sub-lethal dose of camptothecin (CPT). 25nM CPT induced CHK1 activation (Figure 2.3 F) and caused accumulation of cells in G2/M instead of G1/S (Figure 2.3 G) but this treatment did not rescue cell death induced by DDK inhibition (Figure 2.3 E). We also directly tested the role of CHK1 in preventing cell death upon HU pre-treatment. Inhibition of CHK1 using a specific CHK1 inhibitor (LY2603618) (Wang et al., 2014) did not abrogate the rescue seen upon HU pre-treatment (Figure 2.3 H). CHK1 inhibition was confirmed by examining S296 phosphorylation, an auto-phosphorylation site on active CHK1 (Figure 2.3 I). These results show that preventing S-phase or fork progression protects cells against apoptosis upon DDK inhibition, but active CHK1 is neither necessary nor sufficient for this protection.

Figure 2.3. An established checkpoint response prevents cell death induced by DDK inhibition.

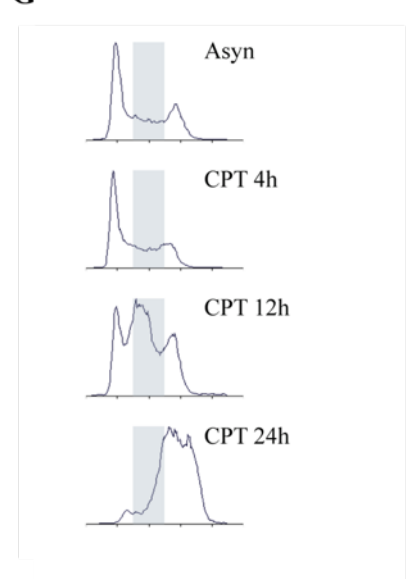




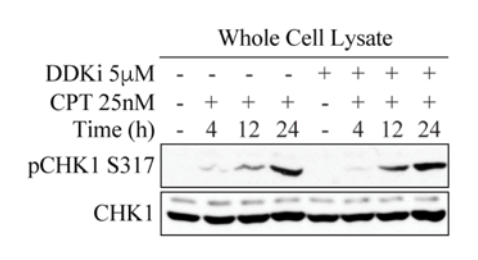




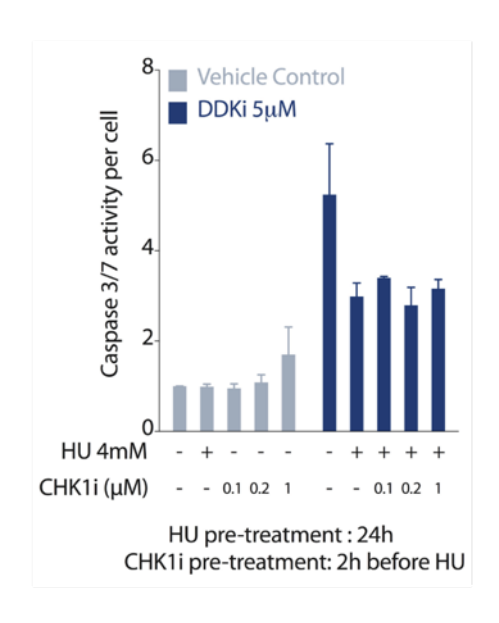




F



H



I

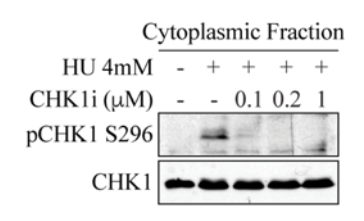


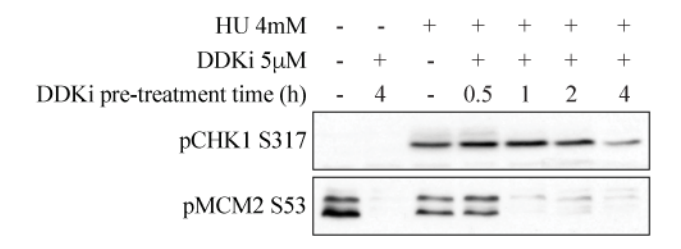
Figure 2.3 (cont'd). (A) HCC1954 cells were pre-treated with or without 4mM HU for 2h followed by incubation with or without 5μM DDKi for 2h, cells were subsequently harvested and subjected to cell fractionation and western blot. (B, C, D) HCC1954 cells were pre-treated with or without HU for the indicated time, followed by incubation with or without DDKi for 12h (B) or 2h (C) followed by Caspase-Glo assay (B) or western blot (C) or flow cytometry (D). (E, F, G) Similar to (B, C, D) except that CPT was used instead of HU. (H, I) HCC1954 cells were pre-treated with or without CHK1i for 2h, then treated with or without HU for 24h followed by exposure to DDKi for an additional 12h (H) or 2h (I) followed by Caspase-Glo assay (H) or western blot (I). For (I) cytoplasmic fraction was used for better visualization of phospho-serine 296 on CHK1.

#### DDK has a primary role in initiating replication checkpoint signaling

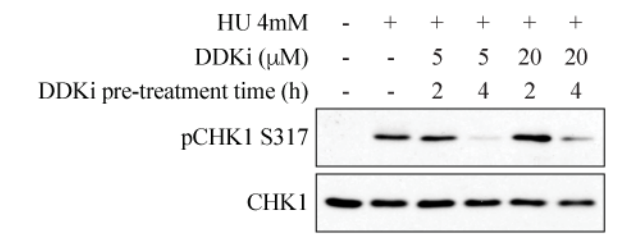
DDK is required to activate CHK1 following replication stress since blocking DDK activity prevents CHK1 phosphorylation upon exposure to HU (Kim et al., 2008; Rainey et al., 2013). We therefore analyzed how DDK influences HU-induced CHK1 phosphorylation in the HCC1954 breast cancer line. We found that 5 µM of DDKi and a pre-treatment time of 4 hours was required to substantially block CHK1 activation by HU in HCC1954 cells (Figure 2.4 A, B). We then looked at various checkpoint markers and also RPA accumulation after HU exposure. As shown previously, CHK1 activation was almost completely eliminated by pre-treatment with DDKi, confirming a role for DDK in activating this checkpoint kinase (Figure 2.4 C). Unexpectedly, we found that RPA2 phosphorylation and chromatin accumulation were also greatly reduced if DDK activity was blocked (Figure 2.4 C). RPA2-S4/S8 phosphorylation showed the strongest reduction. RPA2-S33 phosphorylation was difficult to analyze because the DDKi induces phosphorylation at this site even in the absence of an exogenous replication inhibitor. We saw an identical response when DDK activity was blocked using an siRNA against CDC7 (Figure 2.4 D). We also examined RPA binding and phosphorylation following exposure to topoisomerase inhibitors CPT and etoposide in DDKi-treated cells. DDK inhibition prevented CHK1 phosphorylation, RPA2 accumulation and phosphorylation in response to both CPT and etoposide (Figure 2.5 A, B). These results suggest that DDK promotes formation of ssDNA-RPA complexes upon exposure to various forms of replication stress or DNA damage.

Figure 2.4. DDK is essential for initiating the replication checkpoint pathway.

A



В



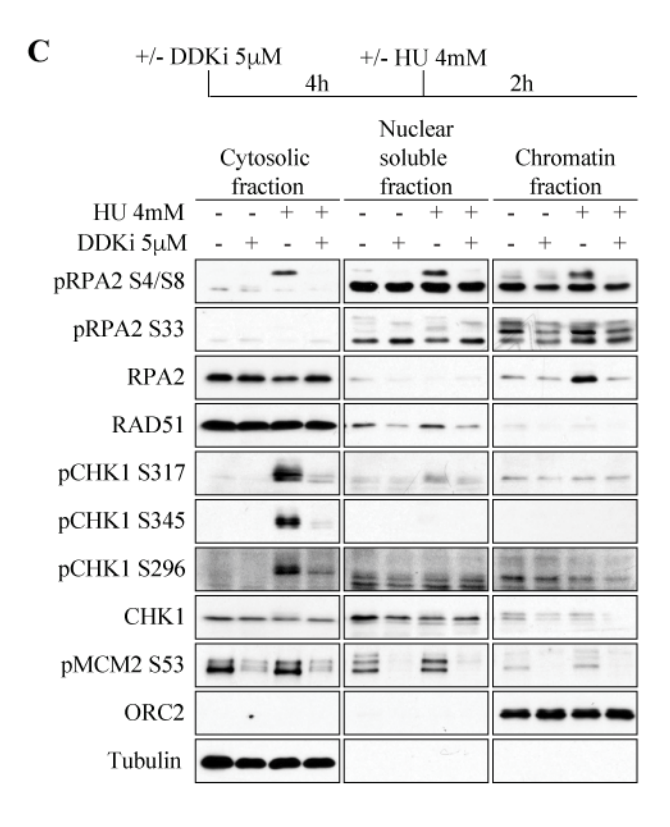
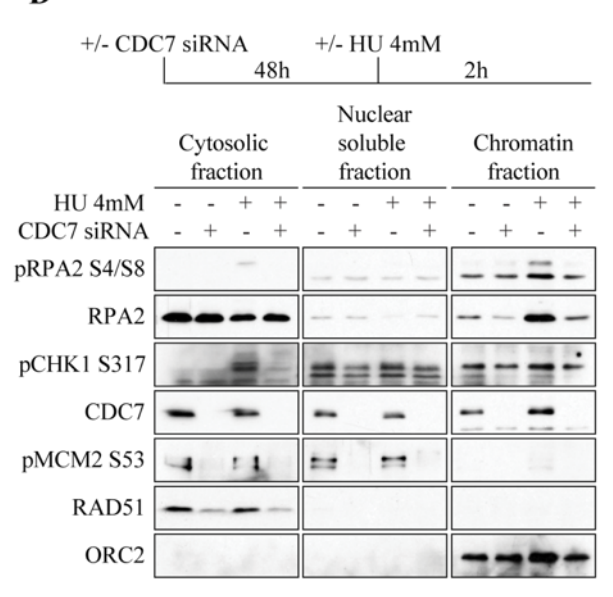


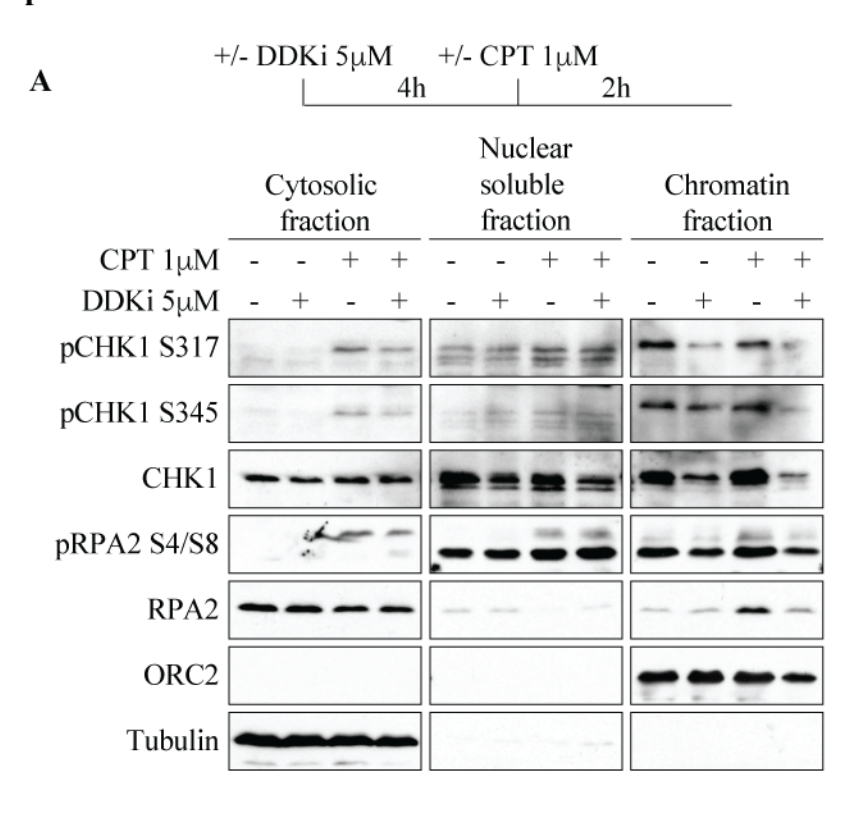
Figure 2.4 (cont'd)





**Figure 2.4 (cont'd). (A, B)** HCC1954 cells were pre-treated with DMSO or DDKi for indicated time followed by incubation with or without HU for 2h. **(C)** HCC1954 cells were pre-treated with DMSO or DDKi for 4h followed by incubation with or without HU for 2h. **(D)** HCC1954 cells were transfected with scrambled siRNA or CDC7 siRNA and 48 hours later treated with or without HU for 2h. All samples were harvested and subjected to cell fractionation.

Figure 2.5. DDK is essential for initiating the replication checkpoint pathway in response to multiple replication inhibitors.



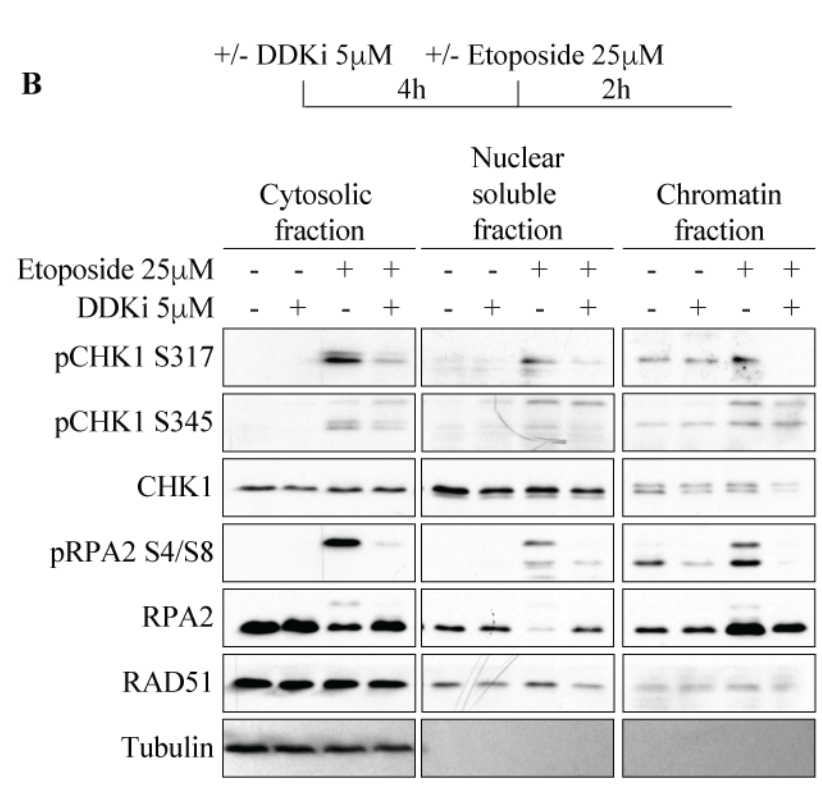


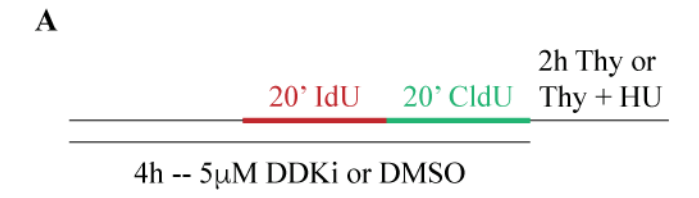
**Figure 2.5 (cont'd). (A, B)** HCC1954 cells were pre-treated with DMSO or DDKi for 4h followed by incubation with or without camptothecin (CPT, **A**) or etoposide (Eto, **B**) for 2h and subjected to cell fractionation assay.

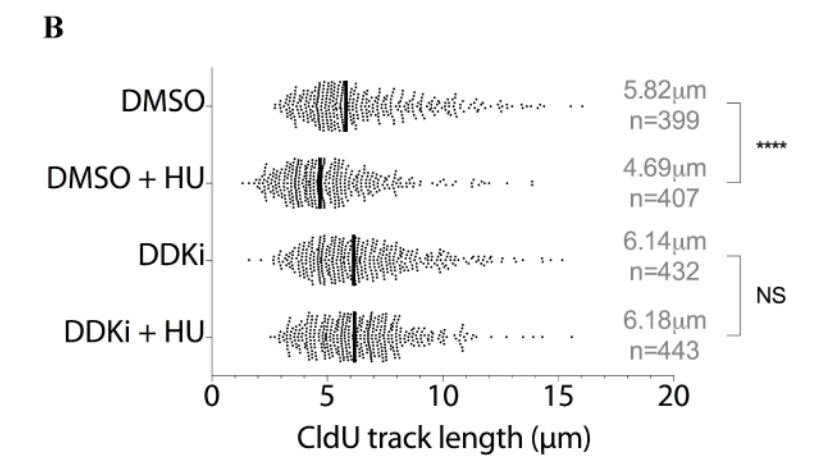
## DDK is required for the processing of stalled replication forks

To rule out the possibility that the reduction in RPA accumulation seen above is due to a reduction in origin firing, we performed DNA fiber analysis to examine the role of DDK at individual replication forks. Using a DNA fiber assay we measured the effect of inhibiting DDK on newly formed DNA strands with or without HU treatment. For these experiments, we used a short (20 minutes) incorporation of IdU followed by 20 minutes of CldU (Figure 2.6 A). A shorter incorporation time allowed detection of smaller changes in the length of nascent DNA than previous assays. Treatment with DDKi alone had no effect on CldU track length indicating that DDK inhibition does not alter nascent strand length in unperturbed cells (Figure 2.6 B, C). We found that 2 hours of HU exposure significantly reduced the length of nascent DNA tracks (CldU tracks) in HCC1954 cells compared to untreated cells (Figure 2.6 B, C). Surprisingly, DDKi treatment completely eliminated the degradation of nascent DNA upon HU exposure. The reduction in the ratio of CldU to IdU lengths (a normalization that allows direct comparison between samples) was also similarly prevented by the DDKi (Figure 2.6 B, C). Moreover, the reduction in nascent strand degradation was dependent on the duration of pre-treatment with DDKi, with 4 hours of pre-treatment resulting in CldU track lengths similar to DMSO treated cells (data not shown, **Figure 2.6 B, C**). Similar results were obtained in MCF7 breast cancer cells (Figure 2.6 D, E, F). These results indicate a role for DDK in the processing of stalled replication forks. We find that the RPA accumulation on chromatin under different conditions correlates well with the length of nascent DNA seen in DNA fiber assay. This suggests that ssDNA formation upon HU treatment might be primarily due to the degradation of newly synthesized DNA. Our data leads us to propose that DDK actively promotes limited resection of stalled replication forks,

which is required for formation of ssDNA, local accumulation of RPA, and activation of downstream checkpoint signaling.

Figure 2.6. DDK has a primary role in processing stalled replication forks.





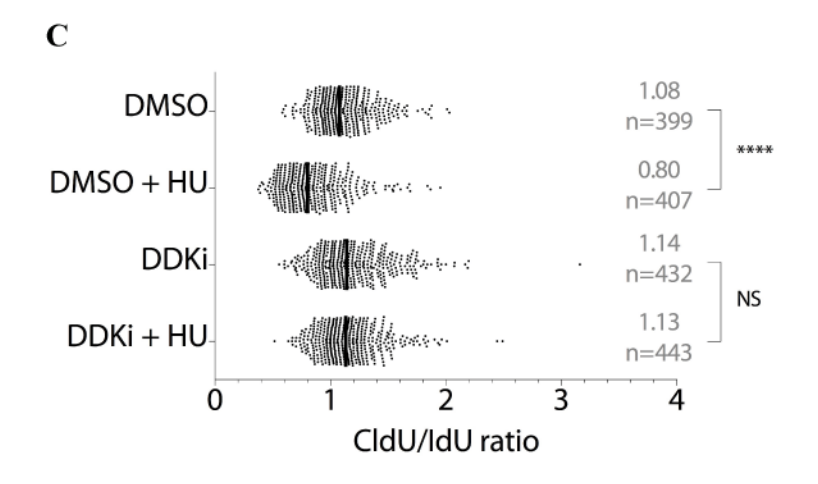
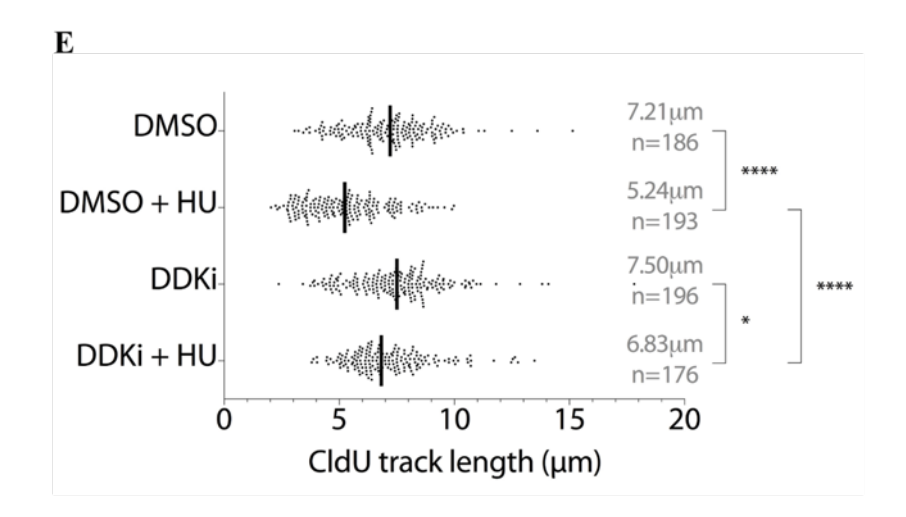
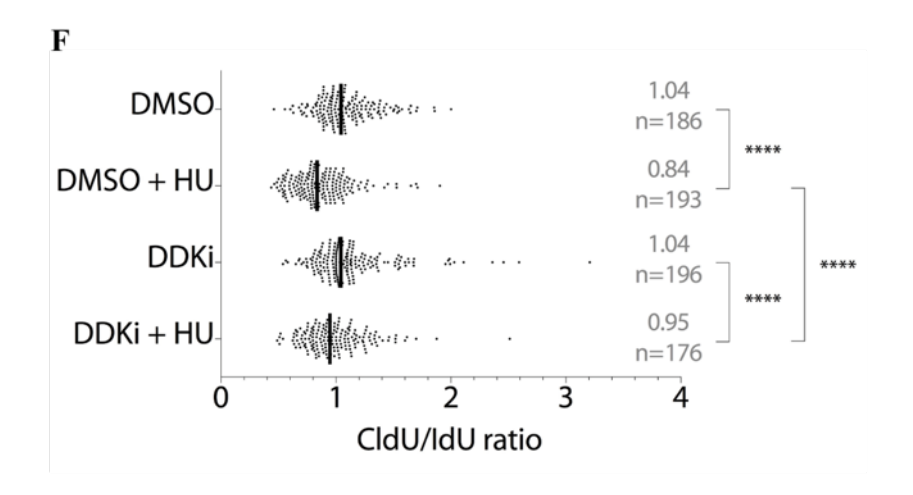


Figure 2.6 (cont'd)

D





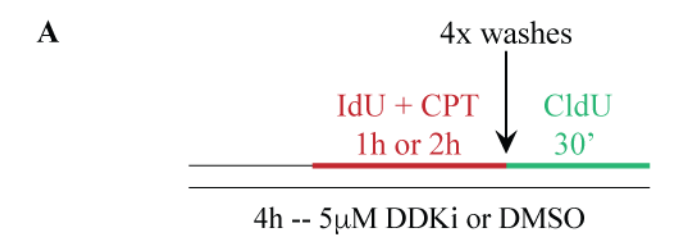


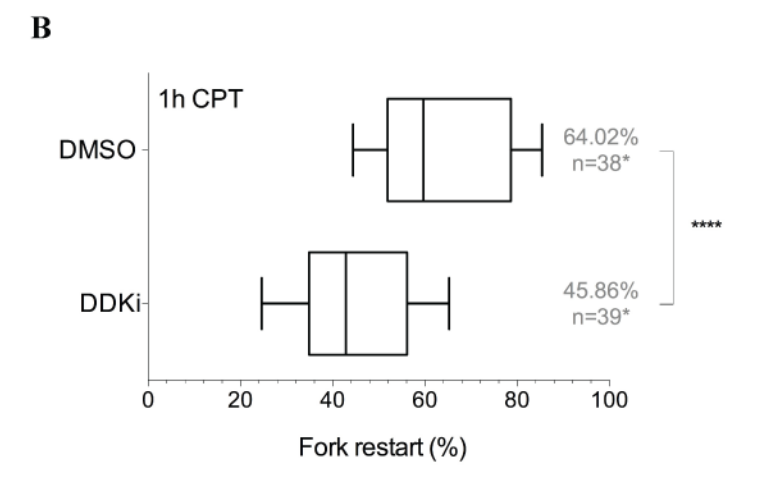
**Figure 2.6 (cont'd). (A, D)** Experimental plan for DNA fiber assay in HCC1954 **(A)** or MCF7 **(D)** cells. Cells were pre-treated with DMSO or DDKi for the indicated time, labelled consecutively with IdU and CldU, subjected to a thymidine chase with or without HU for 2h, and then harvested for DNA fiber assay. Nascent strand resection was measured either as CldU track length **(B, E)** or as a ratio of CldU to IdU incorporation **(C, F)**.

# DDK is required for restart of stalled replication forks

An important function of a replication-checkpoint pathway is to promote DNA repair mechanisms required for rescuing and restarting stalled forks (Sasi and Weinreich, 2016). Since DDK is required for fork processing and checkpoint initiation it might also be necessary for the restart of stalled forks. Using a DNA fiber assay we measured the rate of fork restart following 1 or 2 hours of CPT exposure (Figure 2.7 A). If DDK is required for fork restart, we would expect to see a reduced rate of fork restart in CPT+DDKi treated cells compared to CPT treatment alone. Sixty-four percent of forks restarted after 1h of 1 µM CPT exposure and this was reduced to 46% when cells were pre-treated with DDKi for 4 hours (Figure 2.7 B). The effect of 2 hours of CPT on fork restart was more severe with only 40% of forks restarting after removal of CPT. This was further reduced to 27% when they were pre-treated with DDKi for 4 hours (Figure 2.7 C). These results confirm that DDK is required for efficient replication fork restart, presumably because cells are defective in initiating DNA repair and therefore cannot efficiently restart stalled replication forks.

Figure 2.7. DDK plays an important role in the restart of stalled replication forks.





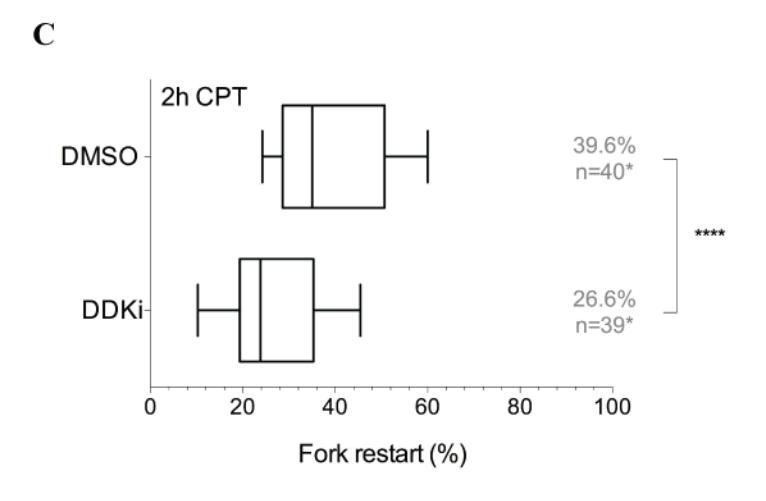


**Figure 2.7 (cont'd). (A)** Experimental plan for DNA fiber assay in HCC1954 cells. Cells were pre-treated with DMSO or DDKi for 4h followed by IdU incorporation in presence of CPT for 1h or 2h. Cells were subsequently washed extensively, exposed to CldU for 30min, and harvested for DNA fiber assay. Replication fork restart was measured by counting DNA fibers with contiguous IdU and CldU tracks after exposure to 1h **(B)** or 2h **(C)** of CPT. \*n indicates the number of images counted per sample. 25 to 30 fibers were counted per image.

# DDK might promote fork processing by regulating the activity of nucleases at stalled forks

CDK is an important cell cycle kinase that phosphorylates and upregulates the activity of several nucleases like CtIP, MRE11, and EXO1 (Ferretti et al., 2013). This ensures high rates of homology directed repair during S and G2 phases, when a sister chromatid is available for error free repair. While the role of nucleases is well understood downstream of dsDNA breaks, their role in replication fork processing is not clear. DDK could exert similar control over nucleases in initiating processing of stalled replication forks. Several pieces of evidence support this idea: (1) mammalian DDK is recruited to chromatin upon DNA damage and fork stalling; (2) high-throughput iPOND studies have identified several nucleases at stalled forks (Dungrawala et al., 2015; Lopez-Contreras et al., 2013; Sirbu et al., 2013); (3) unperturbed replication forks are also enriched for nucleases, probably required for the rescue of naturally stalled forks (Sirbu et al., 2013); and (4) in certain genetic backgrounds nucleases are known to induce hyper resection of replication forks (Iannascoli et al., 2015; Schlacher et al., 2011; Schlacher et al., 2012; Wu et al., 2015).

Most analysis of nucleases upon replication stress look at their roles after a prolonged exposure to HU (Schlacher et al., 2011; Schlacher et al., 2012; Thangavel et al., 2015), which results in collapsed forks and double stranded breaks. However, the nucleases and/or helicases required for processing replication forks immediately after stalling are not known. We therefore examined the effect of inhibiting DDK on the stability of two short range (CtIP and MRE11) and two long range resection enzymes (EXO1, BLM) that are enriched at replication forks and also regulated by CDK (Ferretti et al., 2013).

EXO1 exists in a complex with EEPD1, BLM, and RPA (Nimonkar et al., 2011; Wu et al., 2015) and knockdown of individual proteins destabilizes other proteins in the complex (Wu et al.,

2015). We examined EXO1 protein levels in response to DDK inhibition or knockdown to test if DDK kinase activity or DDK abundance influence EXO1 stability. Interestingly, EXO1 is significantly less abundant following exposure to DDKi with or without prior treatment with DNA damaging agents (Figure 2.8 A). ATR kinase is known to promote degradation of EXO1 presumably to allow only limited degradation of stalled forks (El-Shemerly et al., 2008). We found that the low level of EXO1 following DDK inhibition was not an indirect result of apoptosis or ATR activation (data not shown). We also knocked down CDC7, EXO1, or both using siRNAs and examined the abundance of each protein by immunoblotting. Knocking down either protein significantly reduced expression of the other (Figure 2.8 B). Similar results were seen in HeLa cells (Figure 2.8 C). BLM protein levels were similarly reduced in DDKi treated cells (not shown). In contrast, CtIP stability was only slightly reduced upon DDK inhibition and the levels of MRE11 were unchanged (Figure 2.8 A).

To analyze the contribution of these enzymes to the HU-induced checkpoint signaling, we depleted CtIP, MRE11, EXO1, or BLM using siRNA and looked for markers of checkpoint activation following exposure to HU. Knockdown of each protein was efficient and had little effect on cell cycle progression during the course of the experiment (Figure 2.8 D, data not shown). CtIP knockdown reduced phospho-CHK1 levels but had little effect on either RPA2 phosphorylation or RPA chromatin accumulation (Figure 2.8 D). MRE11 knockdown had no effect on any of these markers (Figure 2.8 D). EXO1 and BLM knockdown significantly reduced CHK1 activation in response to HU, increased RPA2-S4/S8 phosphorylation, but had no effect on RPA chromatin accumulation (Figure 2.8 D). In summary, our data shows that knockdown of CtIP, EXO1, and BLM results in lower levels of CHK1 phosphorylation in response to HU-treatment, similar to the checkpoint-defects seen with DDK inhibition. Since EXO1 has been shown to play a role at stalled

forks in *S. pombe* (Cotta-Ramusino et al., 2005), this role could be conserved in human cells and also be promoted by DDK.

Figure 2.8. DDK might promote fork resection by directly regulating the activity of nucleases.

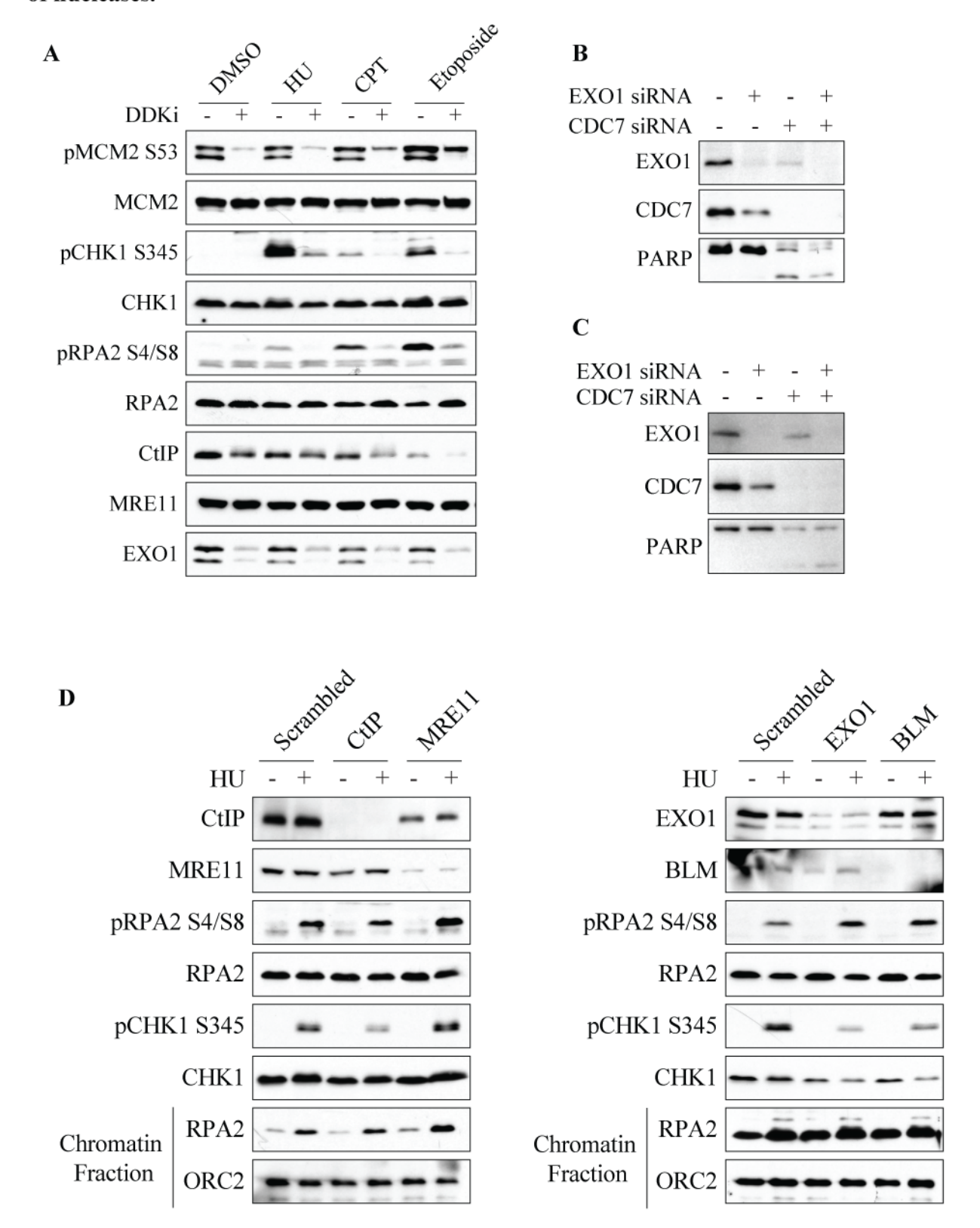
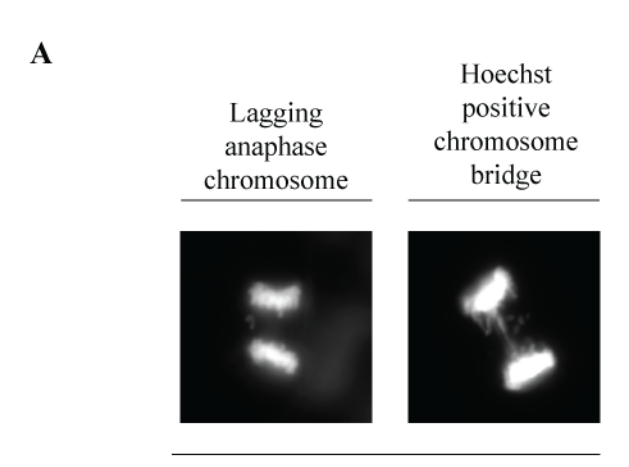


Figure 2.8 (cont'd). (A) HCC1954 cells were pre-treated with DMSO or DDKi for 4h followed by incubation with or without the indicated replication inhibitor for 2h. HCC1954 (B) or HeLa (C) cells were transfected with EXO1 siRNA, 24h later re-transfected with CDC7 siRNA and 72h later harvested for western blot. (D) HCC1954 cells were transfected with indicated siRNAs, 48h later treated with or without HU for 2h, and then harvested for western blot or chromatin fractionation followed by western blot (D, last two panels).

### Low dose DDKi causes aberrant mitotic structures

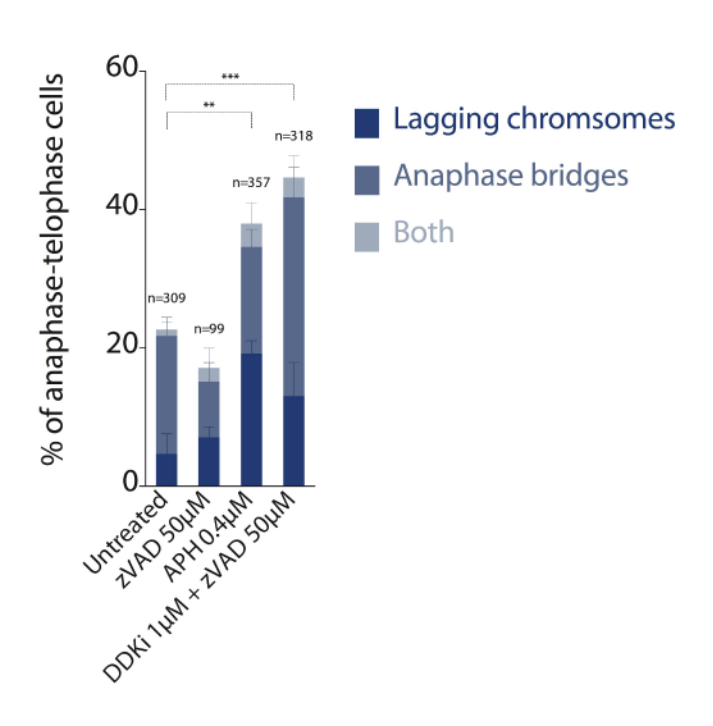
A defect in restarting stalled forks would likely result in incomplete replication and a G2/M arrest in otherwise normal cells. However, DDKi-treated cells are defective in CHK1 and CHK2 activation and therefore would have difficulty restraining mitosis. We therefore examined asynchronous cells after a 24-hour treatment with low dose aphidicolin or low dose DDKi (1µM), which is not sufficient to induce a robust apoptotic response in HCC1954 cells (Sasi et al., 2014). Low dose aphidicolin treatment slows DNA polymerization sufficiently such that some cells complete DNA replication in G2 phase, especially in origin poor regions of the genome, giving rise to lagging chromosomes during mitosis. Surprisingly, we found numerous aberrant mitotic figures in the DDKi-treated cells similar to the aphidicolin-treated cells (Figure 2.9 A, B). Although the increase in lagging chromosomes was similar in aphidicolin and DDKi treated cells, DDKi treatment significantly elevated the number of anaphase bridges compared to aphidicolintreated cells. Anaphase bridges are thought to arise from chromosomes that have long stretches of incompletely replicated DNA or fused telomeres. A small fraction of DDKi-treated nuclei were unique in having highly fragmented chromosomes reminiscent of the "chromosome shattering" or chromothripsis phenotype seen in some cancer cells (not shown). Our data indicates that low level DDKi-treated cells undergo premature mitosis. Acute DDK inhibition may therefore cause high levels of chromosome breakage or abnormalities that triggers cell death in cancer cells.

Figure 2.9. DDK inhibition induces mitotic abnormalities.



Representative Images

В



**Figure 2.9 (cont'd).** HCC1954 cells were treated with DMSO or 1μM DDKi+50μM zVAD or 0.4μM Aphidicolin for 24h.

#### DISCUSSION

We show that ATR kinase is activated and required for apoptosis in response to DDK inhibition. However, inhibiting DDK for up to 6 hours did not cause detectable replication fork stalling or an increase in RPA accumulation, which are normal signals for ATR activation. In the absence of DDK, it is thought the genome cannot be completely replicated because fewer replication origins are activated. So, a fraction of existing forks should eventually stall in replication slow zones or areas where there is a paucity of origins, which often overlap with chromosomal fragile sites (Debatisse et al., 2012). These naturally stalled forks or some other signal might then activate the ATR kinase to induce apoptosis, but without a requirement for CHK1 and CHK2 (the immediate downstream kinases of ATR), since they are not activated in the absence of DDK (Figure 2.2 A) (Montagnoli et al., 2004; Montagnoli et al., 2008).

The ATR-dependent phosphorylation of RPA2-S33 and MCM2-S108 could be markers for such natural stalling events. Human MCM2-S108 is equivalent to MCM2-S92 in Xenopus and MCM2-S95 in chicken cells. In Xenopus egg extracts ATR-mediated MCM2-S92 phosphorylation was shown to be essential for recruitment of the Polo-like kinase Plx1 (the ortholog of human PLK1) to chromatin, and successful completion of DNA replication in presence of mild replication stress – presumably through Plx1-mediated derepression of local checkpoint signaling and firing of dormant origins (Trenz et al., 2008). In DT-40 chicken cells ATR-mediated MCM2-S95 phosphorylation was also associated with increased firing of dormant origins (Schwab et al., 2010). Since MCM2-S108 residue is conserved in vertebrates, but not in yeast, post translational modification of this residue is suggested to be important for processes specific to organisms with large genomes (Shechter and Gautier, 2004) or for dormant origin firing (Alver et al., 2014). We

show that acute DDK inhibition leads to increased MCM2-S108 phosphorylation, which likely represents an ATR signal to fire dormant origins near naturally stalled forks. But in the absence of DDK activity no new origins can be activated. Since RPA2 and MCM2 are components of the replication fork, the signal for cell death might also arise from additional ATR-phosphorylated proteins at the replication fork. How ATR kinase is activated in the absence of ssDNA induction or whether a small amount of ssDNA eventually forms at stalled forks in the absence of DDK is not clear.

Recently, ATR kinase has been shown to mediate cell death induced upon inhibition of transcription in non-cycling cells (Kemp and Sancar, 2016). PHA-767491, the DDK inhibitor used for much of this study, does inhibit transcription by inhibiting CDK9 mediated phosphorylation of RNA-polymerase (Montagnoli et al., 2008). Therefore, it is possible that activation of ATR seen upon treatment with PHA-767491 is due to inhibition of transcription. HCC1954 cells, however, are actively dividing cells and hence ATR would not have a role similar to that in non-cycling cells. Moreover, we tested a structurally distinct DDK inhibitor XL413, with very few off targets (Hughes et al., 2012), and confirmed that XL413 induced apoptosis in an ATR-dependent manner (Figure 2.1 F). Taken together our results show that ATR is required for apoptosis in response to DDK-inhibition, which is accompanied by ATR phosphorylation of RPA2-S33 and MCM2-S108 but without substantial formation of new ssDNA-RPA complexes. The exact mechanism of ATR activation and induction of apoptosis following DDK inhibition remains to be determined.

During the course of our studies we also made a surprising finding regarding a new role for DDK to initiate replication-checkpoint signaling and replication-fork recovery. A role for DDK in error-prone DNA repair in response to UV was first reported more than thirty years ago (Njagi and Kilbey, 1982). Here we report that DDK is required for the resection and early processing of

stalled replication forks consistent with the increased recruitment of DDK to chromatin upon replication stress (Tenca et al., 2007; Yamada et al., 2013b). Furthermore, DDK activity was required for the activation of replication-checkpoint signaling in response to HU, CPT, and etoposide and for efficient recovery of CPT-induced stalled replication forks (Figures 2.5, 2.6, and 2.7). This suggests that DDK promotes proper processing of stalled replication forks, which is essential for the ensuing replication checkpoint signaling and restart of stalled forks.

The reduced rate of fork restart in DDKi-treated cells is reminiscent of phenotypes observed upon knockdown of several nucleases (Petermann and Helleday, 2010; Wu et al., 2015). The degradation of nascent DNA after a short exposure to HU further implicates nucleases in initiating a checkpoint response. However, the study of nucleases and their roles at replication forks have been limited to collapsed forks. DNA2-mediated hyper-resection, for example, is required for the rescue of reversed forks formed after prolonged replication stress (Thangavel et al., 2015). MRE11-mediated hyper-resection, on the other hand, is lethal for cells with certain genetic backgrounds upon prolonged exposure to replication stress (Ray Chaudhuri et al., 2016; Schlacher et al., 2011; Schlacher et al., 2012). Most recently, the double strand break repair factor PTIP was found to promote MRE11-mediated hyper resection of stalled replication fork and genome instability in BRCA1/2-deficient cells. PTIP deficient cells were able to prevent lethal degradation of stalled forks and rescue the lethality of BRCA2-null mouse embryonic stem cells (Ray Chaudhuri et al., 2016). Although these studies have not found a role for CtIP, EXO1, or BLM in resecting stalled forks, iPOND analyses for proteins enriched at forks routinely uncovers multiple nucleases and helicases at unperturbed (eg. BLM, ERCC1, ERCC4, EXO1, MRE11A, CtIP), stalled (eg. BLM, WRN), and collapsed forks (eg. BLM, WRN, EXO1, MRE11A, CtIP) indicating important roles for these enzymes at all times (Dungrawala et al., 2015; LopezContreras et al., 2013; Sirbu et al., 2013). Some nucleases like DNA2 and EXO1 have a role in processing Okazaki fragments during normal replication, and are therefore present at active forks (Balakrishnan and Bambara, 2013). We suggest that DDK recruitment to chromatin facilitates the limited activity of nucleases at stalled forks, which degrades newly synthesized DNA to generate ssDNA-RPA complexes and the activation of replication-checkpoint signaling. Activated ATR-signaling would then attenuate nucleolytic activity at stalled forks to prevent excessive degradation of DNA by described mechanisms (El-Shemerly et al., 2008). Interestingly, fork protection has been associated with increased resistance to chemotherapies like cisplatin and PARP inhibitors, which suggests that aberrant processing of stalled forks is an important mechanism of chemotoxicity (Ray Chaudhuri et al., 2016).

Enzymes like CtIP, EXO1, and BLM might regulate the processing of naturally paused forks, which are likely mimicked by short HU exposure. EXO1 and BLM are present in the same protein complex and our finding that they are much less abundant in DDKi treated cells suggests that DDK might regulate their stability or activity, which could explain the phenotypes observed upon DDK inhibition. In the budding yeast, deletion of non-essential N-terminal BRCT domain in Dbf4 renders cells sensitive to HU, suggesting that this conserved domain mediates the response to replication fork arrest (Gabrielse et al., 2006). DDK activity is also required for DSB formation during meiotic recombination in the budding yeast and phosphorylates the scaffolding protein, Mer2 (Matos et al., 2008; Murakami and Keeney, 2014). This data and others from yeast (Brandao et al., 2014; Day et al., 2010; Furuya et al., 2010) indicates that DDK has multiple roles in DNA metabolism and repair beyond initiating DNA replication.

Treating cells with low doses of replication inhibitors like aphidicolin increases the frequency of UFBs, as well as the formation of anaphase bridges, lagging chromosomes, and

micronuclei (Chan et al., 2009; Naim and Rosselli, 2009). A large fraction of HCC1954 cells had aberrant mitotic figures when DDK was inhibited, consistent with progression through mitosis in the presence of unreplicated DNA. HeLa cells treated with siRNA against CDC7 also showed an aberrant mitotic phenotype (Ito et al., 2012; Montagnoli et al., 2004). Indeed, pre-treating HCC1954 cells with HU for increasing periods of time led to a rescue of cell death following DDK inhibition regardless of CHK1 activation (Figure 2.3 B). But a sub-lethal dose of CPT, which induced CHK1 and a G2/M delay was not sufficient to protect cells from DDKi-induced cell death (Figure 2.3 E). These results show that progression through S-phase in the absence of DDK is deleterious to cells.

We propose that ssDNA generated upon fork stalling is primarily a result of nascent strand degradation and that DDK is required for the efficient processing and recovery of stalled forks even in the absence of exogenous agents (Figure 2.10 A). This activity would especially be important within origin poor regions of the genome. Furthermore, these stalled forks cannot activate a robust checkpoint response in the absence of DDK, and hence cannot stop cells from progressing into M-phase with under-replicated DNA. Aberrant anaphase progression would result in chromosomal breakage, genomic instability, and might be the primary cause of cell death in DDKi-treated cells (Figure 2.10 B).

Figure 2.10. Model for DDK's role at stalled replication fork and events downstream of DDK inhibition.

A

Model for the role of DDK at stalled replication forks

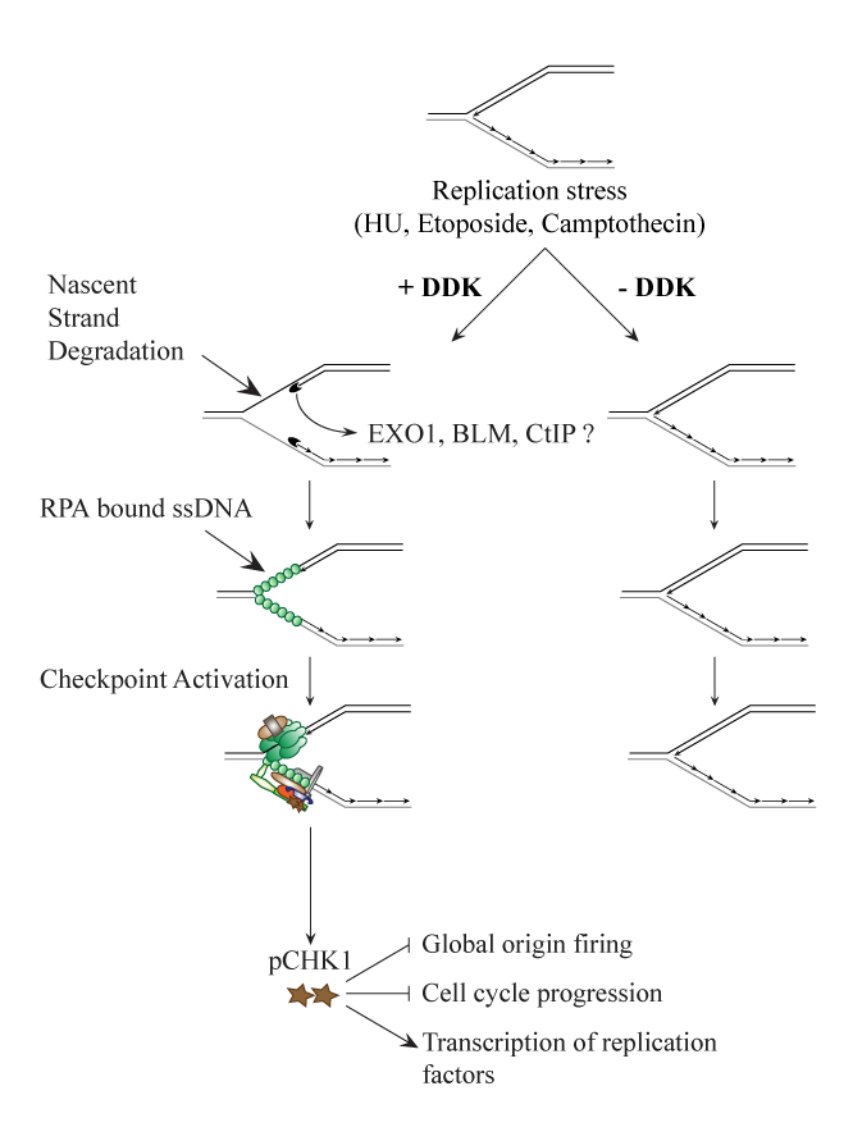
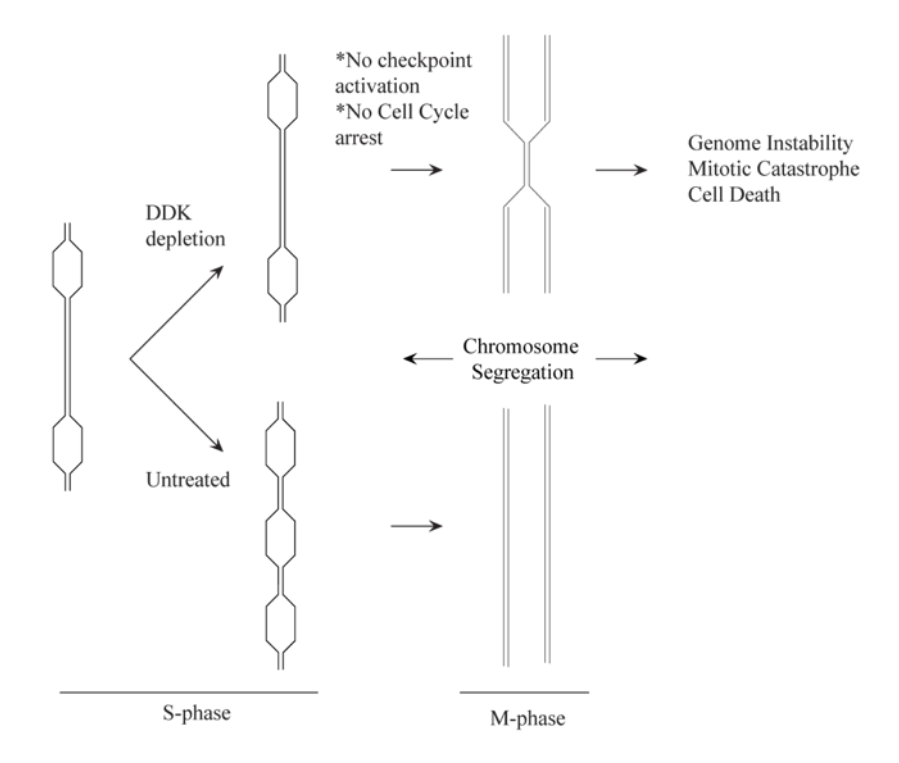


Figure 2.10 (cont'd)

В

# Model for how DDK depletion could lead to cell death



**Figure 2.10 (cont'd).** Model for DDK's role at stalled replication fork (A) and events downstream of DDK inhibition (B). See text for details.

#### **MATERIALS AND METHODS**

# **Cell Lines and Reagents**

HCC1954 cells (ATCC) and Colo-205 (NCI-60) were cultured in RPMI 1640 media supplemented with 10% heat inactivated (HI) FBS, 50units/ml of penicillin, and 50µg/ml of streptomycin. HeLa cells (ATCC) were cultured in MEM supplemented with Earle's salts, 2mM glutamine, 10% HI-FBS, 1.5 g/L sodium bicarbonate, 0.1mM non-essential amino acids, 1mM sodium pyruvate, 50 units/ml of penicillin, and 50µg/ml of streptomycin. The DDK inhibitors, PHA-767491 and XL413, were synthesized as described previously (Sasi et al., 2014), ATR inhibitor (VE-821, #A2521), DNA-PKcs inhibitor (NU 7026, #A8649), Camptothecin (#A2877) were from APExBIO. ATM inhibitor (KU-55933, #S1092) and CHK1 inhibitor (LY2603618, #S2626) were from Selleckchem. Etoposide (#341205) was from EMD Millipore. Hydroxyurea (#H9120) was from USBiological. The antibodies were purchased as indicated: CST: PARP (#9542), pCHK1 S317 (#12302), pCHK1 S345 (#2348), pCHK1 S296 (#2349), CHK1 (#2360), pCHK2 T68 (#2197), CHK2 (#6334), RAD51 (#8875) CtIP (#93110); Bethyl Laboratories Inc.: pMCM2 S53 (A300-756A), pMCM2 S108 (A300-094A), MCM2 (A300-122A), pRPA2 S33 (A300-246A), pRPA2 S4/S8 (A300-245A), ORC2 (A302-735A), EXO1 (A302-639A), MRE11 (A303-998A), BLM (A300-110A); MBL International Corporation: CDC7 (K0070-3S); AbCam: ATR (ab10327); Sigma: β-actin (A5441), Tubulin (T9026); antibodies against RPA1 (NA13, EMD Millipore) and RPA2 (04-1481, EMD Millipore) were gifts from Dr. Bruce Stillman; GE Healthcare: anti-mouse-HRP (NA931V), and anti-rabbit-HRP (NA934V).

#### **RNAi Interference**

Cells were plated in 6-well plates (75000 cells/well) allowed to grow for 36h before transfection. siRNA transfection was performed with Lipofectamine RNAiMAX (Invitrogen) according to manufacturer's instructions. Each well was transfected with 2 µl transfection reagent and a final siRNA concentration of 25nM (CDC7, EXO1, ATR) or 5nM (MRE11, CtIP, BLM) in a total volume of 2ml. Media was replaced 24 hours after transfection and the cells were either harvested or exposed to indicated treatments 48h after transfection. Following siRNAs were used: CDC7 (CDC7-L1, Dharmacon custom siRNA, GGCAAGATAATGTCATGGGA), ATR (Qiagen, SI02664347, GGCACUAAUUGUUCUUCAAtt), EXO1 (Qiagen, SI02665145, GAUGUAGCACGUAAUUCAAtt), MRE11A (Thermo Scientific #s8960, CCCGAAAUGUCACUACUAAtt), **CtIP** (Thermo Scientific, #s142451, CGAAUCUUAGAUGCACAAAtt), **BLM** Scientific #s1999, (Thermo GAUAUCUUCCAAAACGAAAtt).

### **Immunoblotting**

Whole cell extracts were prepared by re-suspending the pellets in RIPA buffer (150mM NaCl, 1% NP-40, 0.5% sodium deoxycholate, 0.1% SDS, 50mM Tris-HCl, pH 8) containing protease inhibitors (100μM PMSF, 1mM Benzamidine, 2.5μg/ml Pepstatin A, 10μg/ml Leupeptin, and 10μg/ml Aprotinin) and phosphatase inhibitors (1mM each NaF, Na<sub>3</sub>VO<sub>4</sub>, Na<sub>2</sub>P<sub>2</sub>O<sub>7</sub>). Protein concentration was measured using the BCA protein assay kit (Pierce, #23227). Cell fractionation into cytosolic, nuclear soluble, and nuclear insoluble (chromatin) fractions was performed as described previously (Mendez and Stillman, 2000). Pellets were re-suspended in lysis Buffer A (10mM HEPES (pH 7.9), 10mM KCl, 1.5 mM MgCl<sub>2</sub>, 0.34M Sucrose, 10% Glycerol, 1mM DTT,

and protease and phosphatase inhibitors) and Triton X-100 was added to a final concentration of 0.1%. After incubation on ice for 8min, lysates were centrifuged at 1,300g, at 4°C, for 5min. The supernatant was collected and clarified by high speed centrifugation (20,000g, 4°C, 5min) to obtain cytosolic fraction. The pellet was washed once with Buffer A and then lysed in Buffer B (3mM EDTA, 0.2 mM EGTA, 1mM DTT, protease and phosphatase inhibitors) for 30min on ice. Soluble nuclear fraction (supernatant) was collected by centrifugation at 1,700g, at 4°C, for 5min. The chromatin fraction (pellet) was washed once with Buffer B, re-suspended in Buffer B, and sonicated briefly. Protein concentration in each fractions was measured using Braford assay (Bio Rad, #500-0006). Equal amounts of proteins were subjected to SDS-PAGE and transferred to nitrocellulose membrane (Millipore, HATF304F0). Transfer efficiency and equal loading was confirmed by Ponceau S staining. Membranes were blocked overnight at 4°C with 5% non-fat milk in TBS-T, followed by incubation in primary and secondary antibodies (1h at RT, 2% milk/BSA in TBS-T). Protein bands were visualized using SuperSignal West Pico solutions (Thermo Scientific).

### Analysis of Caspase 3/7 activity

5000 cells per well were plated in 96 well plates. 24 hours later cells were treated and incubated for the indicated period of time at 37°C. Caspase 3/7 activity and viable cell number were then measured using the Caspase-Glo 3/7 assay (Promega) and CellTiter-Glo assay (Promega), respectively. The 'caspase activity per cell' was obtained by normalizing total caspase activity to cell number. Luminescence was measured using BioTek Synergy Microplate Reader 30 minutes after addition of 'Glo' reagents.

# **Cell Cycle Analysis**

Cells were trypsinized, washed twice with cold PBS, and fixed/permeabilized in 70% ice-cold ethanol (made in water). After fixation on ice for 30mins cells were centrifuged at 400g (4°C, for 5mins), washed once with cold PBS, and centrifuged again. The pellets were resuspended in analysis buffer (10µg/ml propidium iodide and 250µg/ml RNAase) and incubated at 37°C for 30min. Cell cycle profiles were obtained using FACSCalibur<sup>TM</sup> (BD Biosciences) flow cytometer. The data was analyzed using Flowing Software.

## **DNA Fiber Spreading**

DNA fiber spreading was performed as described previously (Breslin et al., 2006; Jackson and Pombo, 1998). Briefly, sub-confluent cells were sequentially labeled first with 10 μM 5-iodo-2'-deoxyuridine (IdU) and then with 100 μM 5-chloro-2'-deoxyuridine (CldU) for the indicated times. One thousand cells were loaded onto a glass slide (StarFrost) and lysed with spreading buffer (200 mM Tris-HCl pH 7.5, 50 mM EDTA, 0.5% SDS) by gently stirring with a pipette tip. The slides were tilted slightly and the surface tension of the drops was disrupted with a pipette tip. The drops were allowed to run down the slides slowly, then air dried, fixed in methanol/acetic acid 3:1 for 10 minutes, and allowed to dry. Glass slides were processed for immunostaining with mouse anti-BrdU to detect IdU (347580, BD Biosciences), rat anti-BrdU (ABC117-7513, Eurobio Abcys) to detect CldU, mouse anti-ssDNA (MAB3868, Millipore) antibodies and corresponding secondary antibodies conjugated to various Alexa Fluor dyes. Nascent DNA fibers were visualized by using immunofluorescence microscopy (Zeiss Apotome 2). The acquired DNA fiber images were analyzed by using MetaMorph Microscopy Automation and Image Analysis Software (Molecular Devices) and statistical analysis was performed with

GraphPad Prism (GraphPad Software). The lengths of at least 150 IdU/CldU tracks were measured per sample.

# ACKNOWLEDGMENTS

I would like to thank Dr. Philippe Pasero, Dr. Yea-Lih Lin, and Flavie Coquel (Institute of Human Genetics, Montpellier, France) for performing and analyzing the DNA fiber experiments and Dr. Bruce Stillman (Cold Spring Harbor) for the RPA antibodies.

# CHAPTER 3.

# DDK PROMOTES TUMOR CHEMORESISTANCE AND SURVIVAL VIA MULTIPLE PATHWAYS

# Modified from

Sasi, N., Bhutkar, A., Lanning, N.J., MacKeigan, J., and Weinreich, M. (2016). DDK promotes tumor chemoresistance and survival via multiple pathways. *Under Review*.

#### **ABSTRACT**

DDK is a two subunit kinase required for initiating DNA replication at individual origins. DDK is composed of the CDC7 kinase and its regulatory subunit, DBF4. Both subunits are highly expressed in many diverse tumor cell lines and primary tumors, which is correlated with poor prognosis. Inhibiting DDK causes apoptosis of tumor cells, but not normal cells, through a largely unknown mechanism. Here we have explored gene expression correlations with DDK high- and DDK low-expressing lung adenocarcinomas. We also performed an RNAi screen to identify kinases and phosphatases that promote apoptosis when DDK is inhibited. Increased DDK expression is highly correlated with inactivation of RB1-E2F and p53 tumor suppressor pathways. Both CDC7 and DBF4 promoters bind E2F suggesting that increased E2F in RB1 mutant cancers promotes increased DDK expression. Surprisingly, the level of DDK expression is strongly correlated with genome-wide gene mutation frequencies suggesting that increased DDK levels promote elevated mutation frequency in lung adenocarcinoma. Our RNAi screen identified 23 kinases and phosphatases that promote apoptosis of both breast and cervical carcinoma cell lines when DDK is inhibited. These hits include checkpoint genes, G2/M cell cycle regulators and known tumor suppressors. Initial characterization of the LATS2 tumor suppressor suggests that it promotes apoptosis independently of the upstream MST1/2 kinases in the Hippo signaling pathway.

#### INTRODUCTION

Increased proliferative capacity and evasion from growth suppressors are classic hallmarks of tumorigenesis (Hanahan and Weinberg, 2011). Tumors can evade growth suppression by mutating key gatekeeper proteins that are responsible for activating cell cycle checkpoints. Unrestricted cell cycle progression in turn results in genome instability, which could arise due to errors in DNA replication, repair, recombination, or chromosome segregation. Genome instability furthers tumor growth through increased mutation rates, chromosomal rearrangements and genome-wide amplification events (Hanahan and Weinberg, 2011). Tumor cells evolve several mechanisms to tolerate genomic instability, frequently by increasing the expression and activity of DNA repair proteins or by altering key cell cycle regulatory proteins. Altered DNA repair pathways have additionally been identified as key drivers of tumorigenesis (Jeggo et al., 2016).

DDK (DBF4-dependent kinase) is a key cell cycle protein required for DNA replication by catalyzing MCM helicase activation at each individual replication origin throughout S-phase (Sasi and Weinreich, 2016). DDK is composed of the CDC7 kinase and its regulatory subunit DBF4, which is required for kinase activity and targeting to various substrates (Sasi and Weinreich, 2016). Both DDK subunits are overexpressed in many primary tumors and in the majority of tumor cell lines tested (Bonte et al., 2008; Chen et al., 2013a; Cheng et al., 2013; Hou et al., 2012b). Overexpression of DDK is correlated with poor prognosis and advanced tumor grade in melanoma, ovarian, breast and other cancers (Bonte et al., 2008; Chen et al., 2013a; Cheng et al., 2013; Hou et al., 2012b). High levels of DDK, however, are not correlated with increased proliferative capacity in tumor cell lines (Bonte et al., 2008). It is therefore not clear what survival advantage, if any, high DDK levels confer on tumors. In addition to its essential role in initiating DNA

replication, DDK also has important functions in mediating replication checkpoint signaling (Kim et al., 2008; Rainey et al., 2013), trans-lesion DNA repair (Brandao et al., 2014; Day et al., 2010), mitotic (Miller et al., 2009), and meiotic phases of cell cycle (Murakami and Keeney, 2014). Most recently, we have identified a primary role for DDK in processing stalled replication forks and initiating replication checkpoint signaling (Sasi et al., 2016). We found that DDK activity is also required for the efficient restart of forks once the replication stress or damage has been repaired (Sasi et al., 2016). It is therefore conceivable that tumor cells rely on these functions of DDK to cope with increased genomic instability and replication stress.

Within the last decade, DDK has emerged as a possible chemotherapeutic target. Depleting CDC7 kinase or inhibiting DDK activity induces apoptosis in tumor cells, while normal cells undergo a reversible cell cycle arrest (Montagnoli et al., 2004; Montagnoli et al., 2008; Tudzarova et al., 2010). A detailed study of the reversible cell cycle arrest induced in normal fibroblast cells uncovered three non-redundant G1-S signaling pathways that inhibit CDK and/or Myc activity when DDK is inhibited, thus restricting progression into S-phase (Tudzarova et al., 2010). Since one or more of these growth suppressors are commonly disrupted in tumor cells, they can progress through a lethal cell cycle in the absence of DDK. The mode of cell death induced in tumor cells upon DDK inhibition involves ATR but is independent of the downstream canonical S-phase checkpoint kinases like CHK1 and CHK2 (Montagnoli et al., 2004; Montagnoli et al., 2008; Sasi et al., 2016). Apoptosis is also independent of p53 activity, although p53 status might influence the timing of apoptosis (Ito et al., 2012; Montagnoli et al., 2004). It is therefore not clear mechanistically how DDK inhibition induces cell death. A better understanding of this pathway is needed to identify tumors that would respond best to DDK inhibition and to uncover mechanisms through which tumors might become resistant to DDK inhibitors. In this study we have addressed how tumors induce and benefit by high levels of DDK. We have also identified a number of kinases and phosphatases that mediate tumor cell death in diverse tumor cell lines when DDK is inhibited.

Our results show that increased DDK expression correlates with tumor response to genotoxic insults and with increased resistance to genotoxic chemotherapy, which could explain the poor prognosis for patients with tumors that overexpress DDK. Using TCGA mutation data we report a strong link between DDK and the tumor mutational load. We also find that DDK expression is highly correlated with RB1 mutation and the "E2F-target" oncogenic signature, suggesting that E2F family members might drive aberrant DDK expression in tumor cells. Using publicly available ChIP-Seq data we show that several E2F family members tightly bind promoters at both CDC7 and DBF4 genes. Finally, using a functional RNAi screen of human kinases and phosphatases we identify multiple mediators of cell death induced upon DDK inhibition. The LATS2 kinase is a novel tumor suppressor that promotes apoptosis when DDK is inhibited and we find that its role is likely independent of the Hippo signaling network. Other top hits from the screen are required for mitotic progression, further strengthening a model where aberrant progression through mitosis in the absence of DDK triggers cell death.

#### RESULTS AND DISCUSSION

## Gene expression signature of tumors differentially expressing CDC7 kinase

Based on previous studies (Day et al., 2010; Kim et al., 2008; Rainey et al., 2013) we hypothesized that tumors with increased expression of DDK are better able to activate a checkpoint or DNA repair pathway in response to genotoxic insults and as a result are more resistant to genotoxic chemotherapies. To test this hypothesis, we used the well annotated lung adenocarcinoma dataset from The Cancer Genome Atlas (TCGA) (Cancer Genome Atlas Research, 2014). We first compared the expression level of DDK in matched normal and tumor tissue. Using a Kolmogorov-Smirnov test for statistical significance we found that all DDK subunits (CDC7, DBF4 and DBF4b) are significantly overexpressed in lung adenocarcinoma tumor tissue when compared to their matched normal tissue (N=57, p-values =  $9.4 \times 10^{-10}$  (CDC7),  $1.1 \times 10^{-16}$  (DBF4),  $5.2 \times 10^{-13}$  (DBF4b)) (**Figure 3.1 A**). Moreover, patients with CDC7overexpressing tumors have significantly worse survival (Hazard Ratio of 1.58, multivariate analysis p-value: 0.00326) (Figure 3.1 B). These results indicate that high level of CDC7 expression is independently prognostic of poor survival in lung adenocarcinoma, which is consistent with previous studies showing similar outcome for CDC7-overexpression in other cancer types. It also suggests that DDK has a universal role in promoting tumor survival.

We then used gene expression data from the top ten CDC7-high expressing tumors and bottom ten CDC7-low expressing tumors to generate a gene expression signature correlated with CDC7. Genes with Z-scores>= +3 were selected as genes upregulated in CDC7-high expressing tumors and those with Z-scores<= -3 were selected as genes downregulated in CDC7-high expressing tumors. The selected lists of genes were then queried for enriched gene sets using Gene

Set Enrichment Analysis (GSEA). Among the genes positively correlated with high CDC7 expression, we found several gene sets indicative of advanced tumor grade or poor prognosis (not shown). We also identified several cell cycle gene sets including (not surprisingly) those involved in DNA replication and activation of the pre-replicative complex, which is the essential role of DDK (Figure 3.2 A). Several mitotic genes sets were also upregulated in CDC7-high expressing tumors including the PLK1 pathway (Figure 3.2 B) supporting the link between the role of DDK throughout S-phase and its interaction with and inhibition of the Polo-like kinases that promote mitotic progression (Chen and Weinreich, 2010; Miller et al., 2009). Gene sets involved in the G2/M checkpoint, activation of the ATR pathway, and response to HU damage were also significantly enriched (Figure 3.2 B). These latter gene sets corroborate our recent finding that DDK activity is essential for processing stalled replication forks and initiating the replication checkpoint response (Sasi et al., 2016). Interestingly, chemoresistance gene sets were significantly enriched in CDC7-high expressing tumors. This correlation could partly explain the poor survival outcome in these patients. Expression of mitotic and G2/M checkpoint genes is enriched in cisplatin-resistant tumor mouse models (Oliver et al., 2010) and CDC7 was among the top genes that were overexpressed in a cisplatin-resistant bladder cancer cell line (Kim et al., 2016). MCM7, a direct target of DDK (Weinreich and Stillman, 1999b), was also overexpressed in the cisplatinresistant cell line (Kim et al., 2016). In budding yeast DDK mediates its essential role in DNA replication initiation by phosphorylating Mcm4 and Mcm6 (Sheu and Stillman, 2010), but Mcm7 was among the most potent DDK targets in vitro and mcm7-1 exhibited strong genetic interactions with CDC7 and DBF4 mutants (Weinreich and Stillman, 1999b). The significance of DDK phosphorylation of MCM2 and MCM7 is not understood but it is possible that their phosphorylation is important for maintenance of genome stability in tumor cells.

Figure 3.1. DDK is overexpressed in tumors and is a predictor of poor survival.

# A Normal (n=57) Matched Tumor (n=57)

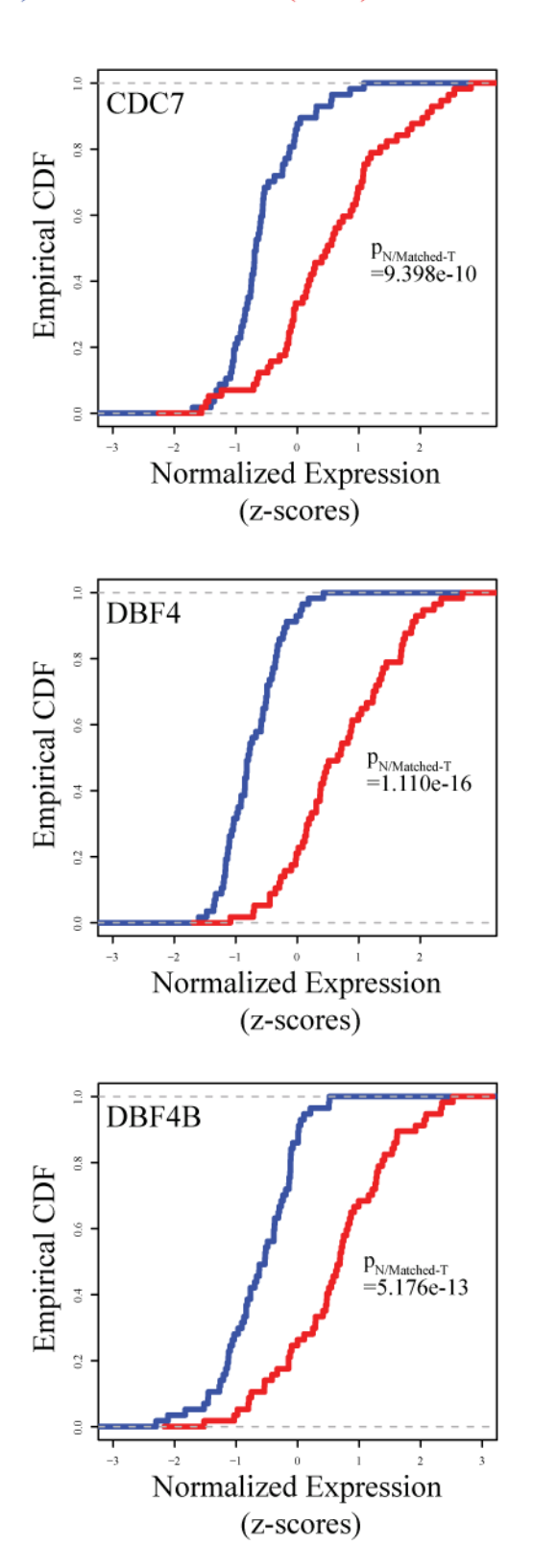


# Figure 3.1 (cont'd)

В

 Table X
 : Results of univariate and multivariable Cox proportional hazards model on overall survival in the TCGA LUAD cohort (all patients).

	Univar	riate	Multivarial	ole	
Charasteristic	HR (95% CI)	р	HR (95% CI)	р	P interaction
CDC7 expression	1.20(1.01-1.42)	0.0389	1.58(1.16-2.14)	0.00326	
DBF4 expression	1.12(0.89-1.40)	0.33	0.94(0.66-1.33)	0.71686	
DBF4B expression	1.13(0.93-1.38)	0.217	0.89(0.67-1.20)	0.45376	
Gender (Male vs Female)	0.98(0.68-1.41)	0.907	0.85(0.55-1.30)	0.44462	
Age (Years)	1.01(0.99-1.03)	0.574	1.02(1.00-1.04)	0.10665	
TNM Stage (Stage III/IV vs I/II)	2.96(2.04-4.29)	9.98E-09	1.82(1.04-3.19)	0.03692	0.6878
T score (T3/T4 vs T1/T2)	2.46(1.53-3.96)	0.000212	2.12(1.17-3.84)	0.01322	0.4766
N score (N1/N2 vs N0)	2.81(1.93-4.10)	7.30E-08	2.35(1.40-3.96)	0.0013	0.5044
Smoking History (reformed > 15yrs vs non-smoker)	1.01(0.53-1.93)	0.968	1.31(0.58-2.95)	0.52119	
Smoking History (reformed < 15yrs vs non-smoker)	1.10(0.61-2.01)	0.747	1.62(0.73-3.59)	0.23811	
Smoking History (current smoker vs non-smoker)	0.71(0.36-1.40)	0.325	0.91(0.38-2.17)	0.83491	
Mutational Load (mutations per coding Mb)	0.98(0.96-1.00)	0.0232	0.97(0.95-1.00)	0.0606	

HR = Hazard ratio; CI = Confidence Interval; TNM Stage = Stage classification per Union for International Cancer Control (UICC);
T score = Primary tumor size/invasiveness; N score = Lymph node metastasis;

p<sub>interaction</sub> = p-value of interaction between CDC7 and other significant covariates (model comparison; likelihood ratio test)

**Figure 3.1 (cont'd). (A)** DDK subunits are significantly overexpressed in lung adenocarcinoma tissue when compared to matched normal tissue. Significance was calculated using Kolmogorov-Smirnov test. CDF, cumulative distribution function. **(B)** CDC7 expression is independently prognostic within the TCGA LUAD cohort (all patients) and is associated with worse patient outcome in univariate (HR = 1.20) and multivariable (HR = 1.58) analyses after controlling for other clinical covariates using a Cox regression model. No significant interaction with other prognostic covariates was detected.

Figure 3.2. Characterization of tumors that differentially express DDK.

# A

# Cell Cycle Progression and DNA Replication

Curated Gene Sets	Brief Description	FDR q-val
REACTOME_CELL_CYCLE	Genes involved in Cell Cycle	0
KEGG_CELL_CYCLE	Cell cycle	0
REACTOME_G1_S_TRANSITION	Genes involved in G1/S Transition	0
REACTOME_S_PHASE	Genes involved in S Phase	0
REACTOME_ACTIVATION_OF_THE_PRE _REPLICATIVE_COMPLEX	Genes involved in Activation of the pre-replicative compl	ex 0
REACTOME_SYNTHESIS_OF_DNA	Genes involved in Synthesis of DNA	0
KEGG_DNA_REPLICATION	DNA replication	0
REACTOME_DNA_STRAND	Genes involved in DNA strand elongation	0
WHITFIELD_CELL_CYCLE_G2	Genes periodically expressed in synchronized HeLa cells, with peak during the G2 phase of cell cycle.	0
REACTOME_MITOTIC_PROMETAPHASE	Genes involved in Mitotic Prometaphase	0
REACTOME_CELL_CYCLE_MITOTIC	Genes involved in Cell Cycle, Mitotic	0
PID_AURORA_B_PATHWAY	Aurora B signaling	0
REACTOME_MITOTIC_M_M_G1_PHASES	Genes involved in Mitotic M-M/G1 phases	0
REACTOME_M_G1_TRANSITION	Genes involved in M/G1 Transition	0
REACTOME_MITOTIC_G1_G1_S_PHASES	Genes involved in Mitotic G1-G1/S phases	0

# В

# Cell cycle checkpoint and drug resistance pathways enriched in CDC7-high expressing tumors

Curated Gene Sets	Brief Description	FDR q-val
REACTOME_CELL_	Genes involved in Cell Cycle Checkpoints	0
CYCLE_CHECKPOINTS HU_GENOTOXIC_DAMAGE_4HR	Genes most consistently regulated at 4 h by all six genotoxins tested: cisplatin, methyl methanesulfonate, mitomycin C, taxol, hydroxyurea and etoposide.	0
REACTOME_ACTIVATION_OF_ATR_IN _RESPONSE_TO_REPLICATION_STRESS	Genes involved in Activation of ATR in response to replication stress	0
REACTOME_CHROMOSOME_MAINTENAN	Genes involved in Chromosome Maintenance	0
REACTOME_G2_M_CHECKPOINTS	Genes involved in G2/M Checkpoints	0
KANG_DOXORUBICIN_RESISTANCE_UP	Genes up-regulated in gastric cancer cell lines: doxorubicin resistant vs. sensitive	0
PID_PLK1_PATHWAY	PLK1 signaling events	0

**Figure 3.2 (cont'd). (A, B)** Gene set enrichment analysis (GSEA) was performed using a gene expression signature differentiating CDC7-high versus CDC7-low tumors. Shown here are enriched gene sets involved in cell cycle progression and DNA replication **(A)** cell cycle checkpoints and drug resistance **(B)**.

#### DDK likely drives increased tumor mutagenesis

To investigate how DDK might contribute to tumorigenesis we looked at the mutation spectrum of CDC7-, DBF4-, and DBF4B-high versus low expressing tumors. The top 25% and bottom 25% of patients were selected based on the expression of CDC7, DBF4, or DBF4B. Over-representation of patients with mutations in specific genes within each group was assessed with respect to the background rate in the whole cohort (hypergeometric test). The group of patients that had tumors with high levels of DDK expression is over-represented with significantly increased mutational load in a large number of genes (CDC7 = 756; DBF4 = 1256; DBF4B = 1443) whereas only a handful of genes in these patients exhibited mutation rates lower than that expected by chance (CDC7 = 22, DBF4 = 17, DBF4B = 10) (Figure 3.3 A). Surprisingly, in patients that had tumors with low levels of DDK expression very few genes had significantly increased rates of mutation (CDC7 = 37; DBF4 = 32; DBF4B = 77). In contrast, in this low DDK expression group several hundred genes had mutation rates significantly *lower* than what is expected by chance (CDC7 = 616; DBF4 = 708; DBF4B = 517) (Figure 3.3 A). It is possible that a few patients with very high mutational load in the DDK-high group might be driving this difference. To directly test this possibility, we compared the mutational load, measured as the number of mutations per Mb of the coding DNA, between the two groups of patients with high and low expression of DDK subunits. We found significantly higher mutational load in tumor patients that overexpress all three DDK subunits (Figure 3.3 B). Together, these analyses suggest that DDK is a driver of tumor mutagenesis.

A positive correlation between DDK expression and the mutational load could be indicative of the improved ability of tumor cells to tolerate genome instability, which is a known mechanism for increased mutation rate in tumor cells (Jeggo et al., 2016). This mechanism,

however, does not explain why patients with "DDK-low" expressing tumors are significantly under-represented in mutational load for such a large number of genes. In the budding yeast, DDK promotes error prone repair and UV/MMS-induced mutagenesis. Yeast strains containing hypomorphic CDC7 alleles are almost immutable in response to these mutagens (Njagi and Kilbey, 1982; Ostroff and Sclafani, 1995). Moreover, yeast strains harboring multiple copies of the wild type CDC7 gene exhibited increased rate of UV-induced mutagenesis (Sclafani et al., 1988). Subsequently, it was found that CDC7 has an epistatic relationship with genes that promote an error-prone DNA repair mechanism known as the trans-lesion DNA synthesis (TLS) (Brandao et al., 2014; Pessoa-Brandao and Sclafani, 2004). In human cell lines, DDK phosphorylates the Rad18 ubiquitin ligase, which is important for the recruitment of TLS polymerase eta to replication stall sites (Day et al., 2010). Therefore, DDK's role in promoting error prone DNA synthesis is likely conserved and could be one of the mechanisms for increased mutagenesis in DDK high expressing tumors. Our finding is the first report that mutational load is strongly correlated with DDK expression in humans and has potentially important chemotherapeutic implications. Inhibiting DDK activity in tumor cells, in addition to promoting cell death, might reduce acquisition of new mutations that would otherwise help promote resistance against chemotherapeutic drugs.

Figure 3.3. DDK likely drives increased tumor mutagenesis.

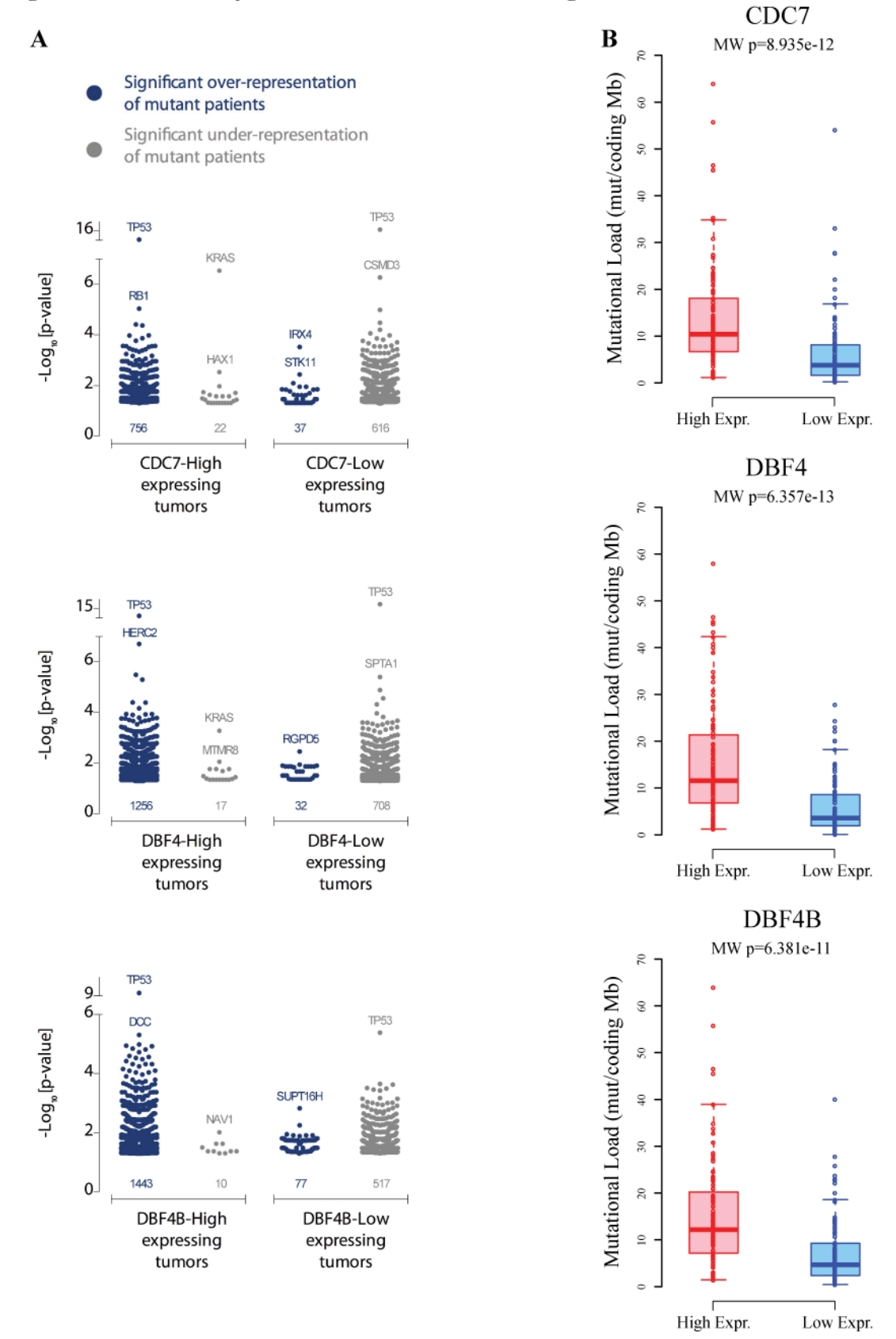


Figure 3.3 (cont'd)

 $\mathbf{C}$ 

Most commonly mutated genes in lung adenocarcinoma.

Ranked in order of decreasing prevalence.

(adapted from Reference [Cancer Genome Atlas Research, 2014, Figure 1a]

TP53	46%
KRAS	33%
KEAP1	17%
STK11	17%
EGFR	14%
NF1	11%
BRAF	10%
SETD2	9%
RBM10	8%
MGA	8%
MET	7%
ARID1A	7%
PIK3CA	7%
SMARCA4	6%
RB1	4%
CDKN2A	4%
U2AF1	3%
RIT1	2%

D

CDC7 high	CDC7 low
expressing tumors	expressing tumors

Gene	p	$\mathbf{q}$	Gene	p	$\mathbf{q}$
TP53	0.00	0.00	KRAS	0.00	0.00
STK11	0.00	0.00	STK11	0.00	0.00
RB1	0.00	0.00	TP53	0.00	0.00
KEAP1	0.00	0.00	EGFR	0.00	0.00
KRAS	0.00	0.00	KEAP1	0.00	0.00
IL32	0.00	0.00	IL32	0.00	0.00
OR8U8	0.00	0.04	HAX1	0.00	0.00
COL5A2	0.00	0.06	NBPF1	0.00	0.00
TMPRSS111	60.00	0.07	RBM10	0.00	0.00
CACNG3	0.00	0.07	SPRR3	0.00	0.01
UBC	0.00	0.07	SYN2	0.00	0.03
FSCB	0.00	0.09	HEBP1	0.00	0.07
FBN2	0.00	0.09	DNMT3B	0.00	0.10
			:	:	:
			RB1	0.33	1.00

Figure 3.3 (cont'd)

E

# Top 25% of patients (tumors with high CDC7 expression)

Gene	# of patients in bucket	# of mutations in bucket	# of patients in total	# of mutations in total	p - enrichment	p - depletion
TP53	112	95	433	231	8.6E-16	1
STK11	112	13	433	64	0.90	0.17
RB1	112	15	433	21	9.2E-06	1
KEAP1	112	22	433	76	0.29	0.80
KRAS	112	12	433	123	1	2.9E-07
RBM10	112	9	433	34	0.54	0.62
EGFR	112	17	433	59	0.25	0.84

# Bottom 25% of patients (tumors with low CDC7 expression)

Gene	# of patients in bucket	# of mutations in bucket	# of patients in total	# of mutations in total	p - enrichment	p - depletion
TP53	106	20	433	231	1	7.2E-17
STK11	106	0	433	12	1	0.03
RB1	106	2	433	21	0.98	0.08
KEAP1	106	17	433	76	0.73	0.38
KRAS	106	39	433	123	0.02	0.99
RBM10	106	7	433	34	0.77	0.38
EGFR	106	16	433	59	0.46	0.66

Figure 3.3 (cont'd). (A) Genes with over-representation of mutant patients within patients' groups that differentially express DDK subunits. Mutational information from the top and bottom 25% of CDC7/DBF4/DBF4B-expressing tumors was used assess significant (p<0.05, hypergeometric test) over-representation (blue) or under-representation (grey) of mutant patients. The number under each data set indicates the total number of genes with significant over- or under-representation of mutant patients within each cohort. (B) Mutational Load (derived as the number of non-silent mutations per 30Mb of coding sequence) in patients with high CDC7/DBF4/DBF4B expression (top 25%, n=122) and low CDC7/DBF4/DBF4B expression (bottom 25%, n=122). Mann-Whitney-Wilcoxon (MW) test was used to assess statistical significance. (C) Significantly mutated genes (p<0.025) identified using MuTSig2CV analysis on mutational data from the TCGA lung adenocarcinoma cohort. Adapted from reference [Cancer Genome Atlas Research, 2014, Figure 1a] (D) MutSig analysis using top and bottom quartiles of CDC7 expressing tumors. Genes commonly mutated in lung adenocarcinoma [from (C)] are highlighted in grey. (E) Genes highlighted in (D) with corresponding mutational data and statistical significance (hypergeometric test) of over- or under-representation of mutant patients within the top and bottom quartiles of patients stratified by CDC7 expression.

### RB1 mutation is strongly correlated with high DDK expression in tumors

The RB1-E2F pathway genes formed a significant subset of gene sets that were positively correlated with high *CDC7* expression (Figure 3.4 A). The expression signature of *CDC7*-high expressing tumors was similar to the oncogenic signature of RB1-E2F pathway (Figure 3.4 B). RB1 is a tumor suppressor that controls the expression of hundreds of genes, especially those involved in G1/S progression. RB1 binds and sequesters the E2F family of transcription factors in G1 phase. In late G1 CDKs hyper-phosphorylate RB1 (pRB), which leads to the release of E2F transcription factors and increased expression of genes required for the G1/S transition and S phase progression (Dyson, 2016). RB1 is frequently mutated in certain tumors, with highest rates of mutation in retinoblastoma, osteosarcoma, and small-cell lung cancers (Dyson, 2016). RB1 mutations are often inactivating but could also increase the phosphorylation of RB1 (Dyson, 2016). In addition, E2F gene loci are amplified and have increased protein expression levels in several cancers (Chen et al., 2009a). Therefore, a strong correlation between high *CDC7* expression and E2F pathway genes could be caused by mutation of RB1 or other pathways that activate the E2F family of transcription factors.

We first tested if RB1 mutation is correlated with high or low DDK expression. Mutational Signature analysis (using MutSig) of tumors from the top-10 *CDC7*-high expressing patients showed that RB1 was among the most highly mutated genes (**Figure 3.3 C**). We then directly tested for the over-representation of RB1 mutant patients within the high and low DDK expression patient groups (hypergeometric test). RB1 had significantly increased rate of mutation in patients with tumors that express high levels of *CDC7*, *DBF4*, or *DBF4B* (**Figure 3.3 A, E**). There was no significant correlation between RB1 mutation and the low *CDC7* expression group (**Figure 3.3 E**). In line with previous findings, DDK expression levels were also strongly correlated with mutations

in p53 (Figure 3.3 A, E). These data strongly suggest that RB1-E2F promotes the expression of DDK in tumor cells. We queried whether E2F family members bind to the CDC7 or DBF4 promoter using publicly available ChIP-Seq datasets. We first searched for E2F transcription factor binding at CDC7 or DBF4 promoter sites using ENCODE-annotated data. Binding of E2F transcription factors at their well-known target gene MCM4 are shown as positive controls (Figure 2C). E2F1, E2F4, and E2F6 transcription factors showed very tight binding at CDC7 and DBF4 promoter regions (Figure 3.4 C, D, E). This finding was verified by E2F ChIP-Seq from multiple cancer cell lines (data not shown). Moreover, analysis of raw ChIP-Seq data also showed binding of E2F3 at CDC7 and DBF4 promoter sites (Kong et al., 2007; Liu et al., 2015). Binding by transcriptional activators (E2F1, E2F3) and repressors (E2F4, E2F6) could be indicative of different phases of cell cycle in an asynchronous cell population since E2F target promoters can be occupied by different E2Fs in a cell cycle dependent manner (Bertoli et al., 2013). A previous report showed that E2F1, 2, and 3 bound to the human DBF4 promoter and promoted DBF4 expression in an atypical manner that was independent of consensus E2F-binding sites (Yamada et al., 2002). The RB1 mutational and E2F ChIP-Seq data is evidence that both CDC7 and DBF4 expression are driven by E2F family members and can explain why RB1 mutations are so strongly correlated with high DDK expression.

Figure 3.4. E2F family of transcription factors strongly bind DDK promoters.

# A

# RB1-E2F pathway

Curated Gene Sets	Brief Description	FDR q-val
KONG_E2F3_TARGETS	Genes up-regulated in MEF cells (embryonic fibroblasts) at 16 hr after serum stimulation and knockdown of E2F3 by	0
ISHIDA_E2F_TARGETS	Genes up-regulated in MEF cells (embryonic fibroblast) after expression of E2F1 or E2F2.	0
CHICAS_RB1_TARGETS_GROWING	Genes up-regulated in growing IMR90 cells (fibroblast) after knockdown of RB1 by RNAi.	0
EGUCHI_CELL_CYCLE_RB1_TARGETS	RB1target genes involved in cell cycle regulation: genes down-regulated by doxorubicin only in cells expressing RB1.	0
VERNELL_RETINOBLASTOMA_PATHWA	Cluster 1: genes up-regulated by RB1, CDNK2A, and one of the E2Fs (E2F1, E2F2, or E2F3).	0
REN_BOUND_BY_E2F	Genes whose promoters were bound by E2F1 and E2F4 in the primary fibroblasts WI-38, by ChIP on chip assay.	0
OLSSON_E2F3_TARGETS_DN	Genes down-regulated in the 5637 cell line (bladder cancer) after knockdown of E2F3 by RNAi.	0

# В

# RB1-E2F Pathway

Oncogenic Signature Gene Sets	Brief Description	FDR q-val
RB_P107_DN.V1_UP	Genes up-regulated in primary keratinocytes from RB1 and RBL1 skin specific knockout mice.	0
E2F3_UP.V1_UP	Genes up-regulated in primary epithelial breast cancer cell culture over- expressing E2F3 gene.	0
E2F1_UP.V1_UP	Genes up-regulated in mouse fibroblasts over-expressing E2F1	0
RB_P130_DN.V1_UP	Genes up-regulated in primary keratinocytes from RB1 and RBL2 skin specific knockout mice.	3.22E-04

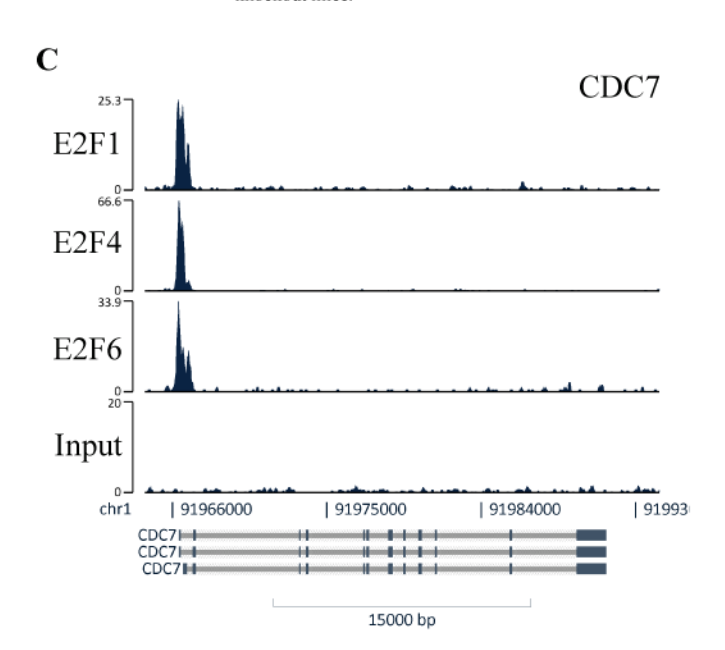
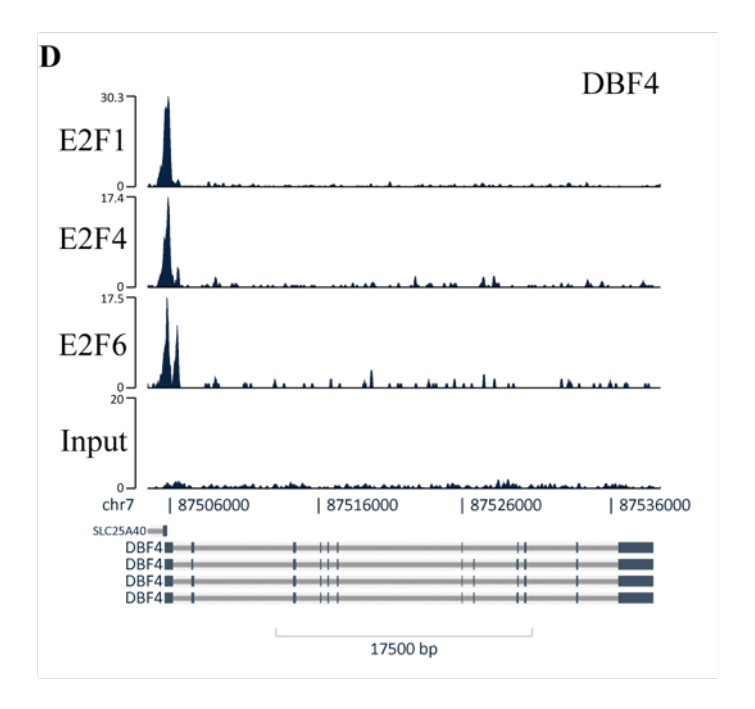
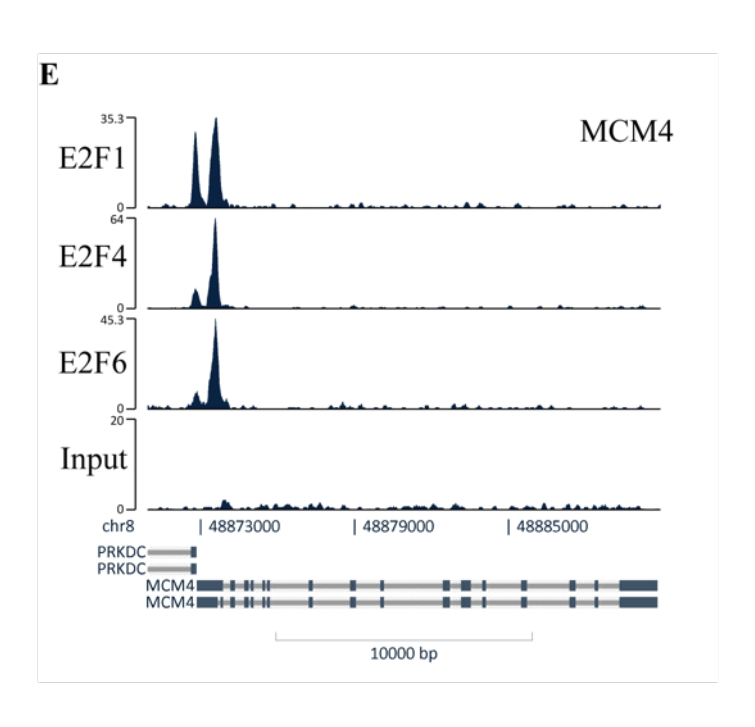


Figure 3.4 (cont'd)





**Figure 3.4 (cont'd).** Gene set enrichment analysis was performed using the gene expression signature derived from a comparison of the top 10 CDC7-high tumors with the bottom 10 CDC-low tumors. Shown here are curated gene sets involved in RB1-E2F pathway (**A**) and oncogenic gene sets (**B**) involved in RB1-E2F pathway. The HeLa-S3 ChIP-Seq data was obtained from ENCODE database and E2F binding analyzed using EaSeq software. (**C**, **D**, **E**). E2F ChIP-Seq signal intensities at the promoter regions of CDC7 (**C**), DBF4 (**D**), and MCM4 (**E**).

# Functional RNAi screen to identify mediators of apoptosis induced following DDK inhibition

Preclinical studies in human cell lines and murine models have demonstrated the therapeutic potential of inhibiting DDK in tumor cells (Montagnoli et al., 2004; Montagnoli et al., 2008). DDK inhibition induces a reversible G1/S cell cycle arrest in normal cells but induces apoptosis in many diverse types of tumors cells through an unknown signaling pathway. Apoptosis is not accompanied by CHK1 and CHK2 kinase activation, which can signal cell death when lethal amounts of DNA damage or irreversible replication fork arrest occurs. The apoptotic response also occurs independently of p53 status. These results suggest that a novel apoptotic pathway is engaged upon DDK inhibition.

To identify mediators of this pathway we used an RNAi screen against all human kinases and phosphatases to test their involvement in cell death upon DDK inhibition. We used the prototype small molecule DDK inhibitor PHA-767491 (DDKi) to inhibit DDK activity in the HCC1954 breast cancer cell line. This cell line was selected from a panel of cancer cell lines that express high levels of DDK based on its reproducible and robust apoptotic response to the DDKi. HCC1954 cells were transfected with pooled siRNAs against individual kinases and phosphatases followed by the addition of DDKi (Figure 3.5) and measurement of cell viability after 72 hours. We screened for instances where knockdown of a target gene prevented the loss of viability induced upon DDK inhibition. The screen was performed in duplicate and was highly reproducible (Figure 3.5 A). The primary screen resulted in 56 hits with a robust Z-score ≥ 2 and 17 hits with Z-scores ≤ -2, i.e. 2 standard deviations above (or below) the median cell viability measurement (Figure 3.5 B). Hits with positive Z-scores (potential mediators of cell death) were ranked using three separate gene ranking software to narrow the list to 41 hits (Figure 3.5 C) (also see experimental procedures). All hits with robust Z-score greater than 3 were included in our list of

41 genes for further analysis regardless of this secondary ranking. These 41 hits were then rescreened in secondary assays with deconvoluted sets of siRNA (4 individual siRNAs per gene) using an assay similar to the primary screen. We then used an alternate readout for cell death by directly measuring the Caspase 3/7 activity of the cell. In this secondary screen in HCC1954 cells we confirmed 29 of the 41 hits from the primary screen (Figure 3.5 D). Finally, we also screened the 41 hits in the independent HeLa cervical cancer cell line for their ability to mediate cell death in response to DDKi. Of the 41 targets tested we identified 23 genes whose knockdown in HeLa cells also prevented the loss of viability induced upon DDK inhibition (Figure 3.5 D). Therefore, we identified multiple potential mediators of the cell death pathway induced upon DDK inhibition. We point out that an earlier study identified the stress kinase p38 MAPK as required for apoptosis following CDC7 siRNA-mediated knockdown in HeLa cells (Im and Lee, 2008). We did not identify p38 MAPK in our initial RNAi screen in HCC1954 cells but we carried it forward nonetheless in the secondary screens. The p38 knockdown did not rescue cell death in the HCC1954 in the secondary screen nor in the HeLa cell line. We cannot explain this discrepancy although another group also found that p38 inhibition did not prevent apoptosis in HeLa cells but instead they found that p38 inhibition actually enhanced apoptosis following DDKi (using PHA-767491) in multiple myeloma cancer cell lines (C. Santocanale, personal communication).

We also identified a small set of genes whose knockdown exacerbated the cell death upon DDK inhibition (hits with Z-scores <= -2). While knocking down some of these genes could result in cell death regardless of DDK inhibition, others might sensitize tumors cells to DDK inhibition. The hits included genes essential for cell growth and division like CSNK1D, CKS1B, SRC, ERBB2, and JAK2. The top hit, PPP2R2B (PP2A-B55β), is an isoform of the Protein Phosphatase 2A (PP2A)-B55 holoenzyme. In fission yeast, Drosophila, Xenopus, and mammalian cells PP2A-

B55 phosphatase inhibits mitotic entry by dephosphorylating both CDC25 phosphatase (inactivating it) and WEE1 kinase (activating it) (Chica et al., 2016; Mochida et al., 2009; Ruvolo, 2016). Inactive CDC25 phosphatase and active WEE1 kinase results in persistent inhibitory phosphorylation of CDK and inhibition of mitotic entry. Therefore, aberrant entry into mitosis might sensitize tumors cells to DDK inhibition. A similar strategy of forced mitotic entry was recently shown to increase tumor sensitivity to ATR inhibitors (Ruiz et al., 2016).

# Proteins involved in mitotic progression are enriched among hits obtained from primary screen

Several hits with positive Z-scores (potential mediators of cell death) are known to be involved in apoptosis or stress response pathways. NME1 is one of only two known mammalian protein histidine kinases (Fuhs et al., 2015). NME1 (also known as NM23-H1 or Nucleotide Diphosphate Kinase) is involved in cellular nucleotide triphosphate homeostasis and was the first identified metastasis suppressor gene (Fuhs et al., 2015). It is also required for maintaining genomic stability, cytokinesis (Conery et al., 2010), and UV-induced DNA repair (Jarrett et al., 2012). Given that DDK also maintains genome stability and regulates error prone repair of UV lesions, NME1 is a potentially interesting mediator of cell death upon DDK inhibition. Knockdown of MAP3K9 also led to rescue of DDKi-mediated cell death. Somatic inactivating mutations in MAP3K9 gene are common in metastatic melanomas and also result in increased chemoresistance (Stark et al., 2012).

To identify potential shared pathways, we used the 29 confirmed hits in HCC1954 cells (Figure 3.5 D) and performed a gene set enrichment analysis (Figure 3.5 E). Due to the inherent bias in the screen (only kinases and phosphatases were targeted) this analysis was not very powerful. Despite this limitation we found that several proteins required for efficient mitotic

progression were enriched in our data set (Figure 3.5 E). The top hit in our screen was Cyclin G associated kinase (GAK). It has important roles in centrosome maturation, chromosome segregation, and clathrin mediated membrane trafficking (Naito et al., 2012; Shimizu et al., 2009). GAK phosphorylates and increases the activity of PP2A-B56 holoenzyme, which is required for mitotic progression (Naito et al., 2012). Importantly, RNAi-mediated knockdown of GAK induces cell cycle arrest at metaphase and activation of the spindle assembly checkpoint (Shimizu et al., 2009). Interestingly, we also identified a component of the PP2A-B56 holoenzyme in our screen, PPP2R5B (Figure 3.5 C, D). PP2A holoenzyme is composed of a catalytic subunit (PPP2CA-B), a regulatory subunit (PPP2R1A), and a substrate targeting subunit (PPP2R5A-E). PP2A-B56 is essential for proper chromosome alignment during metaphase, activation of anaphase promoting complex, and therefore for mitotic progression (Craney et al., 2016; Foley et al., 2011). Another recent finding using budding yeast has shown that PP2A-B56 yeast homolog (Rts1) could be redundant with CDC25 phosphatase in promoting entry into mitosis by dephosphorylating CDK1(Kennedy et al., 2016). CDC25B phosphatase was also identified in our screen (Figure 3.5) C, D). Taken together, these hits strongly suggest that preventing mitotic progression upon DDK inhibition can protect against cell death.

Figure 3.5. RNAi screen to identify mediators of cell death induced upon DDK inhibition.

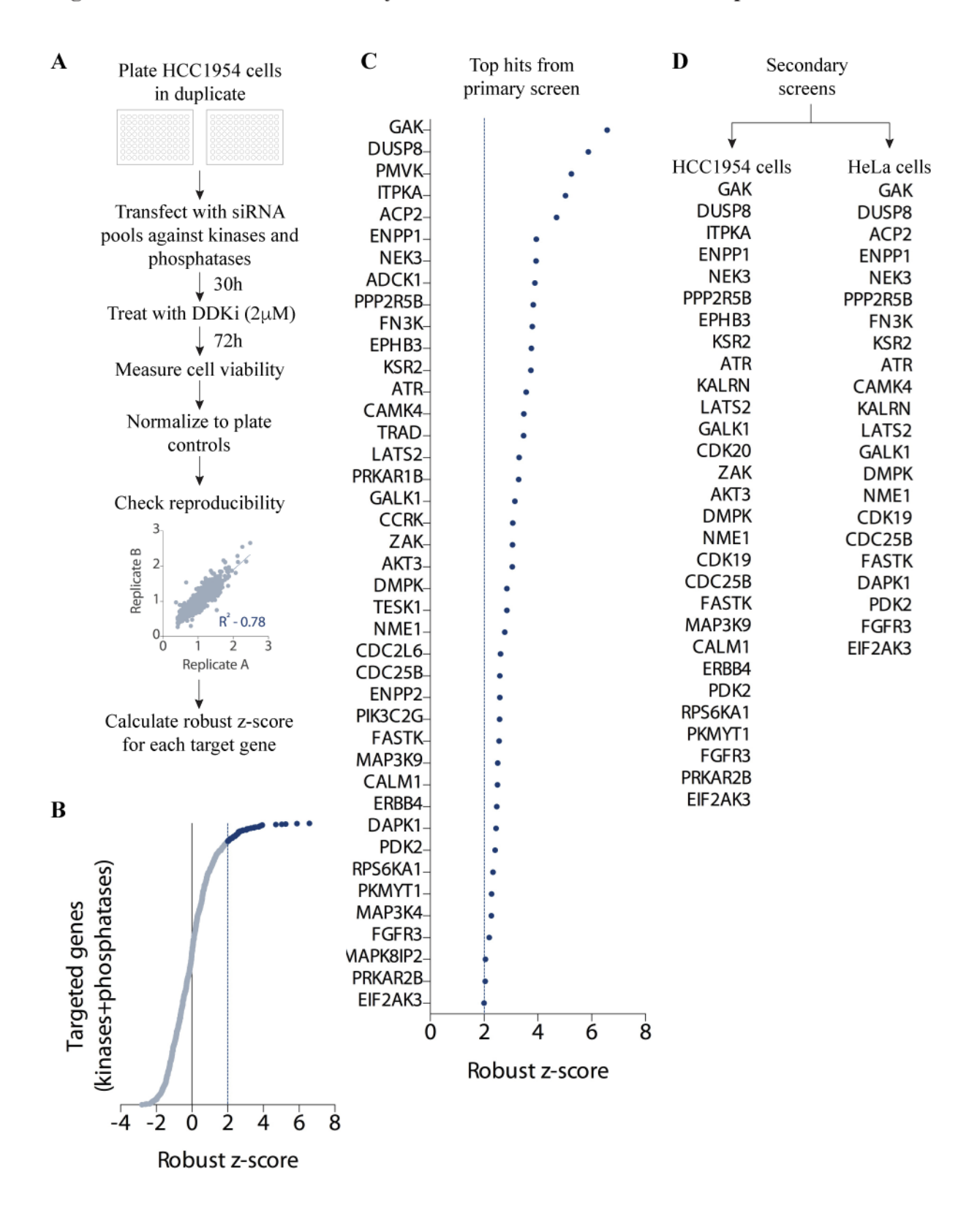


# Figure 3.5 (cont'd)

 $\mathbf{E}$ 

1				
	Gene Set Enrichment Analysis		Ingenuity Pathway Analysis	
	Description	FDR q-val	Description	p-val
	G2/M checkpoint	2.63x10 <sup>-4</sup>	Cell Cycle: G2/M DNA Damage Checkpoint Regulation	6.13E-07
	Candidate substrate proteins of AURKA	1.55x10 <sup>-3</sup>	CREB Signaling in Neurons	8.86E-05
	Genes involved in G2/M phases	3.67x10 <sup>-3</sup>	Sertoli Cell-Sertoli Cell Junction Signaling	1.03E-04
	Genes involved in Cyclin A/B1 associated events during G2/M	6.55x10 <sup>-3</sup>	Mitotic Roles of Polo-Like Kinase	1.05E-04
	Genes involved in Cell Cycle, Mitotic	7.73x10 <sup>-3</sup>	Superpathway of Inositol Phosphate Compounds	1.41E-04

**Figure 3.5 (cont'd). (A)** Outline of the RNAi screen. **(B)** Scatter plot of all targeted genes. Hits with robust Z scores > 2 are highlighted in blue. **(C)** List of top 41 hits from the primary screen. **(D)** Hits validated by secondary screens in HCC1954 cells or HeLa cells. **(E)** G2/M and Mitotic gene sets enriched in hits validated in **(D)**.

### LATS2 kinase mediates cell death upon DDK inhibition

LATS2 kinase, a Hippo signaling component, was among the top positive Z-score hits identified in our siRNA screen. LATS1 and LATS2 kinases are functionally related tumor suppressors involved in mediating growth inhibitory signals in response to a variety of upstream cues (Meng et al., 2016). Both kinases, however, also have roles independent of each other (Hergovich, 2013). LATSI was not recovered in our screen and LATSI knockdown did not rescue cell death upon DDK inhibition (Figure 3.6 A, B). We confirmed the role of LATS2 kinase in mediating cell death upon DDK inhibition using four separate siRNAs against LATS2 (Figure 3.6 **A, B).** The extent of apoptotic rescue seen with LATS2 siRNAs exactly correlated with their knockdown efficiencies, with siRNA#1 showing the strongest knockdown as well as the strongest rescue phenotype (Figure 3.6 A, B). To better visualize LATS2 on the immunoblots we also knocked down LATSI (Meng et al., 2016). Because the DDK inhibitor used to induce cell death could have off target effects, we independently confirmed that LATS2 mediated cell death in response to DDK inhibition following siRNA-mediated knockdown of CDC7. LATS2 knockdown was able to rescue cell death induced by CDC7 siRNA as seen by the rescue of PARP cleavage (Figure 3.6 C). LATS1 knockdown did not have a similar effect on PARP cleavage (Figure 3.6 **D).** We then tested if the upstream kinases involved in the Hippo pathway have a role in DDKmediated apoptosis. MST1 and MST2 are human orthologs of the *Drosophila* Hippo kinase (Meng et al., 2016). These two kinases phosphorylate and activate LATS1/LATS2 kinases. Knockdown of MST1 or MST2 or both did not prevent DDKi-induced cell death (Figure 3.6 E) and neither were identified in our screen. A very recent study has found that MST1 and MST2 are not essential for phosphorylation of LATS1/LATS2 (Meng et al., 2015) and that MAP4K can activate LATS1/LATS2 in parallel with MST1/MST2 (Meng et al., 2015). So although MAP4K kinase

may function to activate LATS2, it also was not identified in our screen. Taken together, our data show that LATS2 is required to promote apoptosis in response to DDK inhibition but it may be activated through an unknown signaling kinase. On the other hand, it is possible that MST1/MST2 functions are redundant with MAP4K for LATS2-dependent apoptosis in this system.

The principal downstream target of the LATS1 and LATS2 kinases is the transcription factor, YAP. Phosphorylation of YAP by LATS1 or LATS2 causes it to be sequestered in the cytoplasm and/or degraded by the proteasome (Meng et al., 2016). As a surrogate for basal LATS2 activity we looked at a canonical YAP phosphorylation site S127 (pYAP S127). Two renal cancer cell lines 786-O and ACHN have inactivating deletions in the Hippo signaling gene SAVI, which acts together with MST1/MST2 upstream of LATS2 kinase (Tapon et al., 2002). We reasoned that these cell lines would therefore have reduced basal levels of LATS2 activity. We probed 786-O and ACHN cells for pYAP S127 levels and found S127 phosphorylation was significantly reduced compared to HCC1954 cells (Figure 3.6 F). Therefore, these cell lines likely also have reduced LATS2 activity and therefore might be resistant to DDK inhibition. We found that both 786-O and ACHN cells had significantly lower rate of cell death (Caspase 3/7 activation) in response to DDK inhibition when compared to the HCC1954 cells (Figure 3.6 G). This was not due to a generalized defect in promoting apoptosis as all three cell lines were equally capable of undergoing apoptosis in response to etoposide, a topoisomerase inhibitor that induces dsDNA breaks and cell death (Figure 3.6 G). Our results show that LATS2 kinase promotes cell death downstream of DDK inhibition through an alternate Hippo signaling pathway. Interestingly, Hippo signaling has previously been shown to induce apoptosis under conditions of stress and LATS2 can promote apoptosis through p53 stabilization and in polyploid cells (Hamilton and O'Neill, 2013). Since LATS2 kinase promotes apoptosis in both breast cancer (HCC1954) and cervical cancer (HeLa)

cell lines, which are both p53 deficient cells, the mechanism of apoptotic induction is likely mediated through another target. Given that ATR is activated and required for apoptosis in response to DDKi, it is tempting to speculate that ATR may directly phosphorylate LATS2 and promote this activity since the MST1, MST2, and MAPK4 kinases are not required for apoptosis. Indeed, there are multiple [ST]Q sites in the C-terminus of LATS2 that could be phosphorylated by ATR. Further studies will be required to understand how LATS2 kinase is activated in response to DDKi and how LATS2 (and the various other kinases/phosphatases we identified) alter the normal apoptotic response.

Figure 3.6. LATS2 mediates cell death upon DDK inhibition.

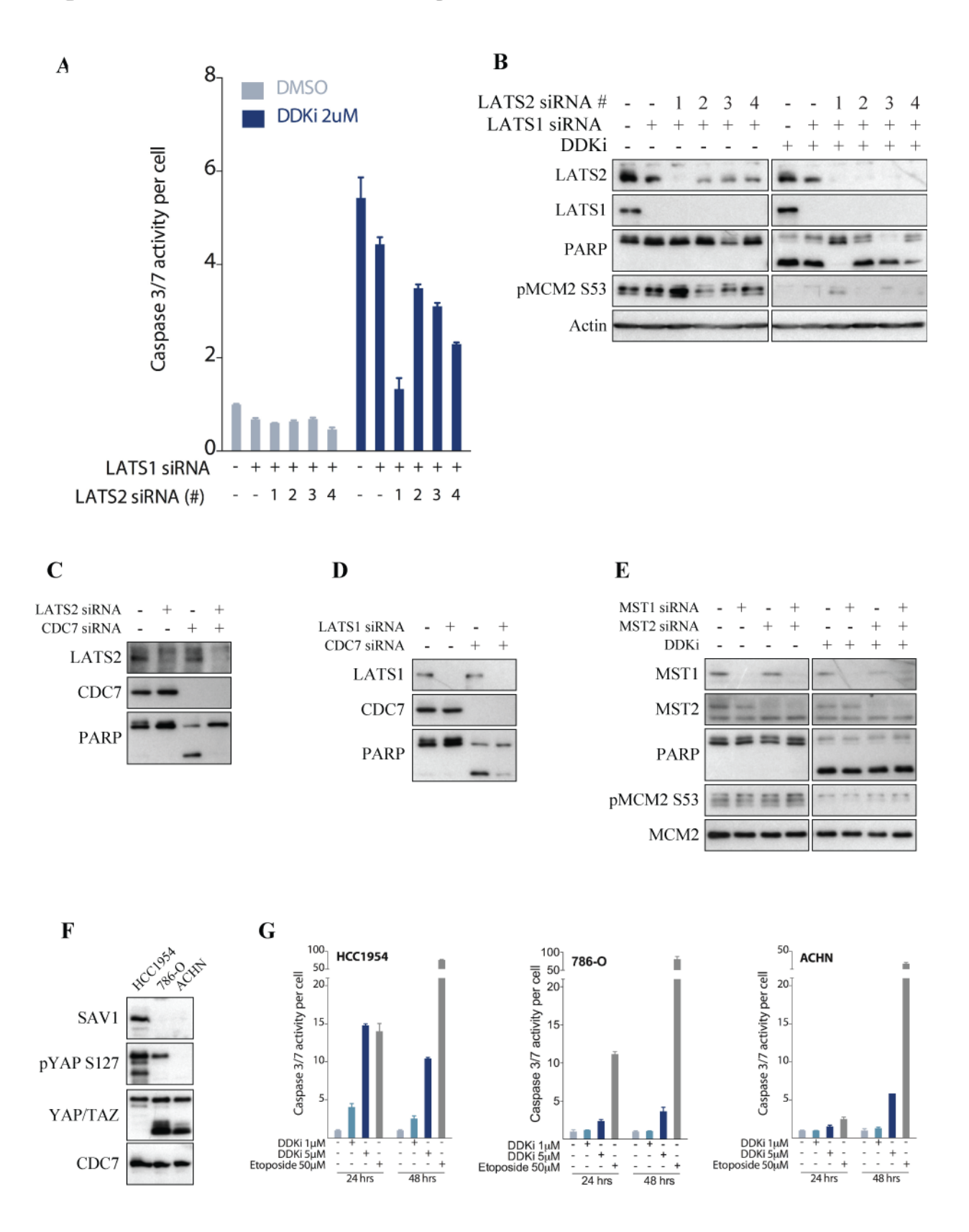


**Figure 3.6 (cont'd). (A, B)** HCC1954 cells were transfected with the indicated siRNAs, 48h later treated with DDKi for 8h and harvested for Caspase 3/7 analysis **(A)** or western blot **(B)**. **(C, D)** HCC1954 cells were transfected with the indicated siRNAs, 72h later harvested for western blot. **(E)** HCC1954 cells were transfected with the indicated siRNAs, 48h later treated with DDKi for 8h and harvested for western blot. **(F)** Sub-confluent population of HCC1954, 786-O, and ACHN were harvested and subject to western blot. **(G)** HCC1954, 786-O, and ACHN cells were plated in 96 well plates, treated with indicated drugs, and Caspase3/7 activity measured at indicated times.

### **MATERIALS AND METHODS**

## Computational data analysis

RNA-seq gene expression profiles of primary tumors and relevant clinical data of 488 lung adenocarcinoma patients were obtained from the Cancer Genome Atlas (TCGA LUAD; cancergenome.nih.gov). The Cox proportional hazards regression model was used to analyze the prognostic value of the CDC7, DBF4, and DBF4B expression across all patients within the TCGA LUAD cohort, in the context of additional clinical covariates. All univariate and multivariable analyses were conducted within a 5-year survival timeframe. The following patient and tumorstage clinical characteristics were used: Gene expression (CDC7, DBF4, DBF4B; log2, continuous); Gender (male vs. female); Age (years, continuous); Smoking History (reformed > 15yrs vs. non-smoker, reformed < 15yrs vs. non-smoker, current smoker vs. non-smoker); Mutational Load (derived as the number of non-silent mutations per 30Mb of coding sequence, continuous); Union for International Cancer Control (UICC) TNM Stage specification (Stage III/IV vs. I/II); UICC T score specification (T2 vs. T1, T3/T4 vs. T1); UICC N score specification (N1/N2 vs. N0). Hazard ratio proportionality assumptions for the Cox regression model were validated by testing for all interactions simultaneously (p = 0.2453). Interaction between CDC7 expression and TNM stage, T score, and N score (significant covariates in the model) were tested using a likelihood ratio test (LRT) to contrast a model consisting of both covariates with another model consisting of both covariates plus an interaction term. No statistically significant difference was found between the two models (TNM: p= 0.6878, T score: p= 0.4766, N score: p= 0.5044; likelihood ratio test).

Empirical Cumulative Distribution Function (ECDF) plots were generated to compare gene expression levels across matched normal and tumor samples (n=57) in the TCGA LUAD cohort. Standardized (z-scores) gene expression values across normal and tumor samples were used and the Kolmogorov-Smirnov (KS) test was used to assess statistical significance. The Mann-Whitney-Wilcoxon test was used to assess statistically significant differences in mutational load between patients with high CDC7 (alternatively DBF4, DBF4B) expression (top 25%, n=122) and low CDC7 (alternatively DBF4, DBF4B) expression (bottom 25%, n=122).

MutSig (Lawrence et al., 2013) was used to identify recurrently mutated genes within the CDC7 high- and low-expression patient groups (n=122) with respect to the background mutational rate in covariate space. Additionally, the statistical significance of patients with mutations in a given gene represented with each of the high- and low-expression groups was assessed using the hypergeometric test (with the total of all patients in the cohort assessed for mutations as the universe). Similar analyses were conducted for patient groups with high- and low- DBF4 and DBF4B expression.

A gene expression signature comprised of differentially expressed genes between patients in the highest CDC7 expression group (n=10) compared to those in the lowest expression group (n=10) was derived using a blind source separation strategy described earlier in (Dimitrova et al., 2016; Li et al., 2015). Subsequent enrichment analyses were performed using Gene Set Enrichment Analysis (GSEA) (Subramanian et al., 2005) and MSigDB (Liberzon et al., 2015). GSEA and Ingenuity Pathway Analysis (IPA, QIAGEN Redwood City, CA) were used for enrichment analyses of targets assessed from RNAi screens.

All statistical analyses were conducted in R (www.R-project.org) and all survival analyses were conducted using the survival package in R.

### ChIP-seq data analysis

HeLa-S3 ChIP-seq data for E2F1, E2F4, E2F6, and input were downloaded from the ENCODE website under accession number ENCFF000XDA (E2F1), ENCFF000XDB (E2F4), ENCFF000XDH (E2F6), and FF459QXO (input). Data analysis and visualization was performed using EaSeq software (Lerdrup et al., 2016).

# Cell lines and reagents

HCC1954 (ATCC), 786-0 (NCI-60), and ACHN (NCI-60) cells were cultured in RPMI-1640 media supplemented with 10% heat inactivated (HI) FBS, 50units/ml of penicillin, and 50½ g/ml of streptomycin. HeLa cells (ATCC) were cultured in MEM supplemented with Earle's salts, 2mM glutamine, 10% HI-FBS, 1.5 g/L sodium bicarbonate, 0.1mM non-essential amino acids, 1mM sodium pyruvate, 50 units/ml of penicillin, and 50µg/ml of streptomycin. The DDK inhibitor, PHA-767491, was synthesized as described previously (Sasi et al., 2014). Etoposide (#341205) was from EMD Millipore. The antibodies were purchased as indicated: CST: PARP (#9542), LATS1 (#3477), MST1 (#3682), MST2 (#3952), SAV1 (#13301), YAP/TAZ (#8418), pYAP S127 (#13008); Bethyl Laboratories Inc.: pMCM2 S53 (A300-756A), MCM2 (A300-122A), LATS2/LATS1 (A300-479A); MBL International Corporation: CDC7 (K0070-3S); Sigma: β-actin (A5441); GE Healthcare: anti-mouse-HRP (NA931V), and anti-rabbit-HRP (NA934V).

## Primary RNAi screen

HCC1954 cells were plated in white-walled, white-bottom 96 well plates (2500/well) and allowed to grow for 24h before transfection. Forward transfection with 25nM pooled-siRNA (4

siRNAs) was performed using Oligofectamine (Invitrogen, 2µl/ml final concentration) in duplicate 96-well plates. 30 hours after transfection cells were treated with fresh media containing DMSO or 2μM DDKi. 72 hours later, growth media was removed and 50 μl of CellTiter-Glo (diluted 1:1 in PBS at room temperature) was added to each well. Luminescence was measured using EnVision 2104 Multilabel Reader (PerkinElmer) 10 minutes after addition of 'Glo' reagent. Three to six wells of negative control (cells transfected with non-targeting siRNA and treated with 2µM DDKi), positive control (cells transfected with non-targeting siRNA and treated with 2µM DDKi+50µM caspase inhibitor zVAD), and transfection control (cells transfected with 25nM ACDC siRNA) were included in each plate. Loss of viability in ACDC siRNA-treated wells (transfection control) was indicative of efficient transfection in each plate. Viability values from the positive and negative controls in each plate were used to calculate Z'-factor (Zhang et al., 1999). All plates had Z'-factor ~0.5 or above, which is indicative of a robust assay with wide separation between positive and negative control values. Raw luminescence values were normalized to the median of each plate (controls were excluded). The normalized values from each plate were subsequently used to calculate robust z-scores as described previously (Birmingham et al., 2009). An arbitrary threshold of z-score>=+2 or z-scores <=-2 was set for hit selection. Only hits with positive z-scores (potential mediators of cell death) were considered for further analysis (56 hits). Gene ranking software GPSy (Britto et al., 2012), Endeavor (Tranchevent et al., 2008), and ToppGene (Chen et al., 2009b) were used to rank hits and some of the low ranking hits were removed from further analysis. All hits with z-scores>=+3 were included irrespective of their ranks. The final list of 41 genes is shown in Figure 3.5 C.

# Secondary RNAi screen

Using a library of 164 deconvoluted siRNAs (4 siRNAs against 41 hits) a secondary screen identical to the primary RNAi screen was performed in HCC1954 cells. A second assay was performed in parallel using caspase 3/7 activity as a direct indicator of apoptosis. Both assays were performed in duplicate and were highly reproducible. The Z'-factor for each plate was calculated as described above. Z-scores were calculated for each hit/siRNA and an arbitrary threshold for hit selection was set for each assay as indicated. 24 (58.5%) of the 41 hits rescreened with at least 2 separate siRNAs. An additional set of 5 hits that rescreened with only one siRNA in *both* viability and apoptosis assays were also included in the final analysis. The list of 29 hits is shown in Figure 3D. Cell line specific effects were tested by performing the secondary screen in HeLa cervical cancer cell line. The assay was performed similar to the secondary screen in HCC1954 cells. Due to higher cytotoxicity in HeLa cells siRNAs were used at a final concentration of 10nM instead of 25nM used in HCC1954 cells. The Z'-factor for each plate was calculated as described above. 23 of the 41 hits rescreened with at least one siRNA and the genes are listed in Figure 3.5 D.

#### RNAi interference

Cells were plated in 6-well plates (75000 cells/well) and allowed to grow for 36h before transfection. siRNA transfection was performed with Lipofectamine RNAiMAX (Invitrogen) according to manufacturer's instructions. Each well was transfected with 2µl transfection reagent and a final siRNA concentration of 25nM in a total volume of 2ml. Media was replaced 24 hours after transfection and the cells were either harvested or exposed to indicated treatments 48h after transfection. Following siRNAs were used: *CDC7* (CDC7-L1, Dharmacon custom siRNA, GGCAAGATAATGTCATGGGA), *LATS1* (Qiagen, SI02223655), *LATS2* # 1 (Qiagen,

SI02660154), LATS2 # 2 (Qiagen, SI02660161), LATS2 # 3 (Qiagen, SI02660168), LATS2 # 4 (Qiagen, SI02660385), MST1 (Qiagen, SI02622270), MST2 (Qiagen, SI02622256).

## **Immunoblotting**

Whole cell extracts were prepared by re-suspending the pellets in RIPA buffer (150mM NaCl, 1% NP-40, 0.5% sodium deoxycholate, 0.1% SDS, 50mM Tris-HCl, pH 8) containing protease inhibitors (100μM PMSF, 1mM Benzamidine, 2.5μg/ml Pepstatin A, 10μg/ml Leupeptin, and 10μg/ml Aprotinin) and phosphatase inhibitors (1mM each NaF, Na<sub>3</sub>VO<sub>4</sub>, Na<sub>2</sub>P<sub>2</sub>O<sub>7</sub>). Protein concentration was measured using the BCA protein assay kit (Pierce, #23227). Equal amounts of proteins were subjected to SDS-PAGE and transferred to nitrocellulose membrane (Millipore, HATF304F0). Transfer efficiency and equal loading was confirmed by Ponceau S staining. Membranes were blocked overnight at 4°C with 5% non-fat milk in TBS-T, followed by incubation in primary and secondary antibodies (1h at RT, 2% milk in TBS-T). Protein bands were visualized using SuperSignal West Pico solutions (Thermo Scientific).

# Analysis of Caspase 3/7 activity

For assays in 96 well plates 5000 cells were plated per well. 24 hours later cells were treated and incubated for the indicated period of time at 37°C. Caspase 3/7 activity and viable cell number were then measured using the Caspase-Glo 3/7 assay (Promega) and CellTiter-Glo assay (Promega), respectively. For assays in six well plates, cells were trypsinized and a suspension was made in 1ml of phosphate buffered saline. Thirty microliters of this suspension was mixed with 30µl of CellTiter-Glo and another 30µl was mixed with 30µl of Caspase-Glo 3/7 reagent. The 'caspase activity per cell' was obtained by normalizing total caspase activity to cell number.

Luminescence was measured using BioTek Synergy Microplate Reader 30 minutes after addition of 'Glo' reagents.

# ACKNOWLEDGMENTS

I would like to thank Dr. Arjun Bhutkar for the computational data analysis and Dr. Nathan J. Lanning for help with the RNAi screen.

# **CHAPTER 4.**

# THE POTENT CDC7-DBF4 (DDK) KINASE INHIBITOR XL413 HAS LIMITED ACTIVITY IN MANY CANCER CELL LINES AND DISCOVERY OF POTENTIAL NEW DDK INHIBITOR SCAFFOLDS

## Modified from

Sasi, N.K., Tiwari, K., Soon, F.F., Bonte, D., Wang, T., Melcher, K., Xu, H.E., and Weinreich, M. (2014). The potent Cdc7-Dbf4 (DDK) kinase inhibitor XL413 has limited activity in many cancer cell lines and discovery of potential new DDK inhibitor scaffolds. PLoS One 9, e113300.

#### **ABSTRACT**

CDC7-DBF4 kinase or DDK (DBF4-dependent kinase) is required to initiate DNA replication by phosphorylating and activating the replicative MCM2-7 DNA helicase. DDK is overexpressed in many tumor cells and is an emerging chemotherapeutic target since DDK inhibition causes apoptosis of diverse cancer cell types but not of normal cells. PHA-767491 and XL413 are among a number of potent DDK inhibitors with low nanomolar IC<sub>50</sub> values against the purified kinase. Although XL413 is highly selective for DDK, its activity has not been extensively characterized on cell lines. We measured anti-proliferative and apoptotic effects of XL413 on a panel of tumor cell lines compared to PHA-767491, whose activity is well characterized. Both compounds were effective biochemical DDK inhibitors but surprisingly, their activities in cell lines were highly divergent. Unlike PHA-767491, XL413 had significant anti-proliferative activity against only one of the ten cell lines tested. Since XL413 did not inhibit DDK-specific MCM2 phosphorylation in multiple cell lines, this compound likely has limited bioavailability. To identify potential leads for additional DDK inhibitors, we also tested the cross-reactivity of ~400 known kinase inhibitors against DDK using a DDK thermal stability shift assay (TSA). We identified 11 compounds that significantly stabilized DDK. Several inhibited DDK with comparable potency to PHA-767491, including CHK1 and PKR kinase inhibitors, but had divergent chemical scaffolds from known DDK inhibitors. Taken together, these data show that several well-known kinase inhibitors cross-react with DDK and also highlight the opportunity to design additional specific, biologically active DDK inhibitors for use as chemotherapeutic agents.

#### INTRODUCTION

The initiation of DNA replication is temporally divided into two phases during the cell cycle. First, an inactive form of the replicative MCM (mini-chromosome maintenance) helicase is loaded onto origin DNA in G1 phase and then activated upon entry into and during S phase by two sets of kinases: cyclin-dependent kinase and DBF4-dependent kinase (DDK) (Karim, 2010). DDK is a two-subunit Ser/Thr kinase composed of the CDC7 kinase and DBF4 regulatory subunits. DDK mediated phosphorylation of the six-subunit MCM2-7 (MCM) helicase is thought to bring about a conformational change in its structure leading to helicase activation (Hardy et al., 1997; Hoang et al., 2007). MCM activation is followed by localized DNA unwinding, recruitment of the replisome machinery and the initiation of bi-directional DNA synthesis (Karim, 2010). Other functions of DDK include facilitation of chromosomal segregation in mitosis and meiosis (Matos et al., 2008; Takahashi et al., 2008), the initiation of meiotic recombination (Sasanuma et al., 2008; Wan et al., 2008), and activation of DNA repair pathways including trans-lesion DNA repair (Day et al., 2010; Yamada et al., 2013b).

CDC7 is a serine/threonine kinase whose activity depends on association with its regulatory subunit, DBF4 (Jiang et al., 1999; Kumagai et al., 1999). DBF4 is a cell cycle regulated protein whose abundance peaks during S-phase and then is degraded by end of mitosis (Ferreira et al., 2000; Oshiro et al., 1999; Weinreich and Stillman, 1999b). Interaction with DBF4 is necessary for CDC7 ATP binding and substrate recognition (Kitamura et al., 2011). Like all protein kinases, the DDK crystal structure reveals an active site in a deep cleft between the N- and C-terminal lobes (Hughes et al., 2012; Huse and Kuriyan, 2002). The DBF4 Zn-finger ("motif C") binds to the N-terminal lobe of DDK and is necessary for human DDK activity. In contrast,

deletions of the budding and fission yeast DBF4 Zn-finger merely impair growth indicating that this motif is not essential for kinase activity (Fung et al., 2002; Harkins et al., 2009; Ogino et al., 2001). DBF4 motif M enhances its association with the CDC7 subunit and is required for the full activity of the kinase in yeast and humans (Harkins et al., 2009; Hughes et al., 2012; Ogino et al., 2001; Sato et al., 2003). DDK phosphorylates multiple subunits of the MCM helicase (Cho et al., 2006; Masai et al., 2006; Montagnoli et al., 2006a) and a recent study in budding yeast indicates that CDC7 and DBF4 physically interact with distinct subunits of the MCM2-7 complex (Ramer et al., 2013).

DDK is over expressed in a number of primary tumors and tumor cell lines (Bonte et al., 2008; Chen et al., 2013a; Cheng et al., 2013; Hou et al., 2012a, b; Malumbres, 2011; Menichincheri et al., 2010). DDK over expression has also been associated with poor prognosis in lung adenocarcinoma (Chapter 3), breast cancers (Choschzick et al., 2010), advanced clinical stage in ovarian carcinoma (Kulkarni et al., 2009), and with aggressive phenotype in papillary thyroid carcinomas (Fluge et al., 2006). Regulating the levels of DDK in tumor cells is an attractive tumor therapeutic strategy. Using neutralizing antibodies, Hunter and colleagues were the first to show that DDK depletion leads to severe disruption of DNA replication in HeLa cells (Jiang et al., 1999). Using small interfering RNAs, Santocanale and colleagues further showed that DDK depletion led to p53-independent apoptosis in HeLa cells whereas a normal human dermal fibroblast cell line underwent a reversible cell-cycle arrest (Montagnoli et al., 2004). HeLa cells were unable to arrest at the G1-S phase transition, progressing through a lethal S phase resulting in cell death via apoptosis. This finding has been corroborated in a number of different cell lines (Im and Lee, 2008; Ito et al., 2012; Tudzarova et al., 2010). Importantly, tumor cell death induced by depletion of DDK is not accompanied by the induction of known checkpoint markers. Similar cellular

responses are seen upon depletion of other components of the replication initiation machinery, including the Cdc6, Cdc45 and MCM2 subunits (Feng et al., 2003; Shreeram et al., 2002). The tumor cell specific killing observed by the depletion of DDK has aroused interest as a pharmaceutical target for cancer therapy. Efforts by multiple pharmaceutical companies have led to a number of small molecule DDK inhibitors (**Table 4.1**).

The first well-characterized DDK inhibitor was a pyrrolopyridinone molecule (PHA-767491, Table 1) (Montagnoli et al., 2008; Vanotti et al., 2008). It is a potent DDK inhibitor with an IC<sub>50</sub> of 10nM using purified kinase. PHA-767491 is also effective in vitro with an average cell proliferation  $IC_{50}$  of  $3.14\mu M$  in 61 tumor cell lines (Montagnoli et al., 2008). PHA-767491 also inhibits purified CDK9 with an IC<sub>50</sub> of 34nM but is a much less potent inhibitor of many other kinases tested (Montagnoli et al., 2008). Hence PHA-767491 is a dual DDK/CDK9 inhibitor. Recent studies have suggested that inhibition of CDK9, a kinase that targets RNA Polymerase II, might enhance the apoptotic response induced by PHA-767491 in some cell lines (Montagnoli et al., 2008; Natoni et al., 2013; Natoni et al., 2011). Modifications of this compound led to the identification of several other potent inhibitors of DDK with some exhibiting superior selectivity and sensitivity (Ermoli et al., 2009; Menichincheri et al., 2010; Menichincheri et al., 2009). XL413, a structurally distinct DDK inhibitor, is a benzofuropyrimidinone based compound with a reported IC<sub>50</sub> of 3.4nM against purified DDK and inhibits cell-proliferation of Colo-205 cells with an IC<sub>50</sub> of 2.69µM (Koltun et al., 2012). It was also highly selective for DDK when tested against a panel of 100 kinases (Koltun et al., 2012).

The increased activity and selectivity of XL413 over PHA-767491 was rationalized by the crystal structure of DDK in complex with the two DDK inhibitors (Hughes et al., 2012). One reason XL413 might be more specific inhibitor is that it made contacts with three of the most

variant residues in the kinase active site when compared to PHA-767491, which interacted with two of these residues. It was therefore unexpected to find that XL413 was not a particularly potent cell growth inhibitor in most of the cell lines we tested, since CDC7 is essential for cell cycle progression. XL413 inhibited proliferation and induced apoptosis in Colo-205 cells as shown previously (Koltun et al., 2012) but had little activity in 9 other tumor cell lines tested. Although both compounds are comparable biochemical DDK inhibitors, PHA-767491 exhibited superior activity to XL413 in cell lines. Analysis of DDK-specific MCM2 phosphorylation levels suggests that XL413 might have poor bioavailability in these and other cancer cell lines. To aid in the development of additional DDK inhibitors, we tested whether known protein kinase inhibitors (i.e., those not designed to inhibit DDK) exhibited cross-reaction with DDK. We screened ~400 compounds using a thermal stability shift assay (TSA) and identified 12 molecules that shifted the thermal stability of DDK, several with nearly equivalent potency as PHA-767491. compounds are therefore unlikely to be highly specific for a single target. Our data highlight the opportunity to design additional specific, biologically active DDK inhibitors for use as chemotherapeutic agents.

Table 4.1. DDK inhibitors synthesized by various pharmaceutical companies

Structure	IUPAC Chemical Name	DDK IC <sub>50</sub> (in vitro)	Cellular Proliferation IC <sub>50</sub>	Company
NH NH	2-pyridin-4-yl-1,5,6,7- tetrahydro-pyrrolo[3,2- c]pyridin-4-one	$10\mathrm{nM}$	3.17µM (average from 61 human cell lines) [42,43]	Nerviano Medical Sciences, Italy
100 NOT	[(S )-2-(2-aminopyrimidin- 4-yl)-7-(2-fluoro-ethyl)- 1,5,6,7- tetrahydropyrrolo[3,2-c ]pyridin-4-one	2nM	1.53μM (average from 12 human cell lines [46]	Nerviano Medical Sciences, Italy
N S S S S S S S S S S S S S S S S S S S	(5Z)-2-(Benzylamino)-5- (1H-pyrrolo[2,3-b]pyridin- 3-ylmethylene)-1,3-thiazol- 4(5H)-one	9nM	0.32μM (on A2780 cell line) [47]	Nerviano Medical Sciences, Italy
11,54	5-(2-Amino-pyrimidin-4- yl)-2-phenyl-1H-pyrrole-3- carboxamide	22nM	5.44µM (average from 16 human cell lines) [48]	Nerviano Medical Sciences, Italy
H <sub>3</sub> C CH <sub>3</sub> N N N N N N N N N N N N N N N N N N N	7,9-dimethyl-8-prop-2- enylpyrido[2,3]thieno[2,4- d]pyrimidin-4-amine	20nM	8.2µM (average from 3 human cell lines) [63]	Roche, USA
CI NOT NOT	(S)-8-chloro-2-(pyrrolidin- 2-yl)benzofuro[3,2- d]pyrimidin-4(3H)-one	3.4nM	2.7μM (Colo-205) [49]	Exelixis, USA
N NOTE NOTE OF THE NAME OF THE	1-(6-aminopyrimidin-4- yl)pyrrolo[2,3-b]pyridine- 6-carbonitrile	9nM	NA [64]	Amgen, USA

#### **RESULTS**

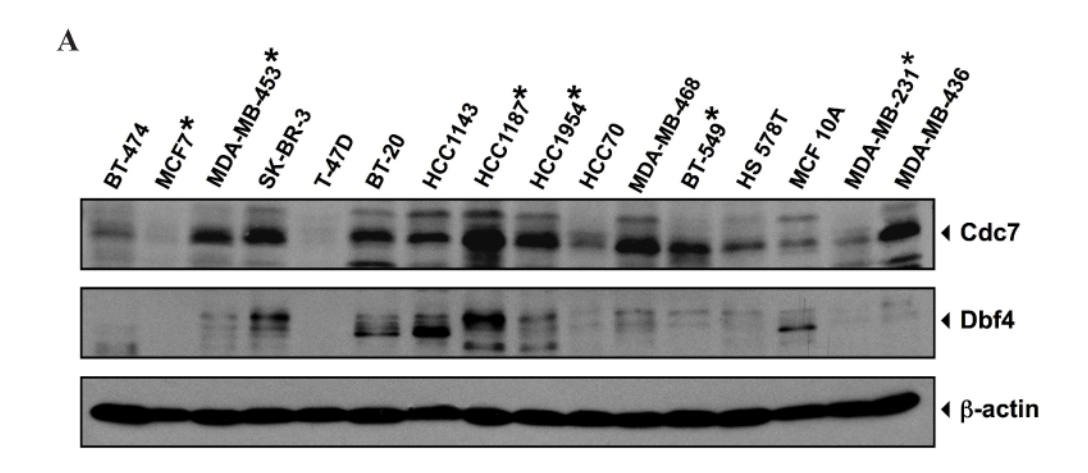
# DDK inhibitors exhibit very different cellular potencies

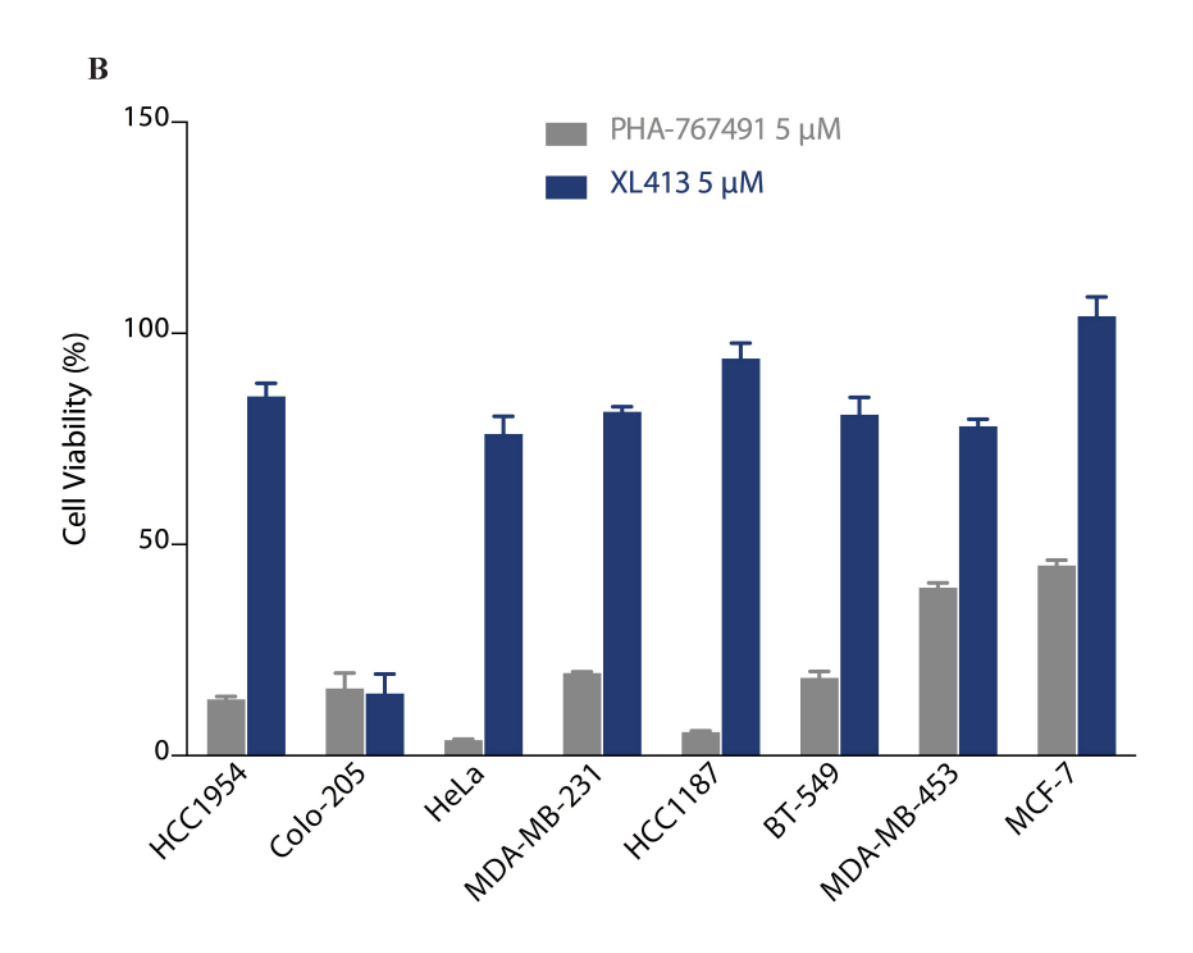
We screened a panel of 15 breast cancer cell lines for CDC7 and DBF4 expression using monoclonal antibodies against each subunit (Bonte et al., 2008). The majority of these express the DDK subunits equivalent to or higher than MCF10A, an immortalized but non-tumorigenic mammary epithelial cell line that served as a non-tumor control (Figure 4.1 A). We used PHA-767491 and XL413 to inhibit DDK in a panel of six breast cancer cell lines that overexpress DDK at various levels (marked with asterisks in **Figure 4.1 A**). Both compounds have been reported to have anti-proliferative activities in the low micromolar range (Koltun et al., 2012; Montagnoli et al., 2008). As controls, we compared these results to PHA-767491 treatment of HeLa cells and XL413 treatment of Colo-205 cells, which inhibit DDK and induce cell death. Since CDC7 kinase is an essential protein, inhibiting its activity should significantly slow or arrest cell proliferation. PHA-767491 significantly inhibited proliferation in all cell lines tested (Figure 4.1 B, values are plotted relative to vehicle controls). PHA-767491 was most effective on the HeLa and HCC1187 cell lines and had the least effect on the MCF-7 (Montagnoli et al., 2008) and the MDA-MB-453 cell lines: 2-fold and 2.5-fold inhibited, respectively. In contrast, XL413 was anti-proliferative only in the Colo-205 cells (Figure 4.1 B).

We then examined the potency profiles of both compounds in more detail using the XL413-sensitive (Colo-205) and XL413-resistant (HCC1954) cell lines. Cells were incubated in presence of increasing concentrations of the inhibitors for 72 hours at  $37^{0}$ C followed by cell viability measurements. PHA-767491 inhibited proliferation in both cell lines with an IC<sub>50</sub> of 0.64 $\mu$ M in HCC1954 cells and 1.3 $\mu$ M in Colo-205 cells (**Figure 4.1 C, E**). These values for PHA-767491 are

consistent with the average IC<sub>50</sub> value calculated using a panel of 61 tumor cell lines,  $3.17\mu M$  (Montagnoli et al., 2008). In contrast, XL413 had an IC<sub>50</sub> of 22.9 $\mu M$  in HCC1954 cells and  $1.1\mu M$  in Colo-205 cells (**Figure 4.1 C, E**). XL413 had minimal effects on two additional colorectal tumor cell lines and the other cell lines tested as seen by the very high IC<sub>50</sub> values (**Figure 4.1 G, H** and data not shown). In correspondence with the viability data, PHA-767491 induced apoptosis in both the HCC1954 and Colo-205 cells, but XL413 induced apoptosis in only the Colo-205 cells (**Figure 4.1 D, F**).

Figure 4.1. Two DDK inhibitors, PHA-767491 and XL413, exhibit differential activity against cultured tumor cells.





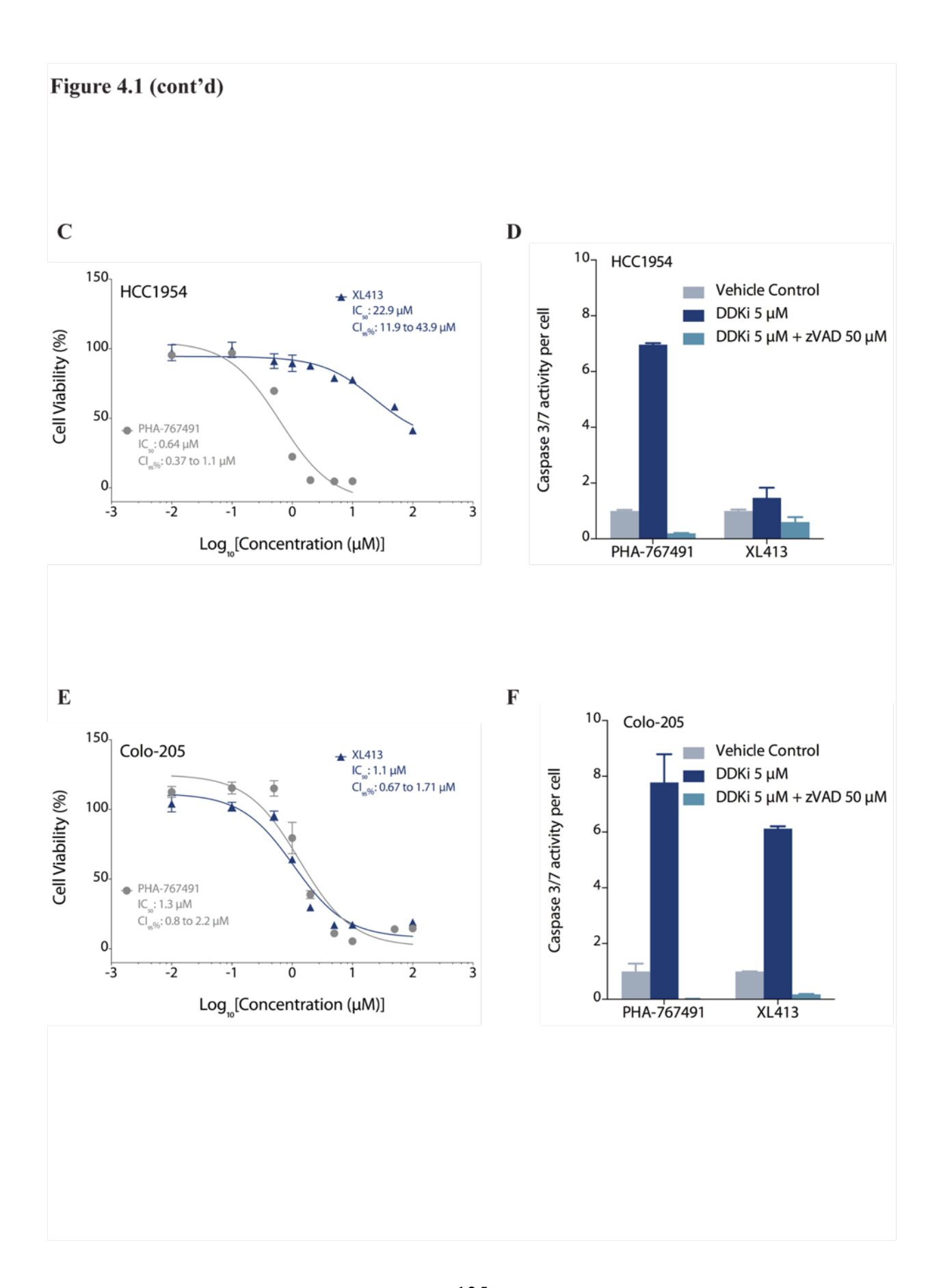
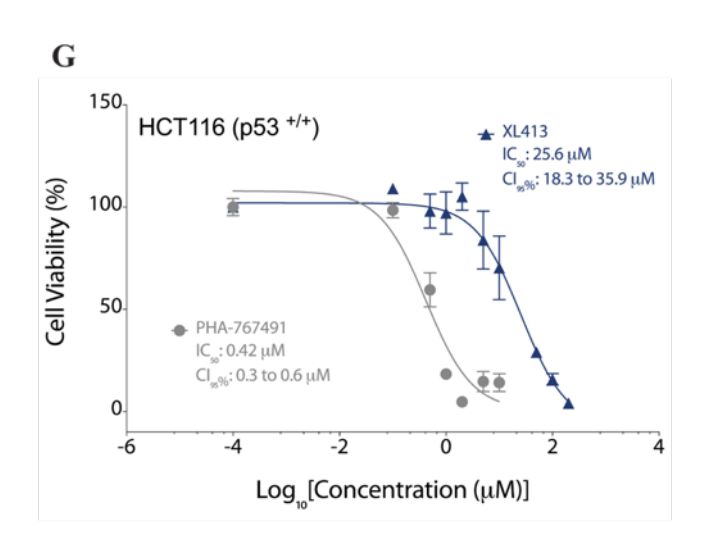
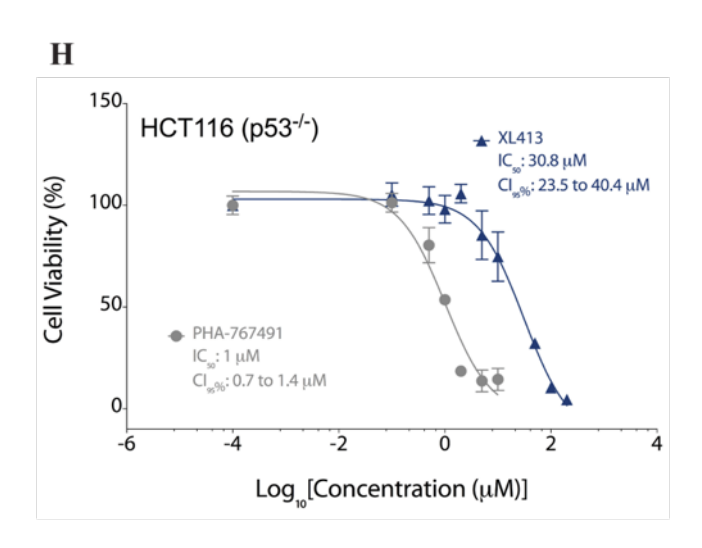


Figure 4.1 (cont'd)





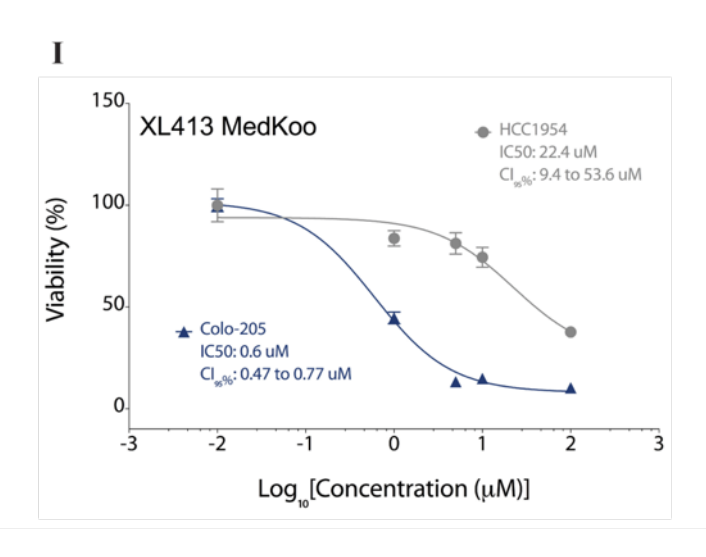
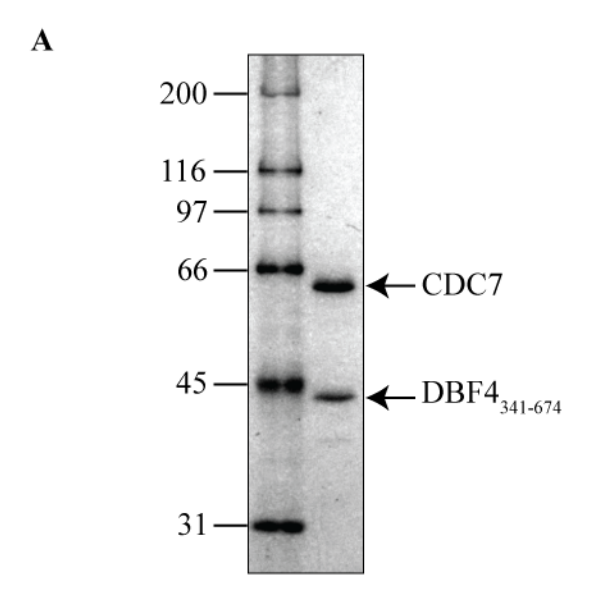


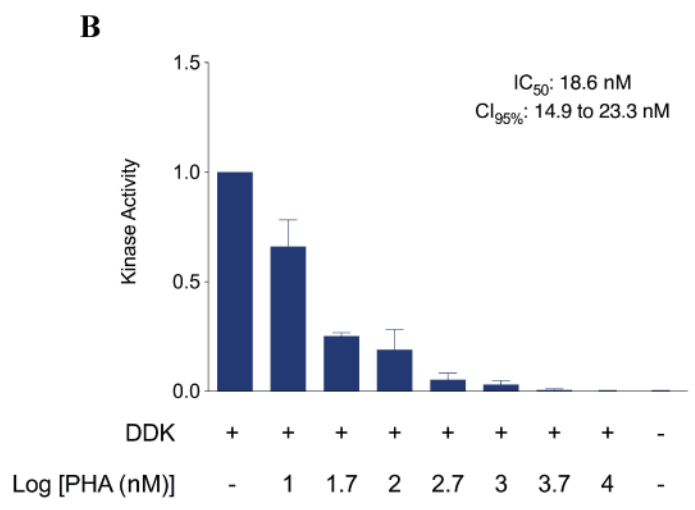
Figure 4.1 (cont'd). (A) DDK is overexpressed in multiple breast cancer cell lines. Immunoblots showing the expression levels of CDC7 and DBF4 in tumor cell lines. β-actin levels indicate equal loading of proteins. (B) Eight tumor cell lines were treated with 5μM of each DDK inhibitor and cell viability was measured 72hrs post drug addition. To determine the IC<sub>50</sub>, HCC1954 cells were treated with increasing concentrations of PHA-767491 or XL413 and the cell viability was measured 72hrs post drug addition. HCC1954 (C, D), Colo-205 (E, F), HCT116 p53WT (G), or HCT116 p53 -/- (H) cells were treated with increasing concentrations of PHA-767491 or XL413 and the cell viability was measured 72hrs post drug addition. The extent of apoptosis induced by the compounds in each cell line relative to vehicle control was measured by Caspase 3/7 activity and is indicated in (D, F). XL413 acquired from a commercial supplier (Medkoo) behaved similar to the chemically synthesized compound (E). All data represent the mean of at least three separate measurements +/- SD and were highly reproducible on separate days.

# PHA-767491 and XI413 are potent DDK inhibitors in vitro

The poor potency of XL413 on most tumor cell lines could be because the synthesized compound is not an effective kinase inhibitor. To test this possibility, we purified recombinant DDK and then measured the IC<sub>50</sub> values of both XL413 and PHA-767491 on purified kinase. We co-expressed His6-SUMO-CDC7 and DBF4 in bacterial cells and then purified the complex as described in Experimental Procedures. Briefly, DDK was bound to a Ni-NTA column followed by elution and removal of the His6-SUMO tag. Untagged DDK was then fractionated over an SP Fast Flow column followed by separation on an S-200 gel filtration column. Kinase assays were performed with purified DDK (**Figure 4.2 A**) in the presence of increasing concentrations of each inhibitor (**Figure 4.2 B, C**). Both PHA-767491 and XL413 were effective DDK inhibitors *in vitro* as shown previously (Hughes et al., 2012; Koltun et al., 2012; Vanotti et al., 2008) with IC<sub>50</sub> values of 18.6nM and 22.7nM, respectively. Since both compounds are effective DDK inhibitors, the cell proliferation profiles indicate that XL413 is unable to act on its target inside the cell.

Figure 4.2. PHA-767491 and XL413 are similarly effective DDK inhibitors in vitro.





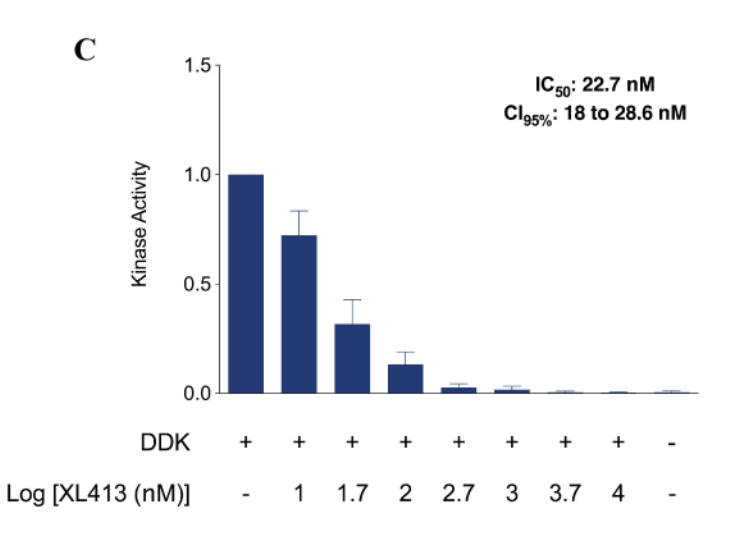


**Figure 4.2 (cont'd). (A)** Coommassie-stained gel showing 1μg purified DDK from bacterial cells. (γ)-<sup>32</sup>P ATP DDK kinase assays in presence of increasing concentrations of PHA-767491 **(B)** and XL413 **(C)**. The kinase assay data represent the mean of four separate measurements +/-SD.

# XL413 is defective in inhibiting DDK-dependent MCM2 phosphorylation in HCC1954 cells

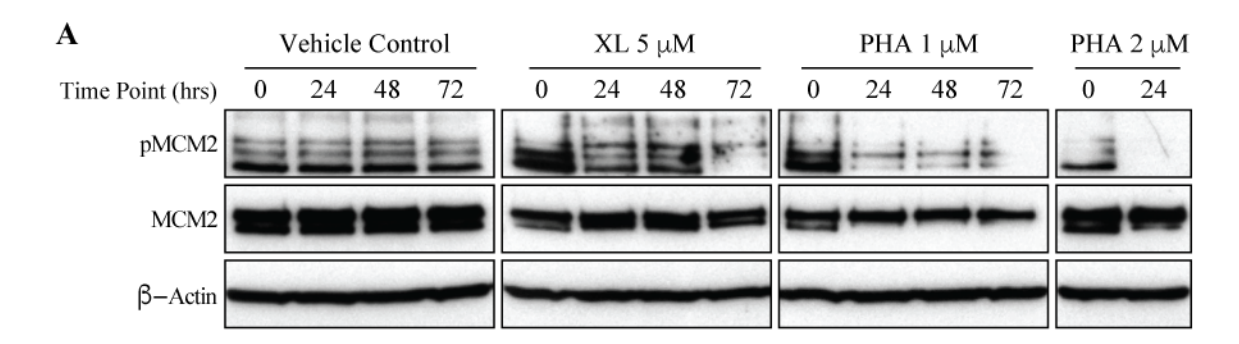
Effective cellular uptake of the DDK inhibitor should compromise DDK activity *in vivo*. Among the many targets of DDK are components of the replicative MCM2-7 helicase. Serine 53 of MCM2 subunit is a well-characterized target site for DDK mediated phosphorylation (Montagnoli et al., 2006a). We quantitated levels of phosphorylation on this site as a measure of DDK activity *in vivo*. HCC1954 cells were incubated in presence of 1μM PHA-767491, 2μM PHA-767491 or 5μM XL413. Cells were then harvested at 0, 24, 48, and 72 hours post drug addition to measure cell proliferation and MCM2 phosphorylation by immunoblotting.

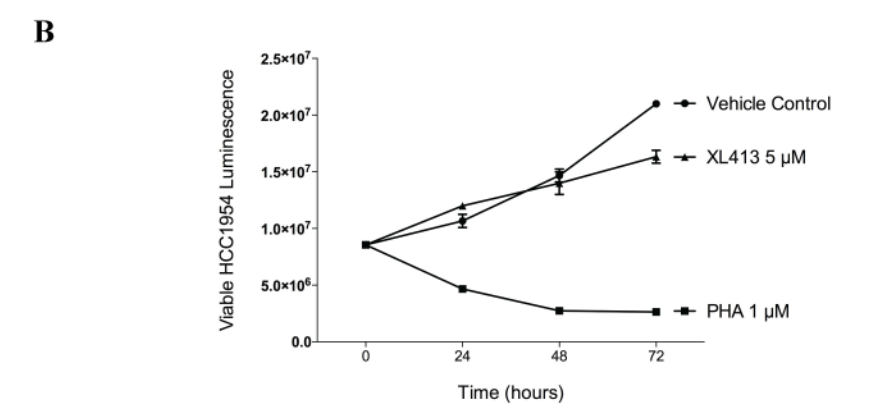
2μM PHA-767491 completely abolished MCM2 phosphorylation by 24 hours in HCC1954 cells (**Figure 4.3 A**), corresponding with its effect on cell growth and viability (**Figure 4.3 B**). In the same cell line, 1μM PHA-767491 resulted in very little residual MCM2 phosphorylation from 24 to 72 hours and was also effective in inhibiting cell proliferation and inducing cell death. In contrast, XL413 did not inhibit MCM2 phosphorylation at 24hrs, even at a higher concentration of 5μM (**Figure 4.3 A**) and there was only a modest decrease in MCM2 phosphorylation at 72 hours. This effect was also seen in the cell proliferation assay, where XL413 treated cells grew only slightly poorer than the vehicle treated cells (**Figure 4.3 B**).

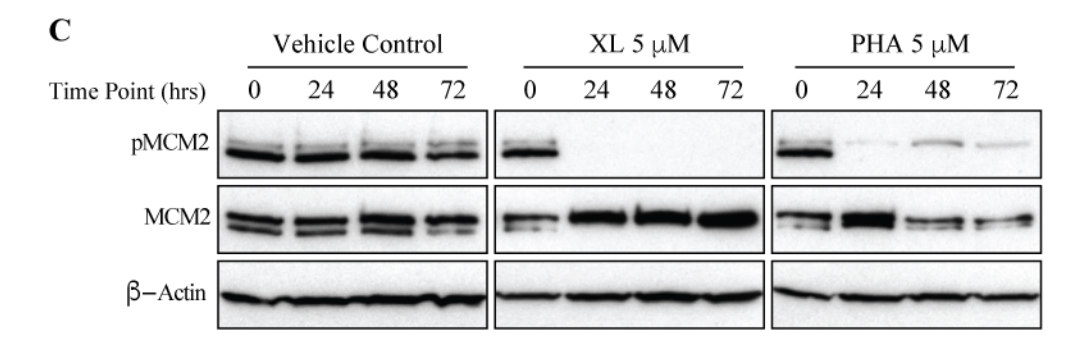
Since both compounds were effective inhibitors in the Colo-205 cells, we examined MCM2 phosphorylation in these cells following drug addition. Again, 5μM PHA-767491 completely abolished MCM2 phosphorylation by 24 hours and was very effective in inducing cell death (Figure 4.3 C, D). However, unlike in HCC1954 cells, XL413 was a very effective inhibitor of DDK activity in Colo-205 cells. 5μM of XL413 completely abolished MCM2 phosphorylation at 24hrs and was also as effective as PHA-767491 in inducing cell death (Figure 4.3 C, D). These results show that the two DDK inhibitors exhibit very different profiles in cell lines despite the

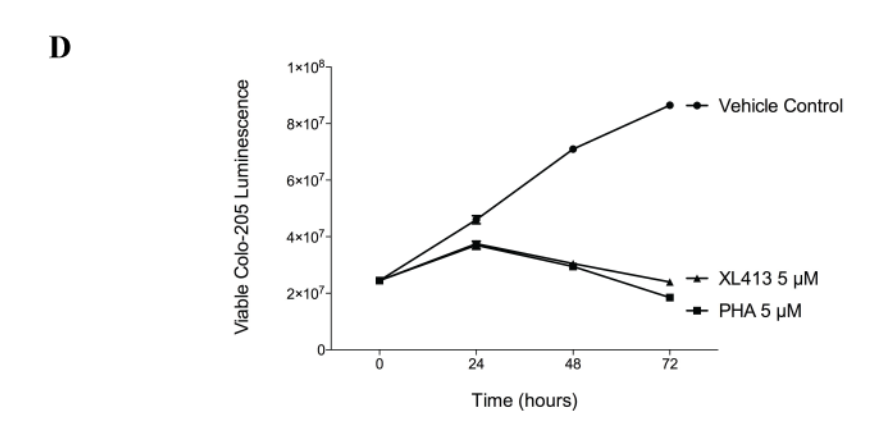
fact that both compounds are highly effective kinase inhibitors *in vitro*. Our data suggest that XL413 is not taken up effectively into many cell lines or is metabolized quickly or modified to an inactive form.

Figure 4.3. XL413 is defective in inhibiting DDK-dependent MCM2 phosphorylation in HCC1954 cells but is effective in Colo-205 cells.









**Figure 4.3 (cont'd). (A)** Immunoblots showing Mcm2 phosphorylation in HCC1954 cells or **(C)** Colo-205 cells in the presence of DMSO, PHA-767491, or XL413. **(B)** Cell proliferation profile of HCC1954 cells or **(D)** Colo-205 cells in presence of DMSO, PHA-767491, or XL413. The cell proliferation data represent the mean of at least two separate measurements +/- SD.

# Screen to determine cross reactivity of known kinase inhibitors with DDK

To identify additional chemical structures that are capable of inhibiting DDK, we tested a panel of  $\sim$ 400 kinase inhibitors against purified DDK in a thermal stability shift assay (TSA) (Niesen et al., 2007). In this assay, inhibitor compounds were incubated with purified DDK and then screened with an increasing temperature gradient to determine the point at which they denature (relative to DDK alone) by following fluorescence changes of the dye SYPRO Orange, which binds to hydrophobic surfaces on unfolded proteins. Inhibitor compounds that bind within the DDK ATP binding pocket are predicted to stabilize the kinase, and  $\Delta T_m$  values (see Materials and Methods) of 2°C or greater are considered significant hits. We identified 12 compounds that caused significant temperature shifts: 11 compounds increased the  $T_m$ , and 1 compound (Genistein) decreased the  $T_m$ .

To estimate the affinity of each compound for DDK we measured  $\Delta T_m$  values for these 12 compounds across a 200-fold range of inhibitor concentrations and compared these values to PHA-767491 (a specific DDK inhibitor), staurosporine (a broad spectrum protein kinase inhibitor), and DMSO as a vehicle control. The data shown in **Figure 4.4 A** represent an average of three independent measurements. The compound genistein, which is an EGFR inhibitor, was unusual in that it increased  $\Delta T_m$  at lower inhibitor concentrations and then decreased  $\Delta T_m$  at 5, 10 and 20 $\mu$ M concentrations. The initial screen was carried out with 20 $\mu$ M inhibitor and explains why genistein was scored as decreasing the  $T_m$ . Perhaps this compound binds to the DDK ATP binding pocket but at higher concentrations disrupts CDC7-DBF4 binding. Each of the other 11 compounds has positive  $\Delta T_m s$ . Examination of the compound titrations reveals that three inhibitors had comparable profiles to PHA-767491 in that they induced a  $\Delta T_m$  of ~2 or more beginning at a 1 $\mu$ M concentration: a Rho kinase inhibitor (Rockout), a protein kinase R (PKR)

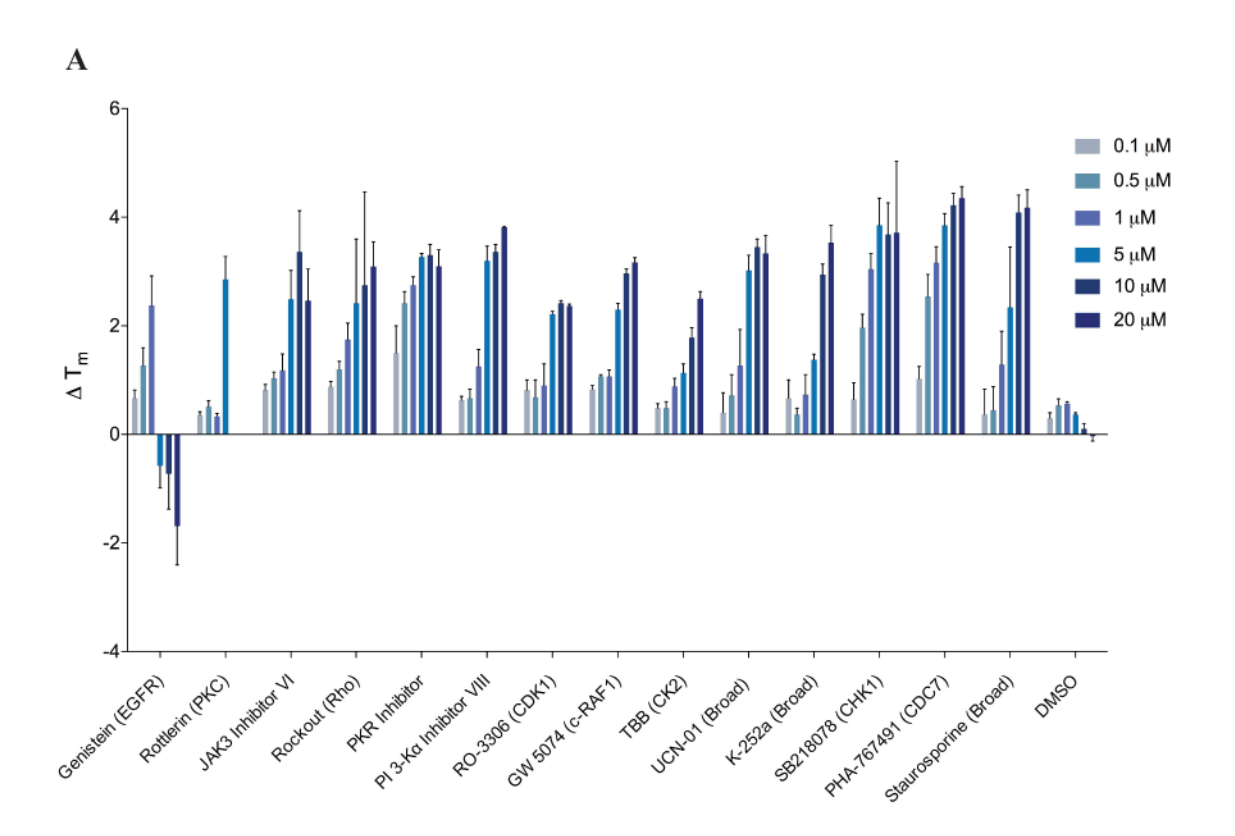
inhibitor, and a CHK1 kinase inhibitor (SB218078). Four additional compounds, the JAK3 inhibitor VI, PI3-Ka inhibitor VII, UCN-01, and K252a gave a 3-fold or higher  $\Delta\Delta T_m$  at 5, 10 and 20 $\mu$ M concentrations.

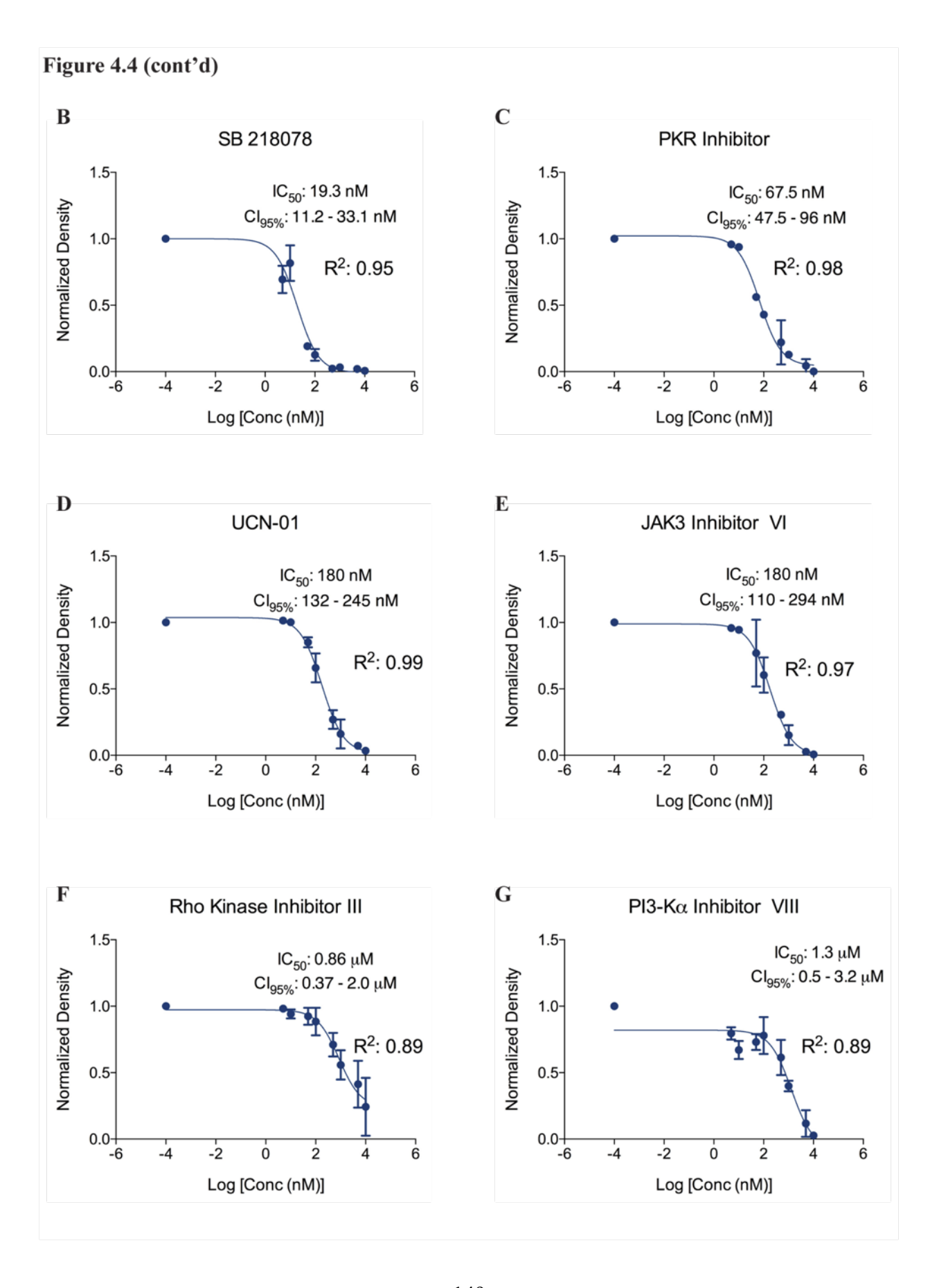
The structures of the top compounds in the TSA screen are shown in **Table 4.2**, revealing a broad range of structural classes that can inhibit DDK. K252a is naturally occurring alkaloid related to staurosporine that inhibits a broad variety of protein kinases including serine/threonine kinases and tyrosine kinases of the Trk family (Kase et al., 1986; Tapley et al., 1992). So, inclusion of K252a in this list (like staurosporine) is perhaps not surprising. Since it is very likely that the inhibitors we recovered in the TSA screen stabilize DDK by their ability to bind in the ATP binding pocket, we performed kinase assays using the top six compounds. Kinase assays revealed that they are indeed DDK inhibitors (**Figure 4.4 B-G**). The CHK1 and the PKR inhibitors were the best compounds *in vitro* and inhibited DDK with IC50s of 19.3nM and 67.5nM, respectively (**Figure 4.5 A, F**). Interestingly, the  $\Delta T_m$  profiles of the CHK1 and PKR inhibitors look strikingly like PHA-767491, raising the possibility that these compounds inhibit DDK in cells. Although SB218078 is derived from staurosporine, it is a potent inhibitor of CHK1 (Jackson et al., 2000). The structures of the other top hits, PKR inhibitor and Rockout, are not derived from staurosporine and also differ from known DDK inhibitors (**Table 4.2**).

We tested whether the PKR and CHK1 inhibitors would alter cell growth and inhibit MCM2 phosphorylation in the HCC1954 breast cancer cell line, which would be strong evidence that they inhibit DDK in cells. Increasing amounts of the PKR inhibitor were incubated with HCC1954 cells over 72 hours, which resulted in a large decrease in the number of viable cells relative to vehicle control (**Figure 4.5 B, IC**<sub>50</sub> of 1.7μM). The large decrease in cell viability was likely the result of significant apoptosis because 2μM PKR inhibitor increased Caspase 3/7 activity

20-fold relative to DMSO control and this was blocked by the pan-caspase inhibitor zVAD (**Figure 4.5 C**). Finally, 2μM PKR inhibitor affected cell growth over a 72 hour time course similar to 2μM PHA-767491 (**Figure 4.5 D**) and also strongly inhibited MCM2 phosphorylation in the HCC1954 cells (**Figure 4.5 E**). These results strongly suggest that the PKR inhibitor is blocking DDK activity in this cell line. We saw the same trend with the CHK1 inhibitor, although it had a reduced ability to block cell growth, induce apoptosis, and inhibit MCM2 phosphorylation relative to the PKR inhibitor and PHA-767491 (**Figure 4.5 F-J**).

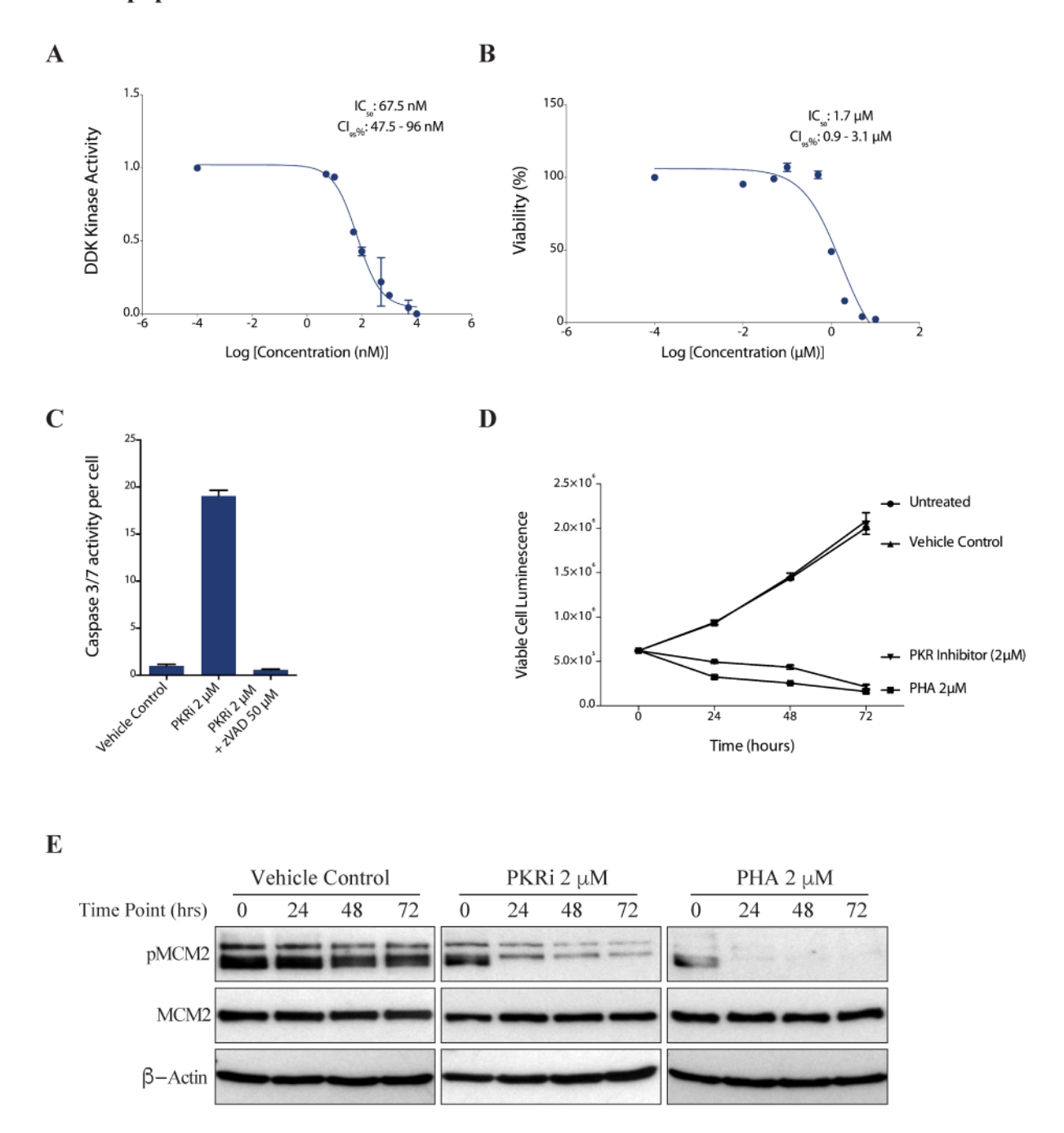
Figure 4.4. Discovery of potential new DDK inhibitor scaffolds.





**Figure 4.4 (cont'd). (A) DDK** thermal stability shift assays (TSA) using known kinase inhibitors. Increasing concentrations of 12 hit compounds discovered in a 400 compound screen were screened against purified DDK using the TSA. PHA-767491 (DDK specific inhibitor), staurosporine (broad spectrum kinase inhibitor) and DMSO are shown as controls. The data represent the mean of three separate measurements +/- SEM. (**B** - **G**) Top hits identified by TSA screen can inhibit DDK in vitro. (γ)- $^{32}$ P ATP DDK kinase assays in presence of increasing concentrations of SB 218078 (**B**), PKR Inhibitor (**C**), UCN-01 (**D**), JAK3 Inhibitor VI (**E**), Rho Kinase Inhibitor III (**F**), and PI3-Kα Inhibitor VIII (**G**). Kinase activities represent the mean of two independent measurements +/- SD on separate days

Figure 4.5. A PKR inhibitor and a CHK1 inhibitor also inhibits DDK activity and induces apoptosis in breast cancer cells.



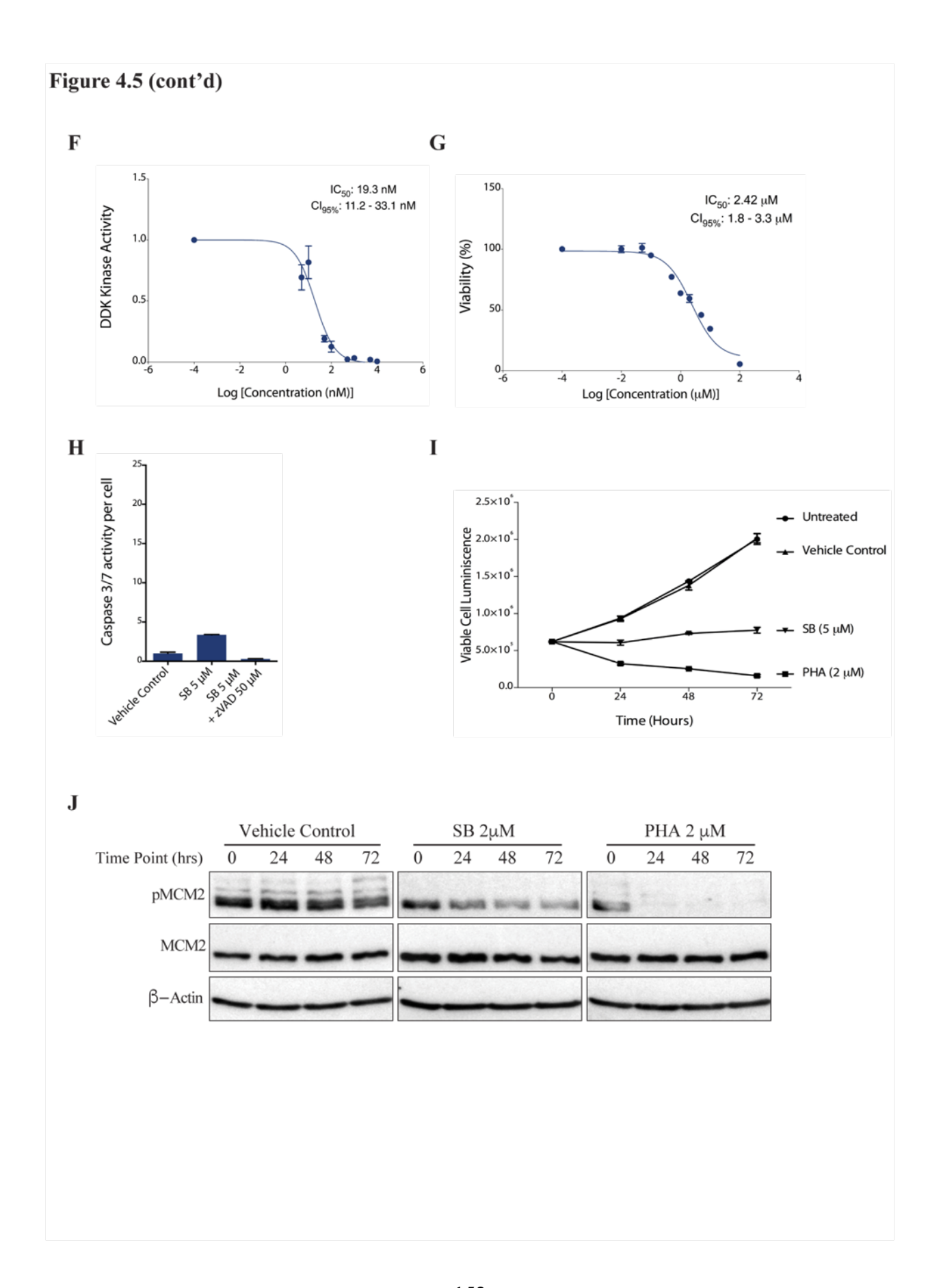


**Figure 4.5 (cont'd).** IC<sub>50</sub> values for the PKR inhibitor and CHK1 inhibitor were determined against purified DDK (**A**, **F**) and HCC1954 cells (**B**, **G**). (**C**, **H**) Caspase 3/7 assays showing that apoptosis was strongly induced at 24 hours following PKR (**C**) and CHK1 inhibitor (**H**) addition and this was eliminated using the pan-caspase inhibitor zVAD. The PKR (**D**) and CHK1 inhibitors (**I**) causes a similar decrease in viability on HCC1954 cells to PHA-767491 over time and also inhibits Mcm2 phosphorylation in cells, a known DDK target (**E**, **J**). The measurements in panels **A-D** & **F-I** represent the averages of at least two measurements +/- SD and were highly reproducible.

Table 4.2. Structures of potential DDK inhibitors

PHA-767491	XL413	Rockout
HN NH	CI NH NH	N HN
JAK3 Inhibitor VI	PI 3-Ka Inhibitor VIII	PKR Inhibitor
NH NH NN NN	O = N+  OCH3  CH3  Br	HN S N
H <sub>3</sub> C K-252a	H <sub>3</sub> C <sub>NH</sub> CH <sub>3</sub> UCN-01	SB218078
H <sub>3</sub> C N N N N N N N N N N N N N N N N N N N	CH <sub>3</sub>	N N N N N N N N N N N N N N N N N N N

#### **DISCUSSION**

Small molecule inhibitors have been successfully employed both in the clinic and laboratory. Despite being initially regarded as too non-specific for deployment in therapy, small molecule kinase inhibitors have emerged as frontrunners in drug development, especially against cancer (Zhang et al., 2009). Clinically useful molecules are often called 'drugs' while the ones used for studying protein functions in the laboratory are called 'chemical probes' (Lipinski, 2004; Workman and Collins, 2010). Both the groups share a basic requirement of high potency against the target of interest. While drugs need to act effectively against the targeted disease and exhibit good pharmacokinetic properties in a physiological setting (Lipinski, 2004), for chemical probes target specificity is of paramount importance (Workman and Collins, 2010). Small molecule inhibitors of DDK are attractive both as drugs as well as chemical probes.

Since the initial description of the tumor specific cell killing observed in response to depletion of DDK, several DDK inhibitors have been synthesized. Very different families of chemical moieties have been shown to exhibit DDK inhibitory activities. Nerviano Medical Sciences, Roche, Abbot, Exelixis, and Amgen have developed and characterized DDK inhibitors. Although DDK inhibitors may be effective anti-cancer drugs, these molecules are also very important for understanding the roles of this multifunctional kinase. As probes, DDK inhibitors would complement the traditional RNAi techniques, which can also have off-target effects (Weiss et al., 2007). RNAi mediated silencing leads to a gradual loss of protein whereas an inhibitor impacts kinase activity and not necessarily protein abundance (Weiss et al., 2007). Chemical inhibitors could also be important in studying the non-kinase roles of DDK.

Two inhibitors of DDK have received more characterization than others: the first was the prototype DDK inhibitor PHA-76749 followed by the highly selective benzofuropyrimidinone XL413. An X-ray crystal structure of DDK in association with both DDK inhibitors has been solved recently (Hughes et al., 2012). The tighter binding of XL413 in the binding pocket of DDK along with its more extensive associations with the non-conserved residues of the active site is thought to be the reason for the superior selectivity profile of XL413. The cellular potency data provided with the initial characterization of XL413 (Koltun et al., 2012) along with the crystal structure evidence made it the best in class DDK inhibitor. XL413 seemed an ideal chemical probe for studies of DDK function in normal and in tumor cells.

It was therefore surprising that in most cell lines we tested XL413 fared very poorly when compared to PHA-767491. This led us to perform a comparative analysis of the biochemical characteristics of both inhibitors. Both inhibitors were quite effective in inhibiting purified DDK complex *in vitro*. Although the cancer cell lines had varying levels of DDK, they all responded well to PHA-767491. XL413, however, had almost no effect on nine of the ten cell lines in our panel. It also did not induce cell cycle arrest in majority of cell lines, indicating that DDK activity was not being inhibited *in vivo*. This was corroborated by the MCM2 phosphorylation analysis in XL413-sensitive Colo-205 cells and XL413-resistant HCC1954 cells. The majority of the original cellular potency profile for XL413 was provided with one cell line, Colo-205. In our analysis, Colo-205 was the sole cell line responsive to XL413. Taken together, our analyses suggest that XL413, while exhibiting impressive chemical characteristics and selectivity, is a poor chemical probe for cell lines.

As described by Workman and Collins (Workman and Collins, 2010), the effectiveness of an inhibitor as a chemical probe is dependent on its (1) chemical properties (2) biological potency

(3) biological selectivity and (4) its context of use. Since XL413 is a product of a high throughput drug-screening program and must have satisfied multiple criteria for selection as lead compound, it is expected to exhibit good pharmacokinetic properties. XL413 was shown to be a highly potent inhibitor with IC<sub>50</sub> values in single digit nanomolar range. Moreover, it was highly selective for DDK over a panel of 100 kinases. With such properties, the poor growth suppressive properties of XL413 among so many cell lines cannot be easily explained. We also performed analyses with XL413 purchased from a separate commercial supplier, MedKoo Inc. This compound, however, had identical cellular potency profiles as the compound synthesized by CGeneTech (Figure 4.1E). Both HCC1954 and Colo-205 cells were cultured in RPMI-1640 media supplemented with 10% fetal bovine serum. Since, the inhibitor functions well in Colo-205 cells, precipitation of XL413 in media cannot be the reason for its inactivity. Possible reasons for its compromised activity on cell lines include poor permeability through the cell membrane, degradation by metabolic enzymes, or higher sensitivity to efflux transporters. In principal, these possible deficits could be circumvented through synthesis of additional chemical derivatives.

Our analysis of XL413 highlights a need for additional biologically active DDK inhibitors. Most ATP competitive inhibitors were optimized by structure activity relationship (SAR) studies on existing scaffolds of chemical inhibitors. PHA-767491 and XL413 were optimized from scaffolds for MK2 and PIM inhibitors, respectively (Anderson et al., 2007; Tsuhako et al., 2012). To identify further chemical scaffolds for development of DDK inhibitors, we tested if any well-known kinase inhibitors cross-reacted with human DDK. This is a possibility since ATP-competitive kinase inhibitors bind within a related ATP-binding pocket. Using a TSA screen, we identified 12 small molecules that significantly shifted the thermal stability of DDK. Several of these functioned comparatively to PHA-767491 in the assay: Rockout (Rho kinase inhibitor), PKR

inhibitor, and SB218078 (CHK1 inhibitor). These compounds fall into different structural classes (Table 4.2) indicating that significant chemical space is available for new DDK inhibitor development. Interestingly, UCN-01, also a CHK1 inhibitor related to staurosporine (Graves et al., 2000), was also identified in our screen and showed a high affinity for DDK. This raises the possibility that more potent and selective derivatives of staurosporine might be designed against DDK. It also raises the possibility that reported biological effects due to CHK1 inhibition may be enhanced by the ability of SB218078 and/or UCN-01 to also inhibit DDK. Rockout is a pyridine-substituted indole derivative and so is somewhat related to PHA-767491. However, the position of the pyridine moiety on the indole ring of Rockout is quite different from the geometry of PHA-767491. In addition, the PKR inhibitor falls into a distinct structural class from either PHA-767491 or XL413.

It was noteworthy that the PKR inhibitor blocked the growth of HCC1954 breast cancer cells, induced apoptosis and inhibited DDK-mediated MCM2 phosphorylation nearly as well as the lead DDK inhibitor PHA-767491. RNA-dependent protein kinase (or PKR) is a ubiquitously expressed protein that blocks protein synthesis in response to a number of stresses and impacts both neurodegenerative diseases and cancer through its ability to promote apoptosis (Marchal et al., 2014). The particular PKR inhibitor we used inhibited PKR with an IC<sub>50</sub> of ~200nM (Jammi et al., 2003) but DDK at 70nM *in vitro* (Figure 4.5 A) and therefore should be classified as a dual PKR/DDK inhibitor. Whether the PKR inhibitor induced apoptosis in HCC1954 cells due to inhibiting DDK activity, PKR activity or both remains to be determined. In summary, our results highlight the cross-reactivity of several kinase inhibitors with DDK and also reveal an opportunity to develop more potent, biologically active DDK inhibitors for future evaluation.

#### **MATERIALS AND METHODS**

# Synthesis of PHA-767491 and XL413

The DDK inhibitors, PHA-767491 and XL413, were synthesized as described previously (Koltun et al., 2012; Vanotti et al., 2008). HPLC analysis and mass spectrometry were performed on both compounds, which confirmed the correct molecular mass and a high level of purity (>99%) for both.

#### **Cell lines**

HeLa cells (ATCC) were cultured in MEM supplemented with Earle's salts, 2mM glutamine, 10% heat-inactivated fetal bovine serum (HI FBS), 1.5g/L sodium bicarbonate, 0.1mM non-essential amino acids, 1mM sodium pyruvate, 50units/ml of penicillin, and 50ug/ml of streptomycin. MDA-MB-453 (ATCC) cells were grown in DMEM supplemented with 4.5g/L D-glucose, 4mM L-glutamine, 110mg/L sodium pyruvate, 10% HI FBS, 50units/ml of penicillin, and 50ug/ml of streptomycin. HCC1954 (ATCC), HCC1187 (ATCC), BT-549 (NCI-60), MCF-7 (NCI-60), and Colo-205 (NCI-60) cells were all cultured in RPMI 1640 media supplemented with 10% HI FBS, 50units/ml of penicillin, and 50ug/ml of streptomycin. All cells were maintained at 37°C with 5% CO<sub>2</sub> in a humidified incubator. HCT-116 p53<sup>+/+</sup> and p53<sup>-/-</sup> cell lines were cultured in McCoy's 5A medium supplemented with 10% HI FBS, 50units/ml of penicillin, and 50μg/ml of streptomycin.

# **DDK** protein induction

pKT37 is a pETDuet-1 (Novagen)-vector that co-expresses His6-Smt3-HsCDC7 (codon optimized, Genescript) and DBF4 residues 341-674, which contains motifs M and C required to bind and activate CDC7. *E. coli* BL21-RIPL was transformed with pKT37 and a fresh colony was grown overnight in LB containing 150µg/ml ampicillin, 50µg/ml chloramphenicol and 1% glucose. Two liters of LB containing 150µg/ml ampicillin and 50µg/ml chloramphenicol were inoculated with ~60 ml of overnight culture to give an OD<sub>600</sub> of 0.1. The culture was grown to an OD<sub>600</sub> of 0.8 and then induced for 6 hrs with 0.5 mM IPTG, at 25°C. The cell pellet was suspended in 20mls Ni-NTA buffer A (20mM HEPES-NaOH (pH 7.4), 250mM NaCl, 10% glycerol) with 1X protease inhibitor cocktail (Roche) and 1mM β-mercaptoethanol. A micro fluidizer was used to lyse the cells, followed by a 30-minute centrifugation (12,000 rpm, F13 rotor) at 4°C.

#### **DDK** purification

DDK was purified step-wise using Nickel-NTA, SP Fast Flow, and S-200 columns. The cell lysate containing 35mM imidazole was applied to a 25ml Ni-NTA column, washed with 20 column volumes, and then eluted with a 250ml 35mM-150mM imidazole gradient. DDK protein fractions (~115mM imidazole) were pooled and dialyzed overnight at 4°C against 20mM HEPES-NaOH, pH 7.4, 1mM EDTA, 10% glycerol with no imidazole. The dialysate was then passed over three 5ml SP Fast Flow columns (connected in tandem), washed and eluted with a 100ml 100 mM-0.5M NaCl gradient. DDK protein fractions (~0.2M) were pooled, MgCl<sub>2</sub> was added to the pooled protein to chelate EDTA, and incubated with PP2C (6His-GST-Hab1) phosphatase using an equivalent milligram amount to the total protein in the pool, and 1/100 equivalent milligram amount of Ulp1 protease to cleave the His6-Smt3 (Sumo) tag at 16°C overnight. DDK was

analyzed on 15% SDS gel to check the extent of dephosphorylation and Sumo cleavage (which was usually greater than 95%). The protein pool was loaded onto a second Ni-NTA column (with no imidazole) and flow through fractions containing DDK were pooled, 1mM EDTA was added to chelate free Ni<sup>++</sup>, and dialyzed overnight at 4°C against 20mM HEPES(pH7.4), 100mM NaCl, 1mM EDTA. The protein was concentrated using 30,000 MWCO spin concentrator (Amicon Ultra, Millipore) at 4°C to a final volume of 10 ml. Concentrated protein was loaded onto a 300 ml S-200 gel exclusion column (Amersham-Pharmacia). HsCDC7-DBF4 eluted at ~150 kDa, close to the dimer value of 110kDa. Total yield was typically 6 to 8 mg.

#### In vitro kinase activation assays

20ng of purified human DDK was pre-incubated with increasing concentrations of each DDK inhibitor for 5 min. Then 10μCi (Y)-<sup>32</sup>P ATP and 1.5μM cold ATP were added in a buffer containing 50mM Tris-HCl (pH 7.5), 10mM MgCl<sub>2</sub>, and 1mM DTT and incubated for 30 min at 30°C. The proteins were denatured in 1X Laemmli buffer at 100°C followed by SDS-PAGE and autoradiography on HyBlot CL film (Denville Scientific, Inc.). Auto-phosphorylation of DDK was used as an indicator of its kinase activity. <sup>32</sup>P-labeled bands were quantified using ImageJ and the IC<sub>50</sub> values were calculated using GraphPad (Prism 6).

#### Analysis of cell viability

For assays in 96 well plates 2500 cells were plated per well. After 24 hours, cells were treated with small molecule inhibitors and incubated for 72 hours at 37°C. Subsequently the cells were lysed and the ATP content was measured as an indicator of metabolically active cells using the CellTiterGlo assay (Promega). IC<sub>50</sub> values were calculated using the GraphPad software. For

assays in six well plates, 100,000 cells were plated per well. After 24 hours, cells were treated with small molecule inhibitors and incubated for varying time points. Cells were trypsinized and a suspension was made in 5ml of phosphate buffered saline. 30µl of this suspension was mixed with 30µl of CellTiterGlo reagent followed by a 10-minute incubation at room temperature. Luminescence was measured using EnVision 2104 Multilabel Reader (PerkinElmer).

#### **Analysis of Caspase 3/7 activity**

5,000 cells per well were plated in a 96 well plate. After 24 hours, cells were treated with small molecule inhibitors and incubated for 24 hours at 37°C. Caspase 3/7 activity and viable cell number were then measured using the Caspase-Glo 3/7 assay (Promega) and CellTiter-Glo assay (Promega), respectively. The "Caspase activity per cell" was obtained by normalizing total Caspase activity to cell number.

#### **Immunoblot Analysis**

Whole cell extracts were prepared by re-suspending the pellets in RIPA buffer (150mM NaCl, 1% NP-40, 0.5% sodium deoxycholate, 0.1% SDS, 50mM Tris HCl, pH8) containing protease inhibitors (100μM PMSF, 1mM Benzamidine, 2.5μg/ml Pepstatin A, 10μg/ml Leupeptin, and 10μg/ml Aprotinin) and phosphatase inhibitors (1mM each NaF, Na<sub>3</sub>VO<sub>4</sub> and Na<sub>4</sub>P<sub>2</sub>O<sub>7</sub>). Protein concentration was measured using the BCA<sup>TM</sup> protein assay kit (Pierce) according to manufacturer's protocol. Equal amounts of protein were subjected to SDS-PAGE and transferred to a nitrocellulose membrane (Millipore). Transfer efficiency and equal loading was confirmed by Ponceau S staining. Following primary and secondary antibody treatments, proteins were visualized using SuperSignal West Pico solutions (Thermo Scientific). Anti-MCM2 and anti-S53-

phospho-MCM2 antibodies were purchased from Bethyl Laboratories; anti-β-actin was from Sigma; anti-mouse and anti-rabbit HRP antibodies were from GE Healthcare; and anti-CDC7 and anti-DBF4 antibodies were described previously (Bonte et al., 2008).

# Thermal Stability Shift Assay (TSA)

All reactions were incubated in a 10  $\mu$ l final volume and assayed in 96-well plates using 20x SYPRO Orange (Invitrogen) and 200 $\mu$ g/ml purified DDK (Niesen et al., 2007). Reactions were incubated with inhibitor compounds on ice for 30 minutes. Compounds from four kinase inhibitor libraries (Calbiochem I, II, III, Tocriscreen Inhibitor Toolbox) were screened at 20 $\mu$ M for T<sub>m</sub> increases with a total DMSO concentration of 2% or less. Thermal melting experiments were carried out using the StepOnePlusTM Real-Time PCR System (Applied Biosystems) melt curve program with a ramp rate of 1°C and temperature range of 15°C to 85°C. Subsequent TSAs on the 12 hits obtained were carried out as above but in triplicate and using a 200-fold range of inhibitor concentrations. Data analysis was performed as described (Niesen et al., 2007). Melting temperatures (T<sub>m</sub>) were calculated by fitting the sigmoidal melt curve to the Boltzmann equation using GraphPad Prism, with R<sup>2</sup> values of > 0.99. The difference in T<sub>m</sub> values calculated for reactions with and without compounds is  $\Delta$ T<sub>m</sub>.

# **ACKNOWLEDGEMENTS**

I would like to thank Kanchan Tiwari for purifying human DDK; Fen-Fen Soon for performing the thermal stability shift assays; Tong Wang for synthesizing the DDK inhibitors; Dr. Bert Vogelstein for the isogenic HCT116 p53+/+ and p53-/- cell lines and FuJung Chang for technical support.

# CHAPTER 5. SUMMARY AND FUTURE DIRECTIONS

This dissertation has addressed several gaps in knowledge in our understanding of DNA replication checkpoint signaling, DDK's role in checkpoint signaling, and in tumorigenesis. In this section I summarize the key findings of this dissertation and discuss the outstanding questions in the field.

# Nucleolytic processing of stalled replication forks

Utilizing tumor cell systems, we found that a short exposure to replication inhibitor like hydroxyurea induces nascent strand degradation at stalled replication forks (Figure 2.6). The extent of nascent strand degradation corresponds to the accumulation of RPA2 on chromatin and activation of CHK1 kinase. It is well known that replication inhibitors stall replication forks, and stalled forks are marked by long stretches of ssDNA, which are bound by RPA2. The existing model for this phenomenon does not satisfactorily explain all the cellular responses to these inhibitors. It is thought that certain replication inhibitors that inhibit DNA polymerase result in an uncoupling of the polymerase and helicase activities. The helicase then unwinds DNA ahead of the stalled replication fork resulting in a long stretch of ssDNA. However, studies in several model systems have shown that the activities of these enzymes are interdependent, making a physical or functional uncoupling of the helicase and polymerase unlikely. Interdependency of polymerase and helicase activity has been shown in T4 (Delagoutte and von Hippel, 2001) and T7 bacteriophage (Stano et al., 2005), bacterial (Kim et al., 1996), yeast (Langston et al., 2014), and human systems (Kang et al., 2012b). Moreover, electron microscopic images of stalled replication forks show long ssDNA at only the leading strand of the replication fork (Lopes et al., 2006). This is inconsistent with a full uncoupling between helicase and polymerase, which would generate long ssDNA on both the leading and lagging strands. Finally, diverse types of replication inhibitors generate ssDNA, including inter-strand crosslinking agents, which would not allow helicase

activity or polymerase activity beyond the crosslink (Berti and Vindigni, 2016). Based on our data we propose that the ssDNA generated upon fork stalling is primarily a result of nascent strand degradation (Figure 2.10 A). The processing of stalled replication fork could be a general mechanism of dealing with a diverse array of replication inhibitors, all of which induce ssDNA formation at the stalled forks. We do not, however, know the mechanism through which the nascent DNA is degraded. This process has to be extremely well regulated as unrestricted degradation of DNA would be lethal. Also, the repertoire of enzymes required for this process is also not known and future studies would be required to better understand this phenomenon.

# DDK has a primary role in processing stalled replication forks

During the course of our studies we also made a surprising finding regarding a new role for DDK to initiate replication-checkpoint signaling and replication fork recovery. We found that the nucleolytic processing of stalled replication forks is dependent on DDK kinase activity. In the absence of DDK activity, the stalled forks are not processed correctly, ssDNA is not generated, and the replication checkpoint signaling is not initiated. Consistent with DDK's role in initiating the replication checkpoint pathway, we found that DDK activity is also essential for replication fork recovery. Our finding places DDK at the apex of the replication checkpoint signaling pathway. While DDK's role in DNA replication has been well studied and understood it is becoming increasingly evident that this kinase has equally important functions in other cellular processes. How DDK regulates fork processing is an important question that remains to be answered.

## High levels of DDK expression confers a survival advantage to tumor cells

DDK is composed of the CDC7 kinase and its regulatory subunit, DBF4. Both subunits are highly expressed in many diverse tumor cell lines and primary tumors, which is correlated with poor prognosis. In this study we have explored gene expression correlations with DDK high- and DDK low-expressing lung adenocarcinomas. We found that DDK-high expressing tumors exhibit a gene expression signature that is enriched for chemoresistance gene sets. This might explain the poor survival rates of patients that carry tumors with high DDK expression. Given our finding that DDK is essential for initiating a replication checkpoint pathway it can be speculated that high DDK expression makes tumor cells more adept at responding to replication stress induced by chemotherapeutic agents like cisplatin, doxorubicin, and other genotoxic drugs.

## DDK likely drives increased tumor mutagenesis

Using data from the Cancer Genome Atlas we uncovered a strong correlation between the mutation load of cancer patients and the expression of DDK subunits. We confirmed this finding by directly comparing the number of mutations per mega bases of the coding DNA between the DDK-high and DDK-low expressing cancer patients. Based on our data we hypothesize that DDK actually drives mutagenesis in mammalian cells. This is in line with evidence from budding yeast where a similar role for DDK has been described in detail (Chapter 3). It has been shown that DDK promotes an error-prone mechanism of DNA repair known as the trans-lesion DNA synthesis, which is known to increase the rate of mutations. It would be important to test this model in human systems using an in vivo assay that directly measures the effect of DDK subunits on the mutation frequency. Furthermore, it remains to be tested if the increased mutagenesis seen upon DDK overexpression is driven by trans-lesion DNA synthesis or through a distinct mechanism.

Since high rates of mutation could result in drug resistance in tumor cells, sub-lethal doses of DDK inhibitors might find use as a combination drug in tumor therapy. Reducing the expression levels of DDK might decrease the rate of acquired drug resistance, which would result in increased long term efficacy of genotoxic drugs. This hypothesis can be tested in mouse models that are used to study resistance to drugs like cisplatin (Oliver et al., 2010). Long term treatment of such mice with cisplatin in combination with low doses of DDK should prolong the time period required to acquire cisplatin resistance.

## DDK as a chemotherapeutic target

DDK is an emerging chemotherapeutic target since inhibiting DDK causes apoptosis of tumor cells, but not normal cells, through a largely unknown mechanism. We performed an RNAi screen to identify kinases and phosphatases that promote apoptosis when DDK is inhibited (Chapter 3). Our RNAi screen identified 23 kinases and phosphatases that promote apoptosis of both breast and cervical carcinoma cell lines when DDK is inhibited. These hits include checkpoint genes, G2/M cell cycle regulators and known tumor suppressors. Initial characterization of the LATS2 tumor suppressor suggests that it promotes apoptosis independently of the upstream MST1/2 kinases in the Hippo signaling pathway. We have also shown that ATR kinase is activated and is required for the tumor cell death induced upon DDK inhibition (Chapter 2). Since our model suggests that cell death primarily occurs due to an aberrant mitosis upon DDK inhibition, it would be interesting to understand the mechanism through which ATR kinase is activated and if the ATR-induced cell death is mediated through LATS2 kinase.

REFERENCES

## REFERENCES

Alexandre, M., Ju-Mei, L., Xiao Ye, J., Ching-Shyi, W., Stephanie, A.Y., Hai Dang, N., Shizhou, L., Amanda, E.J., Jianping, J., and Lee, Z. (2014). PRP19 Transforms into a Sensor of RPA-ssDNA after DNA Damage and Drives ATR Activation via a Ubiquitin-Mediated Circuitry. Molecular cell *53*, 235-246.

Alexandre, M., and Lee, Z. (2015). RPA-coated single-stranded DNA as a platform for post-translational modifications in the DNA damage response. Cell Research *25*, 9-23.

Alver, R.C., Chadha, G.S., and Blow, J.J. (2014). The contribution of dormant origins to genome stability: from cell biology to human genetics. DNA Repair (Amst) 19, 182-189.

Anderson, D.R., Meyers, M.J., Vernier, W.F., Mahoney, M.W., Kurumbail, R.G., Caspers, N., Poda, G.I., Schindler, J.F., Reitz, D.B., and Mourey, R.J. (2007). Pyrrolopyridine inhibitors of mitogen-activated protein kinase-activated protein kinase 2 (MK-2). Journal of medicinal chemistry *50*, 2647-2654.

Balakrishnan, L., and Bambara, R.A. (2013). Okazaki fragment metabolism. Cold Spring Harb Perspect Biol *5*.

Balestrini, A., Cosentino, C., Errico, A., Garner, E., and Costanzo, V. (2010). GEMC1 is a TopBP1-interacting protein required for chromosomal DNA replication. Nature cell biology *12*, 484-491.

Bermejo, R., Capra, T., Jossen, R., Colosio, A., Frattini, C., Carotenuto, W., Cocito, A., Doksani, Y., Klein, H., Gómez-González, B., *et al.* (2011). The replication checkpoint protects fork stability by releasing transcribed genes from nuclear pores. Cell *146*, 233-246.

Berti, M., and Vindigni, A. (2016). Replication stress: getting back on track. Nature structural & molecular biology *23*, 103-109.

Bertoli, C., Klier, S., McGowan, C., Wittenberg, C., and de Bruin, R.A. (2013). Chk1 inhibits E2F6 repressor function in response to replication stress to maintain cell-cycle transcription. Curr Biol *23*, 1629-1637.

Birmingham, A., Selfors, L.M., Forster, T., Wrobel, D., Kennedy, C.J., Shanks, E., Santoyo-Lopez, J., Dunican, D.J., Long, A., Kelleher, D., *et al.* (2009). Statistical methods for analysis of high-throughput RNA interference screens. Nat Methods *6*, 569-575.

Blow, J.J., Ge, X.Q., and Jackson, D.A. (2011). How dormant origins promote complete genome replication. Trends in biochemical sciences *36*, 405-414.

Bonte, D., Lindvall, C., Liu, H., Dykema, K., Furge, K., and Weinreich, M. (2008). Cdc7-Dbf4 kinase overexpression in multiple cancers and tumor cell lines is correlated with p53 inactivation. Neoplasia *10*, 920-931.

- Brandao, L.N., Ferguson, R., Santoro, I., Jinks-Robertson, S., and Sclafani, R.A. (2014). The role of Dbf4-dependent protein kinase in DNA polymerase zeta-dependent mutagenesis in Saccharomyces cerevisiae. Genetics *197*, 1111-1122.
- Branzei, D., and Foiani, M. (2010). Maintaining genome stability at the replication fork. Nature reviews. Molecular cell biology 11, 208-219.
- Breslin, C., Clements, P.M., El-Khamisy, S.F., Petermann, E., Iles, N., and Caldecott, K.W. (2006). Measurement of chromosomal DNA single-strand breaks and replication fork progression rates. Methods Enzymol *409*, 410-425.
- Britto, R., Sallou, O., Collin, O., Michaux, G., Primig, M., and Chalmel, F. (2012). GPSy: a cross-species gene prioritization system for conserved biological processes--application in male gamete development. Nucleic Acids Res *40*, W458-465.
- Brown, G.W., and Kelly, T.J. (1999). Cell cycle regulation of Dfp1, an activator of the Hsk1 protein kinase. Proceedings of the National Academy of Sciences of the United States of America *96*, 8443-8448.
- Buisson, R., Boisvert, J.L., Benes, C.H., and Zou, L. (2015). Distinct but Concerted Roles of ATR, DNA-PK, and Chk1 in Countering Replication Stress during S Phase. Mol Cell *59*, 1011-1024.
- Cancer Genome Atlas Research, N. (2014). Comprehensive molecular profiling of lung adenocarcinoma. Nature *511*, 543-550.
- Cecilia, C.-R., McDonald, E.R., Kristen, H., Mathew, E.S., Harper, J.W., and Stephen, J.E. (2011). A DNA Damage Response Screen Identifies RHINO, a 9-1-1 and TopBP1 Interacting Protein Required for ATR Signaling. Science *332*, 1313-1317.
- Chan, K.L., Palmai-Pallag, T., Ying, S., and Hickson, I.D. (2009). Replication stress induces sister-chromatid bridging at fragile site loci in mitosis. Nat Cell Biol *11*, 753-760.
- Chen, H.J., Zhu, Z., Wang, X.L., Feng, Q.L., Wu, Q., Xu, Z.P., Wu, J., Yu, X.F., Qian, H.L., and Lu, Q. (2013a). Expression of huCdc7 in colorectal cancer. World journal of gastroenterology: WJG *19*, 3130-3133.
- Chen, H.Z., Tsai, S.Y., and Leone, G. (2009a). Emerging roles of E2Fs in cancer: an exit from cell cycle control. Nature reviews. Cancer *9*, 785-797.
- Chen, J., Bardes, E.E., Aronow, B.J., and Jegga, A.G. (2009b). ToppGene Suite for gene list enrichment analysis and candidate gene prioritization. Nucleic Acids Res *37*, W305-311.
- Chen, Y.C., Kenworthy, J., Gabrielse, C., Hanni, C., Zegerman, P., and Weinreich, M. (2013b). DNA replication checkpoint signaling depends on a Rad53-Dbf4 N-terminal interaction in Saccharomyces cerevisiae. Genetics *194*, 389-401.

Chen, Y.C., and Weinreich, M. (2010). Dbf4 regulates the Cdc5 Polo-like kinase through a distinct non-canonical binding interaction. J Biol Chem 285, 41244-41254.

Cheng, A.N., Jiang, S.S., Fan, C.C., Lo, Y.K., Kuo, C.Y., Chen, C.H., Liu, Y.L., Lee, C.C., Chen, W.S., Huang, T.S., *et al.* (2013). Increased Cdc7 expression is a marker of oral squamous cell carcinoma and overexpression of Cdc7 contributes to the resistance to DNA-damaging agents. Cancer letters *337*, 218-225.

Chica, N., Rozalen, A.E., Perez-Hidalgo, L., Rubio, A., Novak, B., and Moreno, S. (2016). Nutritional Control of Cell Size by the Greatwall-Endosulfine-PP2A.B55 Pathway. Curr Biol *26*, 319-330.

Cho, W.H., Lee, Y.J., Kong, S.I., Hurwitz, J., and Lee, J.K. (2006). CDC7 kinase phosphorylates serine residues adjacent to acidic amino acids in the minichromosome maintenance 2 protein. Proc Natl Acad Sci U S A *103*, 11521-11526.

Choschzick, M., Lebeau, A., Marx, A.H., Tharun, L., Terracciano, L., Heilenkotter, U., Jaenicke, F., Bokemeyer, C., Simon, R., Sauter, G., *et al.* (2010). Overexpression of cell division cycle 7 homolog is associated with gene amplification frequency in breast cancer. Human pathology *41*, 358-365.

Chowdhury, A., Liu, G., Kemp, M., Chen, X., Katrangi, N., Myers, S., Ghosh, M., Yao, J., Gao, Y., Bubulya, P., *et al.* (2010). The DNA unwinding element binding protein DUE-B interacts with Cdc45 in preinitiation complex formation. Molecular and cellular biology *30*, 1495-1507.

Christina, K.-R., and Jonathan, M. (2006). Cdc25: mechanisms of checkpoint inhibition and recovery. Trends in cell biology.

Cimprich, K.A., and Cortez, D. (2008). ATR: an essential regulator of genome integrity. Nature reviews. Molecular cell biology *9*, 616-627.

Conery, A.R., Sever, S., and Harlow, E. (2010). Nucleoside diphosphate kinase Nm23-H1 regulates chromosomal stability by activating the GTPase dynamin during cytokinesis. Proc Natl Acad Sci U S A *107*, 15461-15466.

Cortez, D., Glick, G., and Elledge, S.J. (2004). Minichromosome maintenance proteins are direct targets of the ATM and ATR checkpoint kinases. Proceedings of the National Academy of Sciences of the United States of America *101*, 10078-10083.

Costanzo, V., Shechter, D., Lupardus, P.J., Cimprich, K.A., Gottesman, M., and Gautier, J. (2002). An ATR- and Cdc7-dependent DNA damage checkpoint that inhibits initiation of DNA replication. Molecular cell *11*, 203-213.

Cotta-Ramusino, C., Fachinetti, D., Lucca, C., Doksani, Y., Lopes, M., Sogo, J., and Foiani, M. (2005). Exo1 processes stalled replication forks and counteracts fork reversal in checkpoint-defective cells. Mol Cell *17*, 153-159.

Craney, A., Kelly, A., Jia, L., Fedrigo, I., Yu, H., and Rape, M. (2016). Control of APC/C-dependent ubiquitin chain elongation by reversible phosphorylation. Proc Natl Acad Sci U S A *113*, 1540-1545.

Day, T.A., Palle, K., Barkley, L.R., Kakusho, N., Zou, Y., Tateishi, S., Verreault, A., Masai, H., and Vaziri, C. (2010). Phosphorylated Rad18 directs DNA polymerase eta to sites of stalled replication. J Cell Biol *191*, 953-966.

Debatisse, M., Le Tallec, B., Letessier, A., Dutrillaux, B., and Brison, O. (2011). Common fragile sites: mechanisms of instability revisited. Trends in genetics: TIG 28, 22-32.

Debatisse, M., Le Tallec, B., Letessier, A., Dutrillaux, B., and Brison, O. (2012). Common fragile sites: mechanisms of instability revisited. Trends Genet 28, 22-32.

Delagoutte, E., and von Hippel, P.H. (2001). Molecular mechanisms of the functional coupling of the helicase (gp41) and polymerase (gp43) of bacteriophage T4 within the DNA replication fork. Biochemistry 40, 4459-4477.

Dierov, J., Dierova, R., and Carroll, M. (2004). BCR/ABL translocates to the nucleus and disrupts an ATR-dependent intra-S phase checkpoint. Cancer cell *5*, 275-285.

Dimitrova, N., Gocheva, V., Bhutkar, A., Resnick, R., Jong, R.M., Miller, K.M., Bendor, J., and Jacks, T. (2016). Stromal Expression of miR-143/145 Promotes Neoangiogenesis in Lung Cancer Development. Cancer Discov *6*, 188-201.

Duncker, B.P., Shimada, K., Tsai-Pflugfelder, M., Pasero, P., and Gasser, S.M. (2002). An N-terminal domain of Dbf4p mediates interaction with both origin recognition complex (ORC) and Rad53p and can deregulate late origin firing. Proceedings of the National Academy of Sciences of the United States of America *99*, 16087-16092.

Dungrawala, H., Rose, K.L., Bhat, K.P., Mohni, K.N., Glick, G.G., Couch, F.B., and Cortez, D. (2015). The Replication Checkpoint Prevents Two Types of Fork Collapse without Regulating Replisome Stability. Mol Cell *59*, 998-1010.

Dyson, N.J. (2016). RB1: a prototype tumor suppressor and an enigma. Genes Dev 30, 1492-1502.

Edward, A.N., and David, C. (2011). ATR signalling: more than meeting at the fork. The Biochemical journal *436*, 527-536.

El-Shemerly, M., Hess, D., Pyakurel, A.K., Moselhy, S., and Ferrari, S. (2008). ATR-dependent pathways control hEXO1 stability in response to stalled forks. Nucleic Acids Res *36*, 511-519.

Ermoli, A., Bargiotti, A., Brasca, M.G., Ciavolella, A., Colombo, N., Fachin, G., Isacchi, A., Menichincheri, M., Molinari, A., Montagnoli, A., *et al.* (2009). Cell division cycle 7 kinase inhibitors: 1H-pyrrolo[2,3-b]pyridines, synthesis and structure-activity relationships. Journal of medicinal chemistry *52*, 4380-4390.

- Feng, D., Tu, Z., Wu, W., and Liang, C. (2003). Inhibiting the expression of DNA replication-initiation proteins induces apoptosis in human cancer cells. Cancer research *63*, 7356-7364.
- Ferreira, M.F., Santocanale, C., Drury, L.S., and Diffley, J.F. (2000). Dbf4p, an essential S phase-promoting factor, is targeted for degradation by the anaphase-promoting complex. Molecular and cellular biology *20*, 242-248.
- Ferretti, L.P., Lafranchi, L., and Sartori, A.A. (2013). Controlling DNA-end resection: a new task for CDKs. Front Genet 4, 99.
- Fluge, O., Bruland, O., Akslen, L.A., Lillehaug, J.R., and Varhaug, J.E. (2006). Gene expression in poorly differentiated papillary thyroid carcinomas. Thyroid: official journal of the American Thyroid Association *16*, 161-175.
- Foley, E.A., Maldonado, M., and Kapoor, T.M. (2011). Formation of stable attachments between kinetochores and microtubules depends on the B56-PP2A phosphatase. Nat Cell Biol *13*, 1265-1271.
- Fu, Y.V., Yardimci, H., Long, D.T., Ho, T.V., Guainazzi, A., Bermudez, V.P., Hurwitz, J., van Oijen, A., Schärer, O.D., and Walter, J.C. (2011). Selective bypass of a lagging strand roadblock by the eukaryotic replicative DNA helicase. Cell *146*, 931-941.
- Fuhs, S.R., Meisenhelder, J., Aslanian, A., Ma, L., Zagorska, A., Stankova, M., Binnie, A., Al-Obeidi, F., Mauger, J., Lemke, G., *et al.* (2015). Monoclonal 1- and 3-Phosphohistidine Antibodies: New Tools to Study Histidine Phosphorylation. Cell *162*, 198-210.
- Fung, A.D., Ou, J., Bueler, S., and Brown, G.W. (2002). A conserved domain of Schizosaccharomyces pombe dfp1(+) is uniquely required for chromosome stability following alkylation damage during S phase. Molecular and cellular biology *22*, 4477-4490.
- Furuya, K., Miyabe, I., Tsutsui, Y., Paderi, F., Kakusho, N., Masai, H., Niki, H., and Carr, A.M. (2010). DDK phosphorylates checkpoint clamp component Rad9 and promotes its release from damaged chromatin. Mol Cell *40*, 606-618.
- Gabrielse, C., Miller, C.T., McConnell, K.H., DeWard, A., Fox, C.A., and Weinreich, M. (2006). A Dbf4p BRCA1 C-terminal-like domain required for the response to replication fork arrest in budding yeast. Genetics *173*, 541-555.
- Graves, P.R., Yu, L., Schwarz, J.K., Gales, J., Sausville, E.A., O'Connor, P.M., and Piwnica-Worms, H. (2000). The Chk1 protein kinase and the Cdc25C regulatory pathways are targets of the anticancer agent UCN-01. J Biol Chem *275*, 5600-5605.
- Hamilton, G., and O'Neill, E. (2013). Hippo Pathway and Apoptosis. In The Hippo Signaling Pathway and Cancer, M. Oren, and Y. Aylon, eds. (New York, NY: Springer New York), pp. 117-145.
- Hanahan, D., and Weinberg, R.A. (2011). Hallmarks of cancer: the next generation. Cell *144*, 646-674.

- Hardy, C.F., Dryga, O., Seematter, S., Pahl, P.M., and Sclafani, R.A. (1997). mcm5/cdc46-bob1 bypasses the requirement for the S phase activator Cdc7p. Proc Natl Acad Sci U S A *94*, 3151-3155.
- Harkins, V., Gabrielse, C., Haste, L., and Weinreich, M. (2009). Budding yeast Dbf4 sequences required for Cdc7 kinase activation and identification of a functional relationship between the Dbf4 and Rev1 BRCT domains. Genetics *183*, 1269-1282.
- Heffernan, T.P., Unsal-Kaçmaz, K., Heinloth, A.N., Simpson, D.A., Paules, R.S., Sancar, A., Cordeiro-Stone, M., and Kaufmann, W.K. (2007). Cdc7-Dbf4 and the human S checkpoint response to UVC. The Journal of biological chemistry *282*, 9458-9468.
- Hergovich, A. (2013). Regulation and functions of mammalian LATS/NDR kinases: looking beyond canonical Hippo signalling. Cell Biosci 3, 32.
- Hiraga, S.-I., Alvino, G.M., Chang, F., Lian, H.-Y.Y., Sridhar, A., Kubota, T., Brewer, B.J., Weinreich, M., Raghuraman, M.K., and Donaldson, A.D. (2014). Rif1 controls DNA replication by directing Protein Phosphatase 1 to reverse Cdc7-mediated phosphorylation of the MCM complex. Genes & development 28, 372-383.
- Hoang, M.L., Leon, R.P., Pessoa-Brandao, L., Hunt, S., Raghuraman, M.K., Fangman, W.L., Brewer, B.J., and Sclafani, R.A. (2007). Structural changes in Mcm5 protein bypass Cdc7-Dbf4 function and reduce replication origin efficiency in Saccharomyces cerevisiae. Molecular and cellular biology *27*, 7594-7602.
- Hou, Y., Wang, H.Q., and Ba, Y. (2012a). Effects of CDC7 gene silencing and Rituximab on apoptosis in diffuse large B cell lymphoma cells. Journal of cancer research and clinical oncology *138*, 2027-2034.
- Hou, Y., Wang, H.Q., and Ba, Y. (2012b). High expression of cell division cycle 7 protein correlates with poor prognosis in patients with diffuse large B-cell lymphoma. Med Oncol 29, 3498-3503.
- Hughes, S., Elustondo, F., Di Fonzo, A., Leroux, F.G., Wong, A.C., Snijders, A.P., Matthews, S.J., and Cherepanov, P. (2012). Crystal structure of human CDC7 kinase in complex with its activator DBF4. Nature structural & molecular biology *19*, 1101-1107.
- Huse, M., and Kuriyan, J. (2002). The conformational plasticity of protein kinases. Cell *109*, 275-282.
- Hustedt, N., Gasser, S.M., and Shimada, K. (2012). Replication checkpoint: tuning and coordination of replication forks in s phase. Genes 4, 388-434.
- Iannascoli, C., Palermo, V., Murfuni, I., Franchitto, A., and Pichierri, P. (2015). The WRN exonuclease domain protects nascent strands from pathological MRE11/EXO1-dependent degradation. Nucleic Acids Res *43*, 9788-9803.

- Im, J.S., and Lee, J.K. (2008). ATR-dependent activation of p38 MAP kinase is responsible for apoptotic cell death in cells depleted of Cdc7. J Biol Chem 283, 25171-25177.
- Ito, S., Ishii, A., Kakusho, N., Taniyama, C., Yamazaki, S., Fukatsu, R., Sakaue-Sawano, A., Miyawaki, A., and Masai, H. (2012). Mechanism of cancer cell death induced by depletion of an essential replication regulator. PLoS One *7*, e36372.
- Itou, H., Muramatsu, S., Shirakihara, Y., and Araki, H. (2014). Crystal structure of the homology domain of the eukaryotic DNA replication proteins Sld3/Treslin. Structure (London, England: 1993) *22*, 1341-1347.
- Jackson, D.A., and Pombo, A. (1998). Replicon clusters are stable units of chromosome structure: evidence that nuclear organization contributes to the efficient activation and propagation of S phase in human cells. J Cell Biol *140*, 1285-1295.
- Jackson, J.R., Gilmartin, A., Imburgia, C., Winkler, J.D., Marshall, L.A., and Roshak, A. (2000). An indolocarbazole inhibitor of human checkpoint kinase (Chk1) abrogates cell cycle arrest caused by DNA damage. Cancer research *60*, 566-572.
- Jaime, L.-M., Nancy, L.M., Zophonias, O.J., Lisa, G.D.-E., James, W., and David, P.T. (2010). Damage-induced phosphorylation of Sld3 is important to block late origin firing. Nature *467*, 479-483.
- Jammi, N.V., Whitby, L.R., and Beal, P.A. (2003). Small molecule inhibitors of the RNA-dependent protein kinase. Biochem Biophys Res Commun *308*, 50-57.
- Jarrett, S.G., Novak, M., Dabernat, S., Daniel, J.Y., Mellon, I., Zhang, Q., Harris, N., Ciesielski, M.J., Fenstermaker, R.A., Kovacic, D., *et al.* (2012). Metastasis suppressor NM23-H1 promotes repair of UV-induced DNA damage and suppresses UV-induced melanomagenesis. Cancer research *72*, 133-143.
- Jeggo, P.A., Pearl, L.H., and Carr, A.M. (2016). DNA repair, genome stability and cancer: a historical perspective. Nature reviews. Cancer *16*, 35-42.
- Jiang, W., McDonald, D., Hope, T.J., and Hunter, T. (1999). Mammalian Cdc7-Dbf4 protein kinase complex is essential for initiation of DNA replication. EMBO J 18, 5703-5713.
- Jones, R.M., Mortusewicz, O., Afzal, I., Lorvellec, M., García, P., Helleday, T., and Petermann, E. (2013). Increased replication initiation and conflicts with transcription underlie Cyclin E-induced replication stress. Oncogene *32*, 3744-3753.
- José Antonio, T., and John, F.X.D. (2001). Regulation of DNA replication fork progression through damaged DNA by the Mec1/Rad53 checkpoint. Nature *412*, 553-557.
- Kang, Y.-H.H., Galal, W.C., Farina, A., Tappin, I., and Hurwitz, J. (2012a). Properties of the human Cdc45/Mcm2-7/GINS helicase complex and its action with DNA polymerase epsilon in rolling circle DNA synthesis. Proceedings of the National Academy of Sciences of the United States of America *109*, 6042-6047.

Kang, Y.H., Galal, W.C., Farina, A., Tappin, I., and Hurwitz, J. (2012b). Properties of the human Cdc45/Mcm2-7/GINS helicase complex and its action with DNA polymerase epsilon in rolling circle DNA synthesis. Proc Natl Acad Sci U S A *109*, 6042-6047.

Karim, L. (2010). How do Cdc7 and cyclin-dependent kinases trigger the initiation of chromosome replication in eukaryotic cells? Genes & development 24, 1208-1219.

Kase, H., Iwahashi, K., and Matsuda, Y. (1986). K-252a, a potent inhibitor of protein kinase C from microbial origin. The Journal of antibiotics *39*, 1059-1065.

Kaufmann, W.K., and Cleaver, J.E. (1981). Mechanisms of inhibition of DNA replication by ultraviolet light in normal human and xeroderma pigmentosum fibroblasts. Journal of molecular biology *149*, 171-187.

Kemp, M.G., and Sancar, A. (2016). ATR Kinase Inhibition Protects Non-cycling Cells from the Lethal Effects of DNA Damage and Transcription Stress. J Biol Chem *291*, 9330-9342.

Kennedy, E.K., Dysart, M., Lianga, N., Williams, E.C., Pilon, S., Dore, C., Deneault, J.S., and Rudner, A.D. (2016). Redundant Regulation of Cdk1 Tyrosine Dephosphorylation in Saccharomyces cerevisiae. Genetics *202*, 903-910.

Khalid, S., Kin Fan, O., and John, F.X.D. (2013). Regulating DNA Replication in Eukarya. Cold Spring Harbor perspectives in biology 5.

Kim, J.M., Kakusho, N., Yamada, M., Kanoh, Y., Takemoto, N., and Masai, H. (2008). Cdc7 kinase mediates Claspin phosphorylation in DNA replication checkpoint. Oncogene *27*, 3475-3482.

Kim, J.M., Nakao, K., Nakamura, K., Saito, I., Katsuki, M., Arai, K., and Masai, H. (2002). Inactivation of Cdc7 kinase in mouse ES cells results in S-phase arrest and p53-dependent cell death. EMBO J *21*, 2168-2179.

Kim, S., Dallmann, H.G., McHenry, C.S., and Marians, K.J. (1996). Coupling of a replicative polymerase and helicase: a tau-DnaB interaction mediates rapid replication fork movement. Cell *84*, 643-650.

Kim, S.H., Ho, J.N., Jin, H., Lee, S.C., Lee, S.E., Hong, S.K., Lee, J.W., Lee, E.S., and Byun, S.S. (2016). Upregulated expression of BCL2, MCM7, and CCNE1 indicate cisplatin-resistance in the set of two human bladder cancer cell lines: T24 cisplatin sensitive and T24R2 cisplatin resistant bladder cancer cell lines. Investig Clin Urol *57*, 63-72.

Kitamura, R., Fukatsu, R., Kakusho, N., Cho, Y.S., Taniyama, C., Yamazaki, S., Toh, G.T., Yanagi, K., Arai, N., Chang, H.J., *et al.* (2011). Molecular mechanism of activation of human Cdc7 kinase: bipartite interaction with Dbf4/activator of S phase kinase (ASK) activation subunit stimulates ATP binding and substrate recognition. J Biol Chem *286*, 23031-23043.

- Koltun, E.S., Tsuhako, A.L., Brown, D.S., Aay, N., Arcalas, A., Chan, V., Du, H., Engst, S., Ferguson, K., Franzini, M., *et al.* (2012). Discovery of XL413, a potent and selective CDC7 inhibitor. Bioorganic & medicinal chemistry letters *22*, 3727-3731.
- Kong, L.J., Chang, J.T., Bild, A.H., and Nevins, J.R. (2007). Compensation and specificity of function within the E2F family. Oncogene 26, 321-327.
- Kulkarni, A.A., Kingsbury, S.R., Tudzarova, S., Hong, H.K., Loddo, M., Rashid, M., Rodriguez-Acebes, S., Prevost, A.T., Ledermann, J.A., Stoeber, K., *et al.* (2009). Cdc7 kinase is a predictor of survival and a novel therapeutic target in epithelial ovarian carcinoma. Clinical cancer research: an official journal of the American Association for Cancer Research *15*, 2417-2425.
- Kumagai, A., Shevchenko, A., Shevchenko, A., and Dunphy, W.G. (2010). Treslin collaborates with TopBP1 in triggering the initiation of DNA replication. Cell *140*, 349-359.
- Kumagai, H., Sato, N., Yamada, M., Mahony, D., Seghezzi, W., Lees, E., Arai, K., and Masai, H. (1999). A novel growth- and cell cycle-regulated protein, ASK, activates human Cdc7-related kinase and is essential for G1/S transition in mammalian cells. Molecular and cellular biology *19*, 5083-5095.
- Langston, L.D., Zhang, D., Yurieva, O., Georgescu, R.E., Finkelstein, J., Yao, N.Y., Indiani, C., and O'Donnell, M.E. (2014). CMG helicase and DNA polymerase epsilon form a functional 15-subunit holoenzyme for eukaryotic leading-strand DNA replication. Proc Natl Acad Sci U S A *111*, 15390-15395.
- Lawrence, M.S., Stojanov, P., Polak, P., Kryukov, G.V., Cibulskis, K., Sivachenko, A., Carter, S.L., Stewart, C., Mermel, C.H., Roberts, S.A., *et al.* (2013). Mutational heterogeneity in cancer and the search for new cancer-associated genes. Nature *499*, 214-218.
- Leonard, A.C., and Méchali, M. (2013). DNA replication origins. Cold Spring Harbor perspectives in biology 5.
- Lerdrup, M., Johansen, J.V., Agrawal-Singh, S., and Hansen, K. (2016). An interactive environment for agile analysis and visualization of ChIP-sequencing data. Nature structural & molecular biology *23*, 349-357.
- Li, C.M., Gocheva, V., Oudin, M.J., Bhutkar, A., Wang, S.Y., Date, S.R., Ng, S.R., Whittaker, C.A., Bronson, R.T., Snyder, E.L., *et al.* (2015). Foxa2 and Cdx2 cooperate with Nkx2-1 to inhibit lung adenocarcinoma metastasis. Genes Dev *29*, 1850-1862.
- Liberzon, A., Birger, C., Thorvaldsdottir, H., Ghandi, M., Mesirov, J.P., and Tamayo, P. (2015). The Molecular Signatures Database (MSigDB) hallmark gene set collection. Cell Syst *1*, 417-425.
- Lindqvist, A., Källström, H., and Karlsson Rosenthal, C. (2004). Characterisation of Cdc25B localisation and nuclear export during the cell cycle and in response to stress. Journal of cell science *117*, 4979-4990.

Lipinski, C.A. (2004). Lead- and drug-like compounds: the rule-of-five revolution. Drug Discovery Today: Technologies *1*, 337-341.

Liu, H., Tang, X., Srivastava, A., Pecot, T., Daniel, P., Hemmelgarn, B., Reyes, S., Fackler, N., Bajwa, A., Kladney, R., *et al.* (2015). Redeployment of Myc and E2f1-3 drives Rb-deficient cell cycles. Nat Cell Biol *17*, 1036-1048.

Liu, S., Shiotani, B., Lahiri, M., Maréchal, A., Tse, A., Leung, C.C., Glover, J.N., Yang, X.H., and Zou, L. (2011). ATR autophosphorylation as a molecular switch for checkpoint activation. Molecular cell *43*, 192-202.

Lopes, M., Foiani, M., and Sogo, J.M. (2006). Multiple mechanisms control chromosome integrity after replication fork uncoupling and restart at irreparable UV lesions. Mol Cell *21*, 15-27.

Lopez-Contreras, A.J., Ruppen, I., Nieto-Soler, M., Murga, M., Rodriguez-Acebes, S., Remeseiro, S., Rodrigo-Perez, S., Rojas, A.M., Mendez, J., Munoz, J., *et al.* (2013). A proteomic characterization of factors enriched at nascent DNA molecules. Cell Rep *3*, 1105-1116.

Mailand, N. (2000). Rapid Destruction of Human Cdc25A in Response to DNA Damage. Science.

Malumbres, M. (2011). Physiological relevance of cell cycle kinases. Physiological reviews 91, 973-1007.

Mantiero, D., Mackenzie, A., Donaldson, A., and Zegerman, P. (2011). Limiting replication initiation factors execute the temporal programme of origin firing in budding yeast. The EMBO journal *30*, 4805-4814.

Marchal, J.A., Lopez, G.J., Peran, M., Comino, A., Delgado, J.R., Garcia-Garcia, J.A., Conde, V., Aranda, F.M., Rivas, C., Esteban, M., *et al.* (2014). The impact of PKR activation: from neurodegeneration to cancer. FASEB J *28*, 1965-1974.

Masai, H., Taniyama, C., Ogino, K., Matsui, E., Kakusho, N., Matsumoto, S., Kim, J.M., Ishii, A., Tanaka, T., Kobayashi, T., *et al.* (2006). Phosphorylation of MCM4 by Cdc7 kinase facilitates its interaction with Cdc45 on the chromatin. J Biol Chem *281*, 39249-39261.

Matos, J., Lipp, J.J., Bogdanova, A., Guillot, S., Okaz, E., Junqueira, M., Shevchenko, A., and Zachariae, W. (2008). Dbf4-dependent CDC7 kinase links DNA replication to the segregation of homologous chromosomes in meiosis I. Cell *135*, 662-678.

Mendez, J., and Stillman, B. (2000). Chromatin association of human origin recognition complex, cdc6, and minichromosome maintenance proteins during the cell cycle: assembly of prereplication complexes in late mitosis. Molecular and cellular biology *20*, 8602-8612.

Meng, Z., Moroishi, T., and Guan, K.L. (2016). Mechanisms of Hippo pathway regulation. Genes Dev *30*, 1-17.

Meng, Z., Moroishi, T., Mottier-Pavie, V., Plouffe, S.W., Hansen, C.G., Hong, A.W., Park, H.W., Mo, J.S., Lu, W., Lu, S., *et al.* (2015). MAP4K family kinases act in parallel to MST1/2 to activate LATS1/2 in the Hippo pathway. Nat Commun *6*, 8357.

Menichincheri, M., Albanese, C., Alli, C., Ballinari, D., Bargiotti, A., Caldarelli, M., Ciavolella, A., Cirla, A., Colombo, M., Colotta, F., *et al.* (2010). Cdc7 kinase inhibitors: 5-heteroaryl-3-carboxamido-2-aryl pyrroles as potential antitumor agents. 1. Lead finding. Journal of medicinal chemistry *53*, 7296-7315.

Menichincheri, M., Bargiotti, A., Berthelsen, J., Bertrand, J.A., Bossi, R., Ciavolella, A., Cirla, A., Cristiani, C., Croci, V., D'Alessio, R., *et al.* (2009). First Cdc7 kinase inhibitors: pyrrolopyridinones as potent and orally active antitumor agents. 2. Lead discovery. Journal of medicinal chemistry *52*, 293-307.

Miller, C.T., Gabrielse, C., Chen, Y.C., and Weinreich, M. (2009). Cdc7p-Dbf4p regulates mitotic exit by inhibiting Polo kinase. PLoS Genet *5*, e1000498.

Mochida, S., Ikeo, S., Gannon, J., and Hunt, T. (2009). Regulated activity of PP2A-B55 delta is crucial for controlling entry into and exit from mitosis in Xenopus egg extracts. EMBO J 28, 2777-2785.

Montagnoli, A., Moll, J., and Colotta, F. (2010). Targeting cell division cycle 7 kinase: a new approach for cancer therapy. Clinical cancer research: an official journal of the American Association for Cancer Research *16*, 4503-4508.

Montagnoli, A., Tenca, P., Sola, F., Carpani, D., Brotherton, D., Albanese, C., and Santocanale, C. (2004). Cdc7 inhibition reveals a p53-dependent replication checkpoint that is defective in cancer cells. Cancer research *64*, 7110-7116.

Montagnoli, A., Valsasina, B., Brotherton, D., Troiani, S., Rainoldi, S., Tenca, P., Molinari, A., and Santocanale, C. (2006a). Identification of Mcm2 phosphorylation sites by S-phase-regulating kinases. J Biol Chem *281*, 10281-10290.

Montagnoli, A., Valsasina, B., Brotherton, D., Troiani, S., Rainoldi, S., Tenca, P., Molinari, A., and Santocanale, C. (2006b). Identification of Mcm2 phosphorylation sites by S-phase-regulating kinases. The Journal of biological chemistry *281*, 10281-10290.

Montagnoli, A., Valsasina, B., Croci, V., Menichincheri, M., Rainoldi, S., Marchesi, V., Tibolla, M., Tenca, P., Brotherton, D., Albanese, C., *et al.* (2008). A Cdc7 kinase inhibitor restricts initiation of DNA replication and has antitumor activity. Nat Chem Biol *4*, 357-365.

Murakami, H., and Keeney, S. (2014). Temporospatial coordination of meiotic DNA replication and recombination via DDK recruitment to replisomes. Cell *158*, 861-873.

Naim, V., and Rosselli, F. (2009). The FANC pathway and BLM collaborate during mitosis to prevent micro-nucleation and chromosome abnormalities. Nat Cell Biol *11*, 761-768.

- Naito, Y., Shimizu, H., Kasama, T., Sato, J., Tabara, H., Okamoto, A., Yabuta, N., and Nojima, H. (2012). Cyclin G-associated kinase regulates protein phosphatase 2A by phosphorylation of its B'gamma subunit. Cell Cycle *11*, 604-616.
- Natoni, A., Coyne, M.R., Jacobsen, A., Rainey, M.D., O'Brien, G., Healy, S., Montagnoli, A., Moll, J., O'Dwyer, M., and Santocanale, C. (2013). Characterization of a Dual CDC7/CDK9 Inhibitor in Multiple Myeloma Cellular Models. Cancers *5*, 901-918.
- Natoni, A., Murillo, L.S., Kliszczak, A.E., Catherwood, M.A., Montagnoli, A., Samali, A., O'Dwyer, M., and Santocanale, C. (2011). Mechanisms of action of a dual Cdc7/Cdk9 kinase inhibitor against quiescent and proliferating CLL cells. Molecular cancer therapeutics *10*, 1624-1634.
- Niesen, F.H., Berglund, H., and Vedadi, M. (2007). The use of differential scanning fluorimetry to detect ligand interactions that promote protein stability. Nature protocols *2*, 2212-2221.
- Nimonkar, A.V., Genschel, J., Kinoshita, E., Polaczek, P., Campbell, J.L., Wyman, C., Modrich, P., and Kowalczykowski, S.C. (2011). BLM-DNA2-RPA-MRN and EXO1-BLM-RPA-MRN constitute two DNA end resection machineries for human DNA break repair. Genes Dev *25*, 350-362.
- Njagi, G.D., and Kilbey, B.J. (1982). cdc7-1 a temperature sensitive cell-cycle mutant which interferes with induced mutagenesis in Saccharomyces cerevisiae. Mol Gen Genet *186*, 478-481.
- Ogino, K., Takeda, T., Matsui, E., Iiyama, H., Taniyama, C., Arai, K., and Masai, H. (2001). Bipartite binding of a kinase activator activates Cdc7-related kinase essential for S phase. J Biol Chem *276*, 31376-31387.
- Oliver, T.G., Mercer, K.L., Sayles, L.C., Burke, J.R., Mendus, D., Lovejoy, K.S., Cheng, M.H., Subramanian, A., Mu, D., Powers, S., *et al.* (2010). Chronic cisplatin treatment promotes enhanced damage repair and tumor progression in a mouse model of lung cancer. Genes Dev *24*, 837-852.
- On, K.F., Beuron, F., Frith, D., Snijders, A.P., Morris, E.P., and Diffley, J.F. (2014). Prereplicative complexes assembled in vitro support origin-dependent and independent DNA replication. The EMBO journal *33*, 605-620.
- Oshiro, G., Owens, J.C., Shellman, Y., Sclafani, R.A., and Li, J.J. (1999). Cell cycle control of Cdc7p kinase activity through regulation of Dbf4p stability. Molecular and cellular biology *19*, 4888-4896.
- Ostroff, R.M., and Sclafani, R.A. (1995). Cell cycle regulation of induced mutagenesis in yeast. Mutat Res *329*, 143-152.
- Paulovich, A.G., and Hartwell, L.H. (1995). A checkpoint regulates the rate of progression through S phase in S. cerevisiae in response to DNA damage. Cell *82*, 841-847.

Peng, C.Y., Graves, P.R., Thoma, R.S., Wu, Z., Shaw, A.S., and Piwnica-Worms, H. (1997). Mitotic and G2 checkpoint control: regulation of 14-3-3 protein binding by phosphorylation of Cdc25C on serine-216. Science (New York, N.Y.) *277*, 1501-1505.

Pessoa-Brandao, L., and Sclafani, R.A. (2004). CDC7/DBF4 functions in the translesion synthesis branch of the RAD6 epistasis group in Saccharomyces cerevisiae. Genetics *167*, 1597-1610.

Petermann, E., and Helleday, T. (2010). Pathways of mammalian replication fork restart. Nat Rev Mol Cell Biol 11, 683-687.

Petermann, E., Orta, M.L., Issaeva, N., Schultz, N., and Helleday, T. (2010). Hydroxyurea-stalled replication forks become progressively inactivated and require two different RAD51-mediated pathways for restart and repair. Mol Cell *37*, 492-502.

Poh, W.T., Chadha, G.S., Gillespie, P.J., Kaldis, P., and Blow, J.J. (2013). Xenopus Cdc7 executes its essential function early in S phase and is counteracted by checkpoint-regulated protein phosphatase 1. Open biology 4, 130138.

Rainey, M.D., Harhen, B., Wang, G.N., Murphy, P.V., and Santocanale, C. (2013). Cdc7-dependent and -independent phosphorylation of Claspin in the induction of the DNA replication checkpoint. Cell Cycle *12*, 1560-1568.

Raleigh, J.M., and O'Connell, M.J. (2000). The G(2) DNA damage checkpoint targets both Weel and Cdc25. Journal of cell science 113 (Pt 10), 1727-1736.

Ramer, M.D., Suman, E.S., Richter, H., Stanger, K., Spranger, M., Bieberstein, N., and Duncker, B.P. (2013). Dbf4 and Cdc7 proteins promote DNA replication through interactions with distinct Mcm2-7 protein subunits. J Biol Chem *288*, 14926-14935.

Randell, J.C., Fan, A., Chan, C., Francis, L.I., Heller, R.C., Galani, K., and Bell, S.P. (2010). Mec1 is one of multiple kinases that prime the Mcm2-7 helicase for phosphorylation by Cdc7. Molecular cell *40*, 353-363.

Ray Chaudhuri, A., Callen, E., Ding, X., Gogola, E., Duarte, A.A., Lee, J.E., Wong, N., Lafarga, V., Calvo, J.A., Panzarino, N.J., *et al.* (2016). Replication fork stability confers chemoresistance in BRCA-deficient cells. Nature *535*, 382-387.

Reaper, P.M., Griffiths, M.R., Long, J.M., Charrier, J.D., Maccormick, S., Charlton, P.A., Golec, J.M., and Pollard, J.R. (2011). Selective killing of ATM- or p53-deficient cancer cells through inhibition of ATR. Nat Chem Biol *7*, 428-430.

Remus, D., Beuron, F., Tolun, G., Griffith, J.D., Morris, E.P., and Diffley, J.F. (2009). Concerted loading of Mcm2-7 double hexamers around DNA during DNA replication origin licensing. Cell *139*, 719-730.

Ruiz, S., Mayor-Ruiz, C., Lafarga, V., Murga, M., Vega-Sendino, M., Ortega, S., and Fernandez-Capetillo, O. (2016). A Genome-wide CRISPR Screen Identifies CDC25A as a Determinant of Sensitivity to ATR Inhibitors. Mol Cell 62, 307-313.

Ruvolo, P.P. (2016). The broken "Off" switch in cancer signaling: PP2A as a regulator of tumorigenesis, drug resistance, and immune surveillance. BBA Clin 6, 87-99.

Sangrithi, M.N., Bernal, J.A., Madine, M., Philpott, A., Lee, J., Dunphy, W.G., and Venkitaraman, A.R. (2005). Initiation of DNA replication requires the RECQL4 protein mutated in Rothmund-Thomson syndrome. Cell *121*, 887-898.

Santocanale, C., and Diffley, J.F. (1998). A Mec1- and Rad53-dependent checkpoint controls late-firing origins of DNA replication. Nature *395*, 615-618.

Sasanuma, H., Hirota, K., Fukuda, T., Kakusho, N., Kugou, K., Kawasaki, Y., Shibata, T., Masai, H., and Ohta, K. (2008). Cdc7-dependent phosphorylation of Mer2 facilitates initiation of yeast meiotic recombination. Genes Dev *22*, 398-410.

Sasi, N., Coquel, F., Lin, Y., MacKeigan, J., Pasero, P., and Weinreich, M. (2016). DDK has a primary role in processing stalled replication forks to initiate downstream checkpoint signaling. Submitted.

Sasi, N.K., Tiwari, K., Soon, F.F., Bonte, D., Wang, T., Melcher, K., Xu, H.E., and Weinreich, M. (2014). The potent Cdc7-Dbf4 (DDK) kinase inhibitor XL413 has limited activity in many cancer cell lines and discovery of potential new DDK inhibitor scaffolds. PLoS One *9*, e113300.

Sasi, N.K., and Weinreich, M. (2016). DNA Replication Checkpoint Signaling. In The Initiation of DNA Replication in Eukaryotes, L.D. Kaplan, ed. (Cham: Springer International Publishing), pp. 479-502.

Sato, N., Sato, M., Nakayama, M., Saitoh, R., Arai, K., and Masai, H. (2003). Cell cycle regulation of chromatin binding and nuclear localization of human Cdc7-ASK kinase complex. Genes to cells: devoted to molecular & cellular mechanisms 8, 451-463.

Satoshi, Y., Motoshi, H., and Hisao, M. (2013). Replication timing regulation of eukaryotic replicons: Rifl as a global regulator of replication timing. Trends in Genetics *29*, 449-460.

Schlacher, K., Christ, N., Siaud, N., Egashira, A., Wu, H., and Jasin, M. (2011). Double-strand break repair-independent role for BRCA2 in blocking stalled replication fork degradation by MRE11. Cell *145*, 529-542.

Schlacher, K., Wu, H., and Jasin, M. (2012). A distinct replication fork protection pathway connects Fanconi anemia tumor suppressors to RAD51-BRCA1/2. Cancer Cell 22, 106-116.

Schwab, R.A., Blackford, A.N., and Niedzwiedz, W. (2010). ATR activation and replication fork restart are defective in FANCM-deficient cells. EMBO J 29, 806-818.

Sclafani, R.A., Patterson, M., Rosamond, J., and Fangman, W.L. (1988). Differential regulation of the yeast CDC7 gene during mitosis and meiosis. Molecular and cellular biology *8*, 293-300.

Shechter, D., and Gautier, J. (2004). MCM proteins and checkpoint kinases get together at the fork. Proc Natl Acad Sci U S A *101*, 10845-10846.

Sheu, Y.-J.J., and Stillman, B. (2006). Cdc7-Dbf4 phosphorylates MCM proteins via a docking site-mediated mechanism to promote S phase progression. Molecular cell *24*, 101-113.

Sheu, Y.-J.J., and Stillman, B. (2010). The Dbf4-Cdc7 kinase promotes S phase by alleviating an inhibitory activity in Mcm4. Nature *463*, 113-117.

Shimizu, H., Nagamori, I., Yabuta, N., and Nojima, H. (2009). GAK, a regulator of clathrin-mediated membrane traffic, also controls centrosome integrity and chromosome congression. J Cell Sci *122*, 3145-3152.

Shirahige, K., Hori, Y., Shiraishi, K., Yamashita, M., Takahashi, K., Obuse, C., Tsurimoto, T., and Yoshikawa, H. (1998). Regulation of DNA-replication origins during cell-cycle progression. Nature *395*, 618-621.

Shreeram, S., Sparks, A., Lane, D.P., and Blow, J.J. (2002). Cell type-specific responses of human cells to inhibition of replication licensing. Oncogene *21*, 6624-6632.

Silvia, T., Alberto, R., and Christian, S. (2014). Switch on the engine: how the eukaryotic replicative helicase MCM2–7 becomes activated. Chromosoma.

Simon, A.C., Zhou, J.C., Perera, R.L., van Deursen, F., Evrin, C., Ivanova, M.E., Kilkenny, M.L., Renault, L., Kjaer, S., Matak-Vinković, D., *et al.* (2014). A Ctf4 trimer couples the CMG helicase to DNA polymerase α in the eukaryotic replisome. Nature *510*, 293-297.

Sirbu, B.M., and Cortez, D. (2013). DNA damage response: three levels of DNA repair regulation. Cold Spring Harb Perspect Biol 5, a012724.

Sirbu, B.M., McDonald, W.H., Dungrawala, H., Badu-Nkansah, A., Kavanaugh, G.M., Chen, Y., Tabb, D.L., and Cortez, D. (2013). Identification of proteins at active, stalled, and collapsed replication forks using isolation of proteins on nascent DNA (iPOND) coupled with mass spectrometry. J Biol Chem *288*, 31458-31467.

Stano, N.M., Jeong, Y.J., Donmez, I., Tummalapalli, P., Levin, M.K., and Patel, S.S. (2005). DNA synthesis provides the driving force to accelerate DNA unwinding by a helicase. Nature *435*, 370-373.

Stark, M.S., Woods, S.L., Gartside, M.G., Bonazzi, V.F., Dutton-Regester, K., Aoude, L.G., Chow, D., Sereduk, C., Niemi, N.M., Tang, N., *et al.* (2012). Frequent somatic mutations in MAP3K5 and MAP3K9 in metastatic melanoma identified by exome sequencing. Nat Genet *44*, 165-169.

- Subramanian, A., Tamayo, P., Mootha, V.K., Mukherjee, S., Ebert, B.L., Gillette, M.A., Paulovich, A., Pomeroy, S.L., Golub, T.R., Lander, E.S., *et al.* (2005). Gene set enrichment analysis: a knowledge-based approach for interpreting genome-wide expression profiles. Proc Natl Acad Sci U S A *102*, 15545-15550.
- Sun, J., Fernandez-Cid, A., Riera, A., Tognetti, S., Yuan, Z., Stillman, B., Speck, C., and Li, H. (2014). Structural and mechanistic insights into Mcm2-7 double-hexamer assembly and function. Genes & development 28, 2291-2303.
- Sun, T.P., and Shieh, S.Y. (2009). Human FEM1B is required for Rad9 recruitment and CHK1 activation in response to replication stress. Oncogene 28, 1971-1981.
- Takahashi, T.S., Basu, A., Bermudez, V., Hurwitz, J., and Walter, J.C. (2008). Cdc7-Drf1 kinase links chromosome cohesion to the initiation of DNA replication in Xenopus egg extracts. Genes Dev 22, 1894-1905.
- Tanaka, S., Umemori, T., Hirai, K., Muramatsu, S., Kamimura, Y., and Araki, H. (2007). CDK-dependent phosphorylation of Sld2 and Sld3 initiates DNA replication in budding yeast. Nature 445, 328-332.
- Tapley, P., Lamballe, F., and Barbacid, M. (1992). K252a is a selective inhibitor of the tyrosine protein kinase activity of the trk family of oncogenes and neurotrophin receptors. Oncogene 7, 371-381.
- Tapon, N., Harvey, K.F., Bell, D.W., Wahrer, D.C., Schiripo, T.A., Haber, D., and Hariharan, I.K. (2002). salvador Promotes both cell cycle exit and apoptosis in Drosophila and is mutated in human cancer cell lines. Cell *110*, 467-478.
- Tenca, P., Brotherton, D., Montagnoli, A., Rainoldi, S., Albanese, C., and Santocanale, C. (2007). Cdc7 is an active kinase in human cancer cells undergoing replication stress. The Journal of biological chemistry *282*, 208-215.
- Thangavel, S., Berti, M., Levikova, M., Pinto, C., Gomathinayagam, S., Vujanovic, M., Zellweger, R., Moore, H., Lee, E.H., Hendrickson, E.A., *et al.* (2015). DNA2 drives processing and restart of reversed replication forks in human cells. J Cell Biol *208*, 545-562.
- Tranchevent, L.C., Barriot, R., Yu, S., Van Vooren, S., Van Loo, P., Coessens, B., De Moor, B., Aerts, S., and Moreau, Y. (2008). ENDEAVOUR update: a web resource for gene prioritization in multiple species. Nucleic Acids Res *36*, W377-384.
- Trenz, K., Errico, A., and Costanzo, V. (2008). Plx1 is required for chromosomal DNA replication under stressful conditions. The EMBO journal *27*, 876-885.
- Tsuhako, A.L., Brown, D.S., Koltun, E.S., Aay, N., Arcalas, A., Chan, V., Du, H., Engst, S., Franzini, M., Galan, A., *et al.* (2012). The design, synthesis, and biological evaluation of PIM kinase inhibitors. Bioorganic & medicinal chemistry letters *22*, 3732-3738.

Tudzarova, S., Trotter, M.W., Wollenschlaeger, A., Mulvey, C., Godovac-Zimmermann, J., Williams, G.H., and Stoeber, K. (2010). Molecular architecture of the DNA replication origin activation checkpoint. EMBO J *29*, 3381-3394.

Vanotti, E., Amici, R., Bargiotti, A., Berthelsen, J., Bosotti, R., Ciavolella, A., Cirla, A., Cristiani, C., D'Alessio, R., Forte, B., *et al.* (2008). Cdc7 kinase inhibitors: pyrrolopyridinones as potential antitumor agents. 1. Synthesis and structure-activity relationships. Journal of medicinal chemistry *51*, 487-501.

Vassin, V.M., Anantha, R.W., Sokolova, E., Kanner, S., and Borowiec, J.A. (2009). Human RPA phosphorylation by ATR stimulates DNA synthesis and prevents ssDNA accumulation during DNA-replication stress. J Cell Sci *122*, 4070-4080.

Vidal-Eychenie, S., Decaillet, C., Basbous, J., and Constantinou, A. (2013). DNA structure-specific priming of ATR activation by DNA-PKcs. J Cell Biol 202, 421-429.

Walters, R.A., and Hildebrand, C.E. (1975). Evidence that x-irradiation inhibits DNA replicon initiation in Chinese hamster cells. Biochemical and biophysical research communications *65*, 265-271.

Wan, L., Niu, H., Futcher, B., Zhang, C., Shokat, K.M., Boulton, S.J., and Hollingsworth, N.M. (2008). Cdc28-Clb5 (CDK-S) and Cdc7-Dbf4 (DDK) collaborate to initiate meiotic recombination in yeast. Genes Dev *22*, 386-397.

Wang, F.Z., Fei, H.R., Cui, Y.J., Sun, Y.K., Li, Z.M., Wang, X.Y., Yang, X.Y., Zhang, J.G., and Sun, B.L. (2014). The checkpoint 1 kinase inhibitor LY2603618 induces cell cycle arrest, DNA damage response and autophagy in cancer cells. Apoptosis *19*, 1389-1398.

Watase, G., Takisawa, H., and Kanemaki, M.T. (2012). Mcm10 plays a role in functioning of the eukaryotic replicative DNA helicase, Cdc45-Mcm-GINS. Current biology: CB *22*, 343-349.

Weinreich, M., and Stillman, B. (1999a). Cdc7p-Dbf4p kinase binds to chromatin during S phase and is regulated by both the APC and the RAD53 checkpoint pathway. The EMBO journal *18*, 5334-5346.

Weinreich, M., and Stillman, B. (1999b). Cdc7p-Dbf4p kinase binds to chromatin during S phase and is regulated by both the APC and the RAD53 checkpoint pathway. EMBO J 18, 5334-5346.

Weiss, W.A., Taylor, S.S., and Shokat, K.M. (2007). Recognizing and exploiting differences between RNAi and small-molecule inhibitors. Nat Chem Biol *3*, 739-744.

Wenyi, F., David, C., Max, E.B., Lindsay, A.F., Gina, M.A., Walton, L.F., Mosur, K.R., and Bonita, J.B. (2006). Genomic mapping of single-stranded DNA in hydroxyurea-challenged yeasts identifies origins of replication. Nature cell biology *8*, 148-155.

Workman, P., and Collins, I. (2010). Probing the probes: fitness factors for small molecule tools. Chemistry & biology 17, 561-577.

Wu, Y., Lee, S.H., Williamson, E.A., Reinert, B.L., Cho, J.H., Xia, F., Jaiswal, A.S., Srinivasan, G., Patel, B., Brantley, A., *et al.* (2015). EEPD1 Rescues Stressed Replication Forks and Maintains Genome Stability by Promoting End Resection and Homologous Recombination Repair. PLoS Genet *11*, e1005675.

Yamada, M., Sato, N., Taniyama, C., Ohtani, K., Arai, K., and Masai, H. (2002). A 63-base pair DNA segment containing an Sp1 site but not a canonical E2F site can confer growth-dependent and E2F-mediated transcriptional stimulation of the human ASK gene encoding the regulatory subunit for human Cdc7-related kinase. J Biol Chem *277*, 27668-27681.

Yamada, M., Watanabe, K., Mistrik, M., Vesela, E., Protivankova, I., Mailand, N., Lee, M., Masai, H., Lukas, J., and Bartek, J. (2013a). ATR-Chk1-APC/CCdh1-dependent stabilization of Cdc7-ASK (Dbf4) kinase is required for DNA lesion bypass under replication stress. Genes & development 27, 2459-2472.

Yamada, M., Watanabe, K., Mistrik, M., Vesela, E., Protivankova, I., Mailand, N., Lee, M., Masai, H., Lukas, J., and Bartek, J. (2013b). ATR-Chk1-APC/CCdh1-dependent stabilization of Cdc7-ASK (Dbf4) kinase is required for DNA lesion bypass under replication stress. Genes Dev 27, 2459-2472.

Yan, L., and Hiroyuki, A. (2013). Loading and activation of DNA replicative helicases: the key step of initiation of DNA replication. Genes to Cells 18, 266-277.

Yanow, S.K., Gold, D.A., Yoo, H.Y., and Dunphy, W.G. (2003). Xenopus Drf1, a regulator of Cdc7, displays checkpoint-dependent accumulation on chromatin during an S-phase arrest. The Journal of biological chemistry *278*, 41083-41092.

Yardimci, H., and Walter, J.C. (2013). Prereplication-complex formation: a molecular double take? Nature structural & molecular biology *21*, 20-25.

Yekezare, M., Gómez-González, B., and Diffley, J.F. (2013). Controlling DNA replication origins in response to DNA damage - inhibit globally, activate locally. Journal of cell science *126*, 1297-1306.

Zegerman, P., and Diffley, J.F. (2007). Phosphorylation of Sld2 and Sld3 by cyclin-dependent kinases promotes DNA replication in budding yeast. Nature *445*, 281-285.

Zegerman, P., and Diffley, J.F. (2010). Checkpoint-dependent inhibition of DNA replication initiation by Sld3 and Dbf4 phosphorylation. Nature *467*, 474-478.

Zhang, J., Yang, P.L., and Gray, N.S. (2009). Targeting cancer with small molecule kinase inhibitors. Nature reviews. Cancer *9*, 28-39.

Zhang, J.H., Chung, T.D., and Oldenburg, K.R. (1999). A Simple Statistical Parameter for Use in Evaluation and Validation of High Throughput Screening Assays. J Biomol Screen *4*, 67-73.

Zou, L., and Elledge, S.J. (2003). Sensing DNA damage through ATRIP recognition of RPAssDNA complexes. Science (New York, N.Y.) 300, 1542-1548.

Zou, L., Liu, D., and Elledge, S.J. (2003). Replication protein A-mediated recruitment and activation of Rad17 complexes. Proceedings of the National Academy of Sciences of the United States of America *100*, 13827-13832.